Impact of IL-7 signaling on adoptive T cell therapy

D i s s e r t a t i o n

zur Erlangung des akademischen Grades
d o c t o r r e r u m n a t u r a l i u m
(Dr. rer. nat.)

im Fach Biologie
eingereicht an der

Lebenswissenschaftlichen Fakultät
der Humboldt-Universität zu Berlin
von

M. Sc. Katrin Deiser

Präsident der Humboldt-Universität zu Berlin
Prof. Dr. Jan-Hendrik Olbertz

Dekan der Lebenswissenschaftlichen Fakultät
Prof. Dr. R. Lucius

Gutachter: 1. Prof. Dr. W. Uckert
2. Prof. Dr. T. Schüler
3. Prof. Dr. I. Schmitz

Tag der mündlichen Prüfung: 21.05.2015

1 Summary

Interleukin-7 (IL-7) is an essential and nonredundant cytokine required for the development and maintenance of mature T cell. Its availability is limited under normal conditions, but rises during lymphopenia, leading to increased T cell proliferation. The administration of recombinant IL-7 to normal or lymphopenic mice and humans results in increased T cell numbers and altered T cell phenotype. Hence, IL-7 administration could mediate therapeutic benefits in immunocompromised patients and is currently tested in several clinical trials, including anti-cancer trials. However, besides its well-studied effects on T cells little is known about the effect of IL-7 on other immune and non-immune cells and their influence on T cell homeostasis. Therefore, we evaluated the effect of IL-7 therapy on adoptively transferred T cells in IL-7 receptor (IL-7R)-competent and IL-7R-deficient lymphopenic mice. We confirm the benefits of IL-7 therapy on T cell responses but additionally show that many of these effects are dependent on IL-7R expression by host cells, indicating that IL-7R signaling in host cells modulates T cell responses. Surprisingly, peptide vaccination blunted the beneficial effect of IL-7 treatment on adoptive T cell therapy against cancer. Irrespective of peptide vaccination however, we show that efficient T cell responses against cancer are dependent on host IL-7R signaling. Based on studies in bone-marrow chimeric mice, we identify non-hematopoietic host cells as main regulators of IL-7 therapy-modulated T cell differentiation. We conclude from these data that IL-7 therapy affects non-hematopoietic stromal cells that modulate the success of adoptive T cell therapy. Our results confirm that stromal cells in various organs express *il-7* and show that these cells are targeted by IL-7 therapy *in vivo*. Hence, we propose that *il-7*-expressing cells regulate IL-7 therapy-modulated T cell homeostasis. To identify and study these *il-7* expressing stromal cells in more detail, we characterized a new transgenic mouse model that will facilitate determining the molecular pathways to improve the success of adoptive T cell therapy.

2 Introduction

Our interactions with the environment affect the quality of our lives, especially the period that we spend in health. Our body fights invaders with complex defense mechanisms, comprised of the outer physical layer of epithelial barriers and the inner motile cells of the immune system. The immune system can discriminate between normal - "healthy" and infected - "sick" cells by recognizing a variety of "danger cues". When the immune system recognizes pathogen associated molecular patterns (PAMPs) or other foreign structures such as antigens (Ag) of pathogens, it responds. If the immune response is not strong enough, it leads to severe infection and disease. On the other hand, when the immune response is activated inappropriately strong or long, it causes immunopathology. Therefore, it is pivotal that each and every component of the immune response is tightly regulated. The immune system is comprised of various cell types and proteins that either circulate through the body or reside in particular tissues. All immune cell types are derived from the hematopoietic lineage, and each immune cell type plays a unique role in recognition of different hazardous factors, performing specialized functions and communicating with other cells. Based on their function, immune cells can be classified into two main arms, the innate and the adaptive immune cells (1).

2.1 Innate immune system

In general, innate immune cells recognize threats by their pattern recognition receptors (PRR) that bind PAMPs such as bacterial carbohydrates (e.g. lipopolysaccharide or mannose) and bacterial or viral nucleic acids (2). The main components of the innate immune system include the complement system, phagocytes and innate lymphoid cells (ILCs).

The complement system is comprised of proteins that circulate in the blood stream in an inactive state. Upon triggering by pathogens, a chain reaction is set off and a cascade of proteins gets activated. These proteins directly kill bacteria or label them for better clearance by immune cells. In addition, they drive the innate immune response by attracting and activating phagocytes (3).

Phagocytes ingest bacteria, viruses, dead and infected cells. Upon activation, they release proteins from their granules to help killing the invaders and to attract other immune cells. The population of phagocytes is very heterogeneous and includes neutrophils, macrophages and dendritic cells (DCs). Neutrophils belong to the early line of immune defense. Upon danger cues, they leave the bloodstream, trap, ingest and thus remove bacteria e.g. by release of net-like structures or by antimicrobial substances (4). Similarly, macrophages also clear invaders and damaged or dead cells. Moreover, they alert and attract other immune cells and can present Ags (5–8).

Other members of the innate immune system are the functionally diverse group of innate

lymphoid cells (ILC). They include subsets that regulate lymphoid organ development, tissue homeostasis at mucosal surfaces but can also display antimicrobial activity (9). One of their members are natural killer (NK) cells. They recognize and kill virus-infected or mutated cells by releasing enzymes that e.g. perforate the target's membrane. Besides, they express surface molecules that can trigger programmed cell death of infected or mutated cells (10).
A small but functionally significant innate immune cell population consists of DCs. Immature DCs reside in tissues and take up pathogens or other foreign material by constantly sampling their surrounding with finger-like structures called dendrites. Upon activation through ligation of their PRRs immature DCs start to mature and migrate via the lymphatic system to local secondary lymphoid organs. The maturation changes their phenotype from a phagocytic cell to an Ag-presenting cell (APC) (11, 12). Ags are molecules that can stimulate lymphocytes by binding to T or B cell receptors (TCR or BCR). The TCR is restricted to recognize antigenic peptides only when bound to appropriate major histocompatibility complex (MHC) molecules. Maturing DCs upregulate MHC class I and II molecules as well as the expression of costimulatory surface molecules such as CD80/86 (cluster of differentiation 80/86). Higher surface MHC levels correlate with increased levels of Ag presentation. Additionally, CD80/86 are ligands for the costimulatory receptor CD28 on T cells, thus allowing efficient Ag-mediated T cell activation (13). Hence, activated DCs turn to the most powerful activators of the adaptive immune system. The different roles of activated adaptive immune cells will be described below.

2.2 Adaptive immune system

T and B lymphocytes form the adaptive immune system. Their response to threats that have not been eliminated by the innate immune system is delayed (14). Generally, adaptive immune responses are not induced at the site of infection but rather in secondary lymphoid organs (SLO) to which lymphocytes and APCs migrate (15). In SLOs, lymphocyte activation is mediated through specific Ag recognition by the appropriate TCR or BCR. Activated lymphocytes mediate highly specific responses and can memorize the Ag leading to faster and stronger reactivation upon reencounter (16). The ability of the adaptive immune system to provide a very specific protection against a broad range of pathogens requires an exceptionally diverse recognition capacity. Diversity is generated in early stages of development by random rearrangement of genes encoding for the BCR and TCR. To generate cells with receptors that recognize only foreign proteins, T and B cells have to undergo several selection processes.

2.2.1 B cell development and function

B cell development starts in the bone marrow and continues in peripheral lymphoid tissues such as the spleen. In the bone marrow, B cell development progresses through several

stages involving random gene rearrangements at the locus encoding the BCR, which result in the surface expression of a BCR capable of binding Ag. To avoid generation of B cells that target the own body, only those cells that did not encounter Ag during their maturation in the bone marrow can be activated after entry into the periphery (17). If B cells recognize an Ag in SLOs, they internalize and process it to present antigenic peptides via MHC-II molecules. $CD4^+$ T cells recognizing such peptide-MHC-II complexes, get activated and provide help to further promote B cell activation. Then, B cells start to proliferate and develop into antibody-(Ab)-secreting plasma cells or long-lived memory B cells. Upon reencounter with the Ag, memory B cells can immediately mount a secondary response that provides an instant and high level of protection and thus the basis for vaccinations. For the development into such effective defense cells, activated B cells need to undergo several maturation processes, including somatic hypermutation. As a result of this process, mutations are introduced into the BCR gene and those B cells expressing a functionally improved BCR are positively selected. This affinity maturation ensures that highly effective BCRs are produced and released as cell-free Abs. Additionally, B cells undergo Ab class switching to produce Abs with different effector functions. For example, Abs can neutralize toxins or label infected cells for killing. Ab class switch is triggered by signals from T cells involving cytokine receptor and CD40 engagement on B cells (18). Other functions of T cells and their generation are described below.

2.2.2 T cell development and function

2.2.2.1 T cell development in the thymus

Similar to B cells, T cell development also starts in the bone marrow. However, T cell progenitors leave the bone marrow and migrate into the thymus where they develop into thymocytes. During their development, thymocytes migrate through different stromal microenvironments called the thymic cortex and medulla where they receive unique signals that allow their maturation (Fig. 2.1). Early committed thymocytes lack expression of TCR and its coreceptors CD4 and CD8, and are therefore termed CD4/8 double-negative (DN) thymocytes. During the late DN stage, the TCR gene segments encoding the TCR-α and -β chain are recombined and an αβ-TCR first becomes expressed on the cell. This leads to proliferation and differentiation into the CD4 and CD8 double-positive (DP) stage. Then, thymocytes strongly interact with self-peptides presented by MHC-I and MHC-II molecules on cortical epithelial cells (cTECs). The interaction of the TCR with these self-peptide-MHC complexes determines the fate of the DP thymocytes. Too weak TCR signals result in death by neglect. Appropriate, intermediate signals lead to survival called positive selection. This process is accompanied by CD4 or CD8 lineage commitment. Then, CD4 and CD8 single-positive (SP) thymocytes rapidly relocate to the medulla, where they scan DCs and medullary TECs (mTECs) for self-peptide-MHC ligands. Too strong TCR signaling promotes

cell death. This so-called negative selection ensures the elimination of potentially auto-destructive T cells. Instead, the host provides just enough TCR-mediated stimulation by self-peptide MHC-complexes to keep T cells alive (19). Ultimately, only about 5% of DP thymocytes survive selection and finally enter SLO as mature $CD4^+$ T helper and $CD8^+$ T killer cells (20, 21).

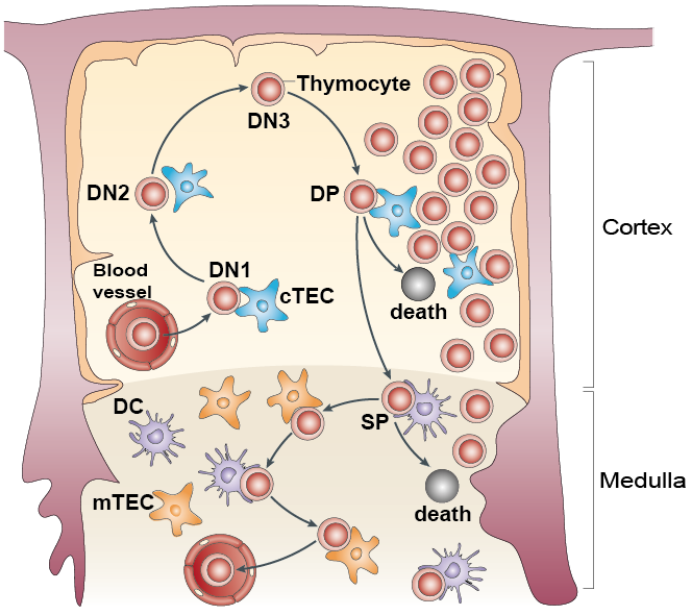

Figure 2.1: T cell development is directed by interactions with stromal cells.
T cell development proceeds along a well-ordered passage through different thymic stromal microenvironments. T cell progenitors enter the thymus through blood vessels near the junction of cortex and medulla. Early committed T cells, termed double-negative DN thymocytes can be further subdivided into four stages (DN1-4). At the DN3 stage, a TCR as well as CD4 and CD8 first become expressed on the cell surface. In the double-positive (DP) stage, the T cells scan self-peptide-MHC ligands presented by cortical epithelial cells (cTECs). Too weak TCR signaling results in death by neglect, whereas intermediate signals lead to survival and CD4 or CD8 lineage commitment. Then, CD4 or CD8 single positive (SP) thymocytes migrate to the medulla, where they bind to self-peptide-MHC ligands presented by DCs and medullary TECs (mTECs). Too strong TCR signaling promotes acute cell death. This negative selection ensures that T cells do not target the host and is known as central tolerance. (Adapted from Klein et al., 2009)

2.2.2.2 T cell activation

Once mature, naive $CD4^+$ and $CD8^+$ T cells circulate through the blood stream and lymphoid tissues until they are activated by encounter of their specific Ag presented by mature APCs in SLOs. The type of T cell response is dependent on the pathogen itself, the presentation of its Ags and the resulting inflammatory environment.

Extracellular pathogens are ingested by professional APCs and digested by lysosomal enzymes. The resulting peptide fragments are presented to Ag-specific $CD4^+$ T cells via MHC-II. Upon primary Ag contact, naive $CD4^+$ T cells start to proliferate and differentiate into effector T cells that secrete multiple cytokines which help e.g. to activate the antimicrobial

properties of macrophages, provide support for $CD8^+$ T cell responses and induce Ab production by B cells (1, 22).

APCs process cytosolic pathogens as well as altered endogenous or viral proteins by the enzyme complex called proteasome and present resulting peptides via MHC-I molecules. Ags presented on MHC-I molecules activate naive Ag-specific $CD8^+$ T cells. These cells proliferate and differentiate into cytotoxic T cells (CTL) that kill infected or mutated target cells and secrete pro-inflammatory cytokines. Activated T cells expand massively and acquire effector functions. The peak of the response is reached after 7-8 days resulting in maximal pathogen clearance. However, most effector cells die and only few cells survive to form a small but stable pool of memory T cells (23). Upon reencounter with their cognate Ag, memory $CD8^+$ T cells exert effector functions within minutes (24). Hence, the generation of memory T cells ensures efficient and long-lasting protection against recurrent infections (Fig. 2.2).

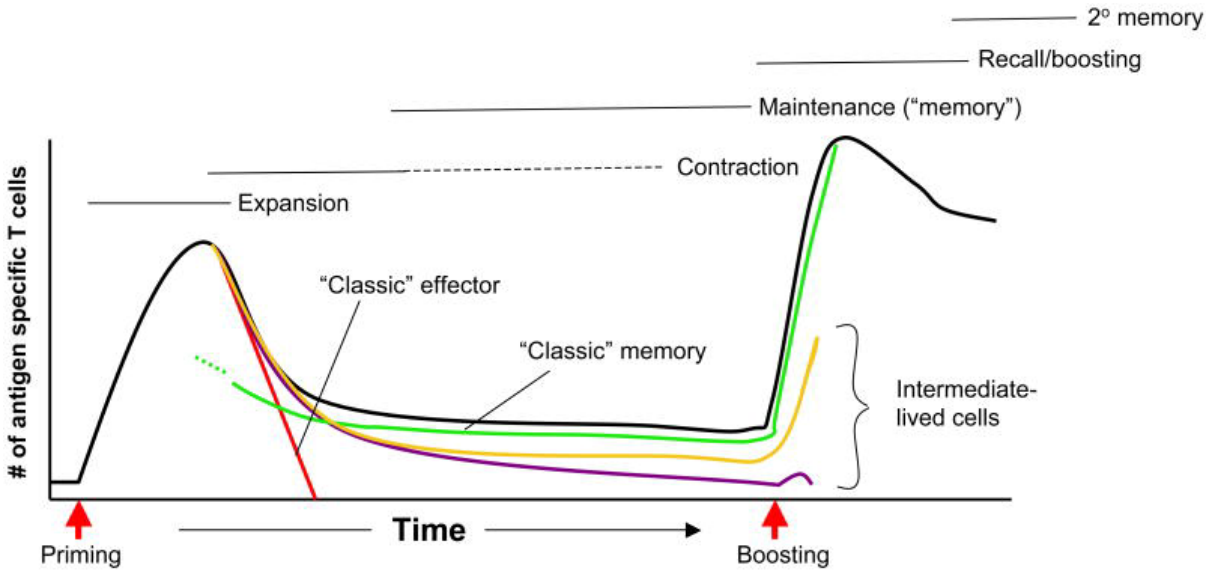

Figure 2.2: Ag-specific T cell response.
The scheme of an acute immune response shows numbers of Ag-specific T cells (black line) at different stages after primary (Priming) and secondary Ag contact (Boosting). During the primary response, the fate of typical effector (red line) and memory (green line) T cells is shown. In addition, populations of intermediate longevity are depicted as purple and yellow lines. (Adapted from Jameson and Masopust, 2009)

Yet, it is not completely clear how cell fate is determined and why some memory T cells live shorter and are less protective than others (25) (Fig. 2.2). Since this work is focused on the activation, expansion and anti-tumor function of $CD8^+$ T cells under different experimental conditions, the factors influencing these processes will be discussed in more detail in the following section.

The mere presentation of Ag, often referred to as "Signal 1", is not sufficient to fully prime T cells and induce effector and memory cells. Costimulation (so-called "Signal 2") needs to be provided simultaneously. This is delivered by ligation of T cell expressed CD28 to CD80

or CD86 expressed on the surface of APCs. Additionally, inflammatory cytokines including interleukin-12 (IL-12) and interferons (IFNs) promote $CD8^+$ T cell expansion and act as "Signal 3" (Fig. 2.3A vs. 2.3B). These cytokines are released by innate immune cells in response to the pathogen (26–28). Interestingly, absence of IFN receptors on TCR-transgenic T cells does not impede proliferation but survival of effector T cells (29).

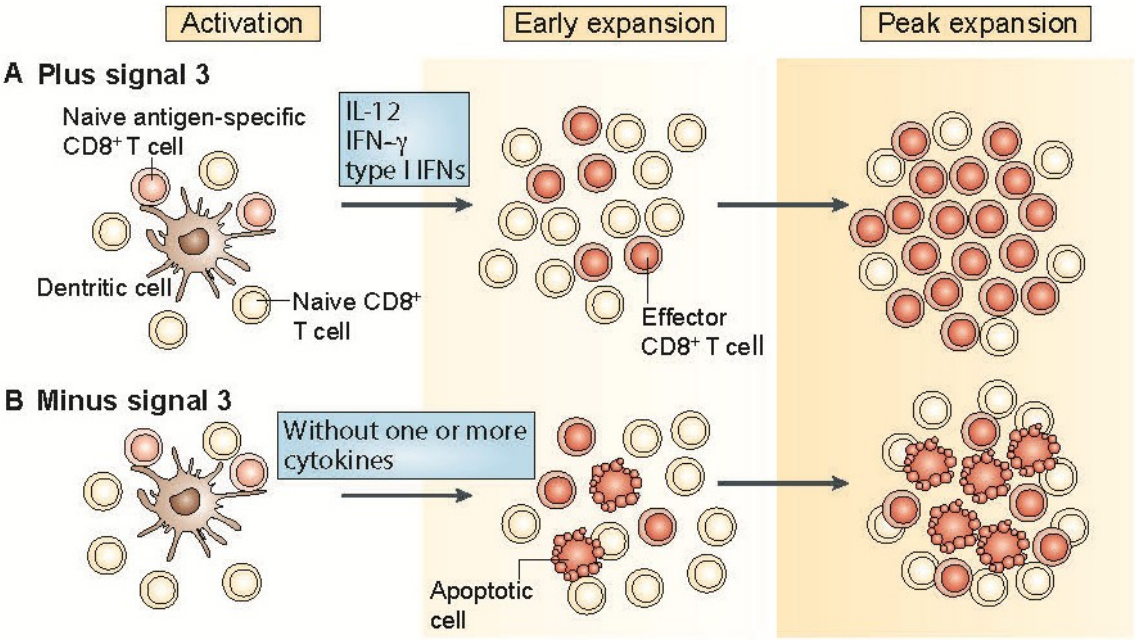

Figure 2.3: Signal 3 is required for efficient generation of $CD8^+$ effector T cells. Maximal expansion, function, and survival of effector $CD8^+$ T cells depend on the cytokine milieu during the early stages of the $CD8^+$ T cell response. Several cytokines (IL-12, type I IFNs, and IFN-γ) can serve as Signal 3 *in vitro*. During an infection, the type of Signal 3 may mainly depend on the type of pathogen. (Adapted from Harty and Badovinac, 2008)

$CD4^+$ T cells also help to generate highly functional $CD8^+$ effector T cells. They condition DCs via CD40 ligand-mediated signals to become more effective stimulators of $CD8^+$ T cells (30–32). Fully activated $CD8^+$ T cells start to proliferate and secrete cytokines like IL-2, IFN-γ as well as apoptosis-inducing tumor-necrosis factor (TNF). Importantly, they also release cytolytic mediators such as perforin and granzymes (Fig. 2.4). Most effector T cells downregulate the expression of the lymph node homing molecule L-Selectin (CD62L) and the α-chain of the cytokine receptor for IL-7 (IL-7Rα, CD127). The majority of effector T cells will die by apoptosis in the contraction phase, but some will give rise to long-lived, CD127-expressing memory T cells (Fig. 2.4).

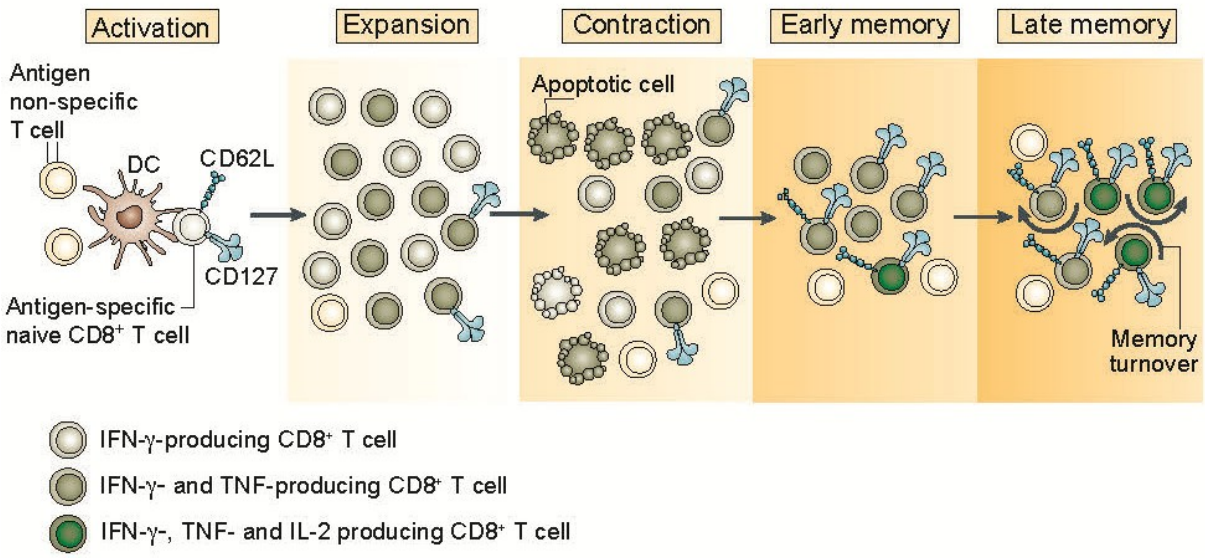

Figure 2.4: CD8$^+$ T cell response to infection or vaccination.
Upon activation of Ag-specific CD8$^+$ T cells by antigenic peptides and co-stimulatory molecules presented by mature DCs, T cells proliferate and differentiate into effector T cells releasing cytokines. Most effector T cells loose expression of CD127 and CD62L and finally die. Many of the surviving memory precursor T cells express CD127. Upregulation of CD62L expression occurs in addition to other phenotypical changes that result in formation of memory T cells. A stable pool of memory T cells is maintained by a dynamic process comprised of slow proliferation (memory turnover) and cell death. (Adapted from Harty and Badovinac, 2008)

Although the molecular mechanisms controlling contraction of Ag-specific CD8$^+$ T cells are incompletely understood, it was shown that the onset and kinetics of CD8$^+$ T cell contraction after *Listeria monocytogenes* and lymphocytic choriomeningitis virus infections are independent of dose and duration of the infection and amount of Ag displayed (33). Therefore it is assumed that contraction is “programmed” by early signals after infection independently of Ag clearance (28, 33). In proof-of-principle experiments using T cells with a mutated TCR-signaling domain, it was shown that qualitatively distinct TCR signals can separate effector from memory fates (34). The prevailing view that strong TCR ligation is required for inducing cytotoxic T cell responses and CD8$^+$ T cell memory generation was challenged in 2009. It was reported that even very weak TCR-ligand interactions are sufficient to activate naive T cells, induce proliferation and promote formation of effector as well as memory cells in response to microbial infection. The strength of the TCR-ligand interaction determined only the size of the memory pool. Interestingly, these findings correlated with the fact that strongly stimulated T cells contracted and exited lymphoid organs later than weakly stimulated cells (35). However, the decisive pathways and environmental conditions required for efficient memory T cell development still remain largely elusive.

2.2.2.3 Formation of memory T cell subsets

After contraction of the effector T cell population, a small pool of surviving memory $CD8^+$ T cells containing diverse and convertible populations is maintained (Fig. 2.4). Two major subsets of memory cells were defined by the expression CD62L and chemokine (C-C motif) receptor 7 (CCR7). Effector-memory T cells (T_{EM}) express low amounts of both molecules while central-memory T cells (T_{CM}) express high amounts of CD62L and CCR7 (36). High expression of both molecules guides T_{CM} into lymphoid tissues where they can self-renew. This process is termed homeostatic turnover (Fig 2.4). Compared to T_{CM}, T_{EM} rather reside in peripheral non-lymphoid tissues (37–40). How these two memory subsets develop and whether they are interconvertible has been actively debated in the literature for many years. Several models have been proposed to explain the divergent developmental fates of Ag-experienced T cells (41). According to the “linear differentiation model”, most effector cells mature into terminally differentiated effector cells that finally die (39). However, some effector cells differentiate into T_{EM}, which then convert into T_{CM}, the population with self-renewal capacity (Fig. 2.5A). The “branching differentiation model” suggests that one activated T cell can give rise to progeny with distinct differentiation fates (Fig. 2.5B). Generation of heterogenic daughter cells might be achieved through mechanisms such as epigenetic changes or asymmetric cell division. In the latter case, the part of the cell distal to the APC-contact-zone forms a daughter cell that gives rise to T_{CM} while the part of cell including the APC-contact zone forms a daughter cell that gives rise to T_{EM} (42). In the “self-renewing effector model”, activated T cells can develop into effector T cells or T_{CM} that can self-renew (Fig. 2.5C) (43). These cells home to lymphoid tissues and undergo homeostatic turnover, but may also give rise to T_{EM} that migrate to sites of infection and will finally die as terminally differentiated effector T cells. The branching and self-renewing effector models are partially questioned by lineage-tracing experiments demonstrating that memory responses are raised by cells that have already developed a full effector phenotype (44). In this context, it has also been proposed that very strong stimulation leads to terminally differentiated effector cells, which die during the contraction phase (45), whereas T_{CM} preferentially develop from weakly activated T cells, which are e.g. recruited at later stages of the immune response and have superior survival capacities (‘‘latecomers’’) (46). Notably, the huge potential of T cells to adopt various fates was shown in two elegant studies in which a single adoptively transferred naive $CD8^+$ T cells could give rise to effector as well as diverse memory populations (47, 48).

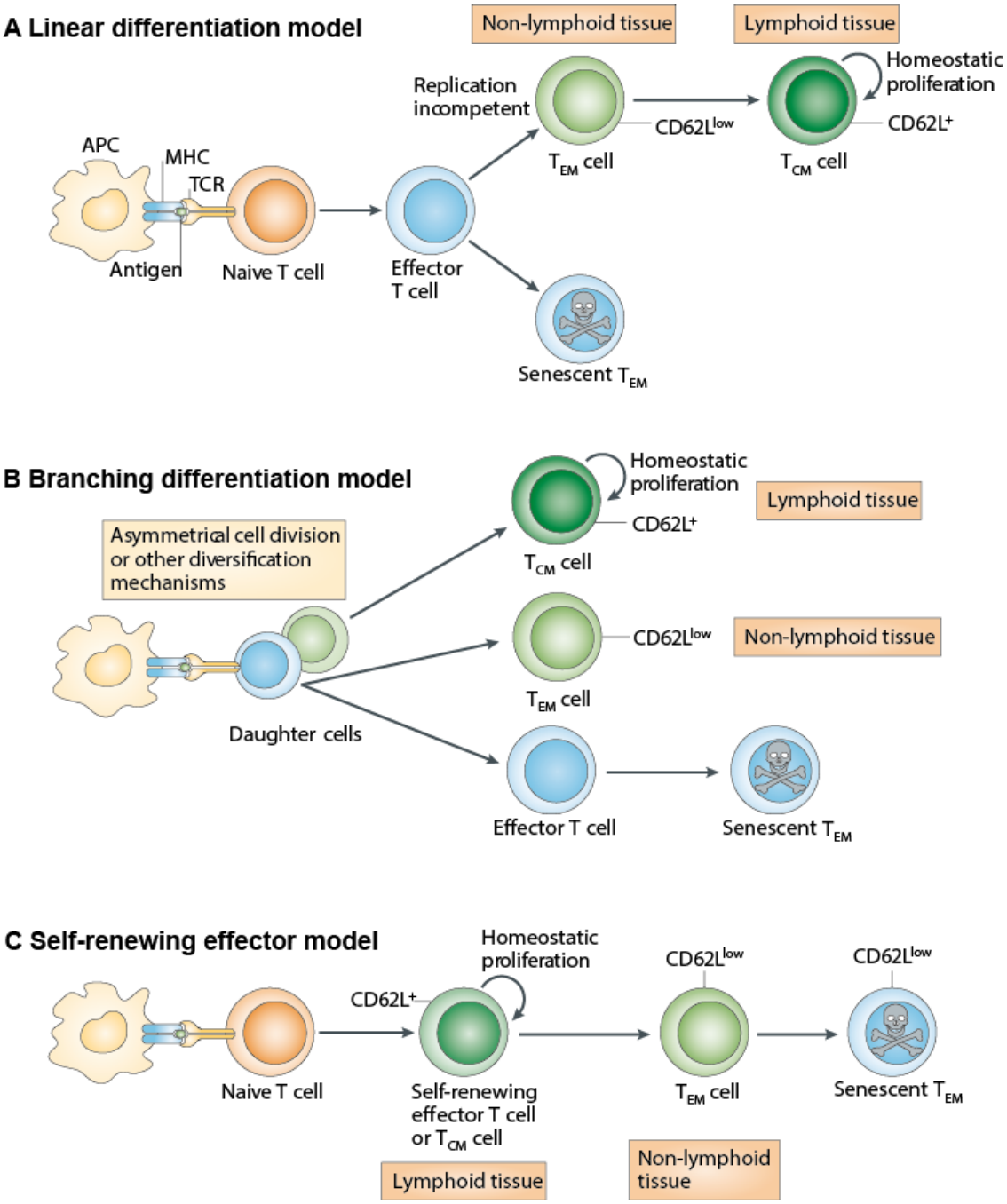

Figure 2.5: Models of memory T cell differentiation.
(A) In the linear differentiation model, efficient activation of naive T cells results in generation of effector T cells, that die by apoptosis soon after pathogen clearance (senescent T_{EM}), or differentiate into T_{EM} that express low levels of CD62L, do not home to lymphoid tissues, and are replication incompetent. Yet, some T_{EM} can give rise to T_{CM} that express CD62L and are long-lived since they undergo homeostatic turnover in lymphoid tissues. (B) In the branched differentiation model it is proposed that one activated T cell can give rise to two daughter cells with different fates. (C) In the self-renewing effector model, it is suggested that a naive T cell can directly develop into a T_{CM} or an effector T cell that can self-renew. (Adapted from Ahmed et al., 2009)

Besides the classical way of generating memory T cells in response to specific Ag contact, another pathogen-independent route exists in hosts with reduced numbers of lymphocytes (lymphopenia). Congenital genetic defects leading to the severe combined immunodeficiency syndrome or interventions like chemo- or radiotherapy can cause lymphopenia (49, 50). When only few or no T cells are present in a host, newly generated or adoptively transferred T cells undergo lymphopenia-induced proliferation (LIP). In this state, T cells divide at a slow rate in response to higher amounts of homeostatic cytokines and more frequent contact with low-affinity, self-Ag presented by APCs (51, 52). Thereby, under LIP, T cells gradually acquire characteristics of memory T cells (53).

2.2.2.4 T cell differentiation and effector function

The protective capacity of naive and memory T cells was assessed in several studies. They consistently showed that T_M respond faster and more effectively at lower doses of Ag (54–56). Whether T_{CM} or T_{EM} provide more protection against infections is still controversially discussed. It was reported that predominant generation of T_{EM} correlated best with protection against *Listeria monocytogenes* (57). However, in another study it was demonstrated that T_{CM} are more efficient in mediating protective immunity against lymphocytic choriomeningitis virus (39). In terms of adoptive T cell therapy, tumor-specific T_{CM} cells showed increased anti-tumor activity compared to T_{EM} cells (58, 59). Therefore, development of therapeutic strategies for the generation of large amounts of tumor-specific T_{CM} are demanded to promote the success of adoptive T cell therapy against cancer. However, it is still unclear how differentiation and expansion of these T cells is regulated. As IL-7R-mediated signaling is involved in critical steps of naive and memory T cell development and homeostasis, a better understanding of this pathway may help to generate better therapeutic T cells (60).

2.3 Regulation of $CD8^+$ T cell homeostasis by IL-7R signaling

2.3.1 Essential role of IL-7 signals for T cell generation and survival

IL-7 was first described as growth factor for B cell progenitors in 1988 (61, 62). It is a highly homologous protein in mice and humans with a predicted size of 15 and 17 kDa, respectively. IL-7 is a non-classical interleukin, since it is mainly produced by non-immune cells such as fibroblasts and epithelial cells (63–66). The essential role of IL-7 signals for T cells was discovered in experiments with IL-7-deficient ($IL\text{-}7^-$) mice, which contain only very few T cells (67). This defect is largely attributed to the lack of IL-7R signaling during very early stages of lymphocyte development such as in common lymphoid progenitors (CLP) and DN thymocytes (Fig. 2.6) (67, 68). However, the transfer of naive T cells from WT to $IL\text{-}7^-$ mice does not compensate for the developmental block suggesting that naive T cells are not able to survive in an $IL\text{-}7^-$ environment (69, 70). Recently, these findings were supported by elegant experiments using $IL\text{-}7^-$ mice with transgenic, thymus-specific *il-7* expression. T cells

emigrating form the *il-7* expressing thymus to the IL-7$^-$ periphery did not survive, showing that IL-7 is also needed for survival of mature T cells (71). By contrast, high levels of IL-7, as in IL-7-transgenic (-tg) mice or after IL-7 injections, dramatically raise the numbers of naive and memory T cells (72–76). Moreover, the overabundance of IL-7 in IL-7-tg mice leads to autoimmunity (77, 78). These results indicate that IL-7 availability must be tightly controlled for regulating immune responses. Furthermore, identifying regulators of IL-7 production but also of IL-7R expression is required in order to exploit its functions for immunotherapy.

2.3.2 Regulation of IL-7R expression during T cell ontogeny

The IL-7R is composed of the IL-7Rα-chain and the IL-2Rγ-chain, also known as common cytokine receptor γ-chain (γ_c-chain) (79). While the γ_c-chain is assumed to be expressed at constant levels by T cells (80, 81), the IL-7Rα is subjected to strong regulation throughout the T cell's ontogeny (82). It is first induced on CLPs in the bone marrow (Fig. 2.6). Both, hematopoietic stem cells (HSCs) and CLP can probably generate early T cell lineage progenitors lacking IL-7Rα expression. In the following differentiation steps, the IL-7Rα is expressed on DN thymocytes promoting TCR gene rearrangement, then downregulated on DP thymocytes probably due to TCR signaling and finally reexpressed by SP thymocytes, which migrate to the periphery and form the naive T cell pool (75). Naive, mature T cells need signals from self-peptide-MHC complexes and IL-7 in order to survive (51, 83–85). Upon activation, most mature Ag-specific T cells lose the expression of IL-7Rα. Only a small population of effector T cells retains IL-7Rα on the surface, which marks, but not directs them to become memory T cells (86, 87). Memory T cell survival is dependent on less specific peptide-MHC interactions than naive T cells (88). While their basic turnover rate is rather dependent on IL-15R signals, IL-7R signaling promotes their survival (70, 89, 90). Increased levels of IL-7 together with more frequent contact to low-affinity self-Ag, as found under lymphopenic conditions, can even drive the proliferation of naive T cells that finally acquire a memory-like phenotype with similar characteristics as conventional T_M (52, 70, 91).

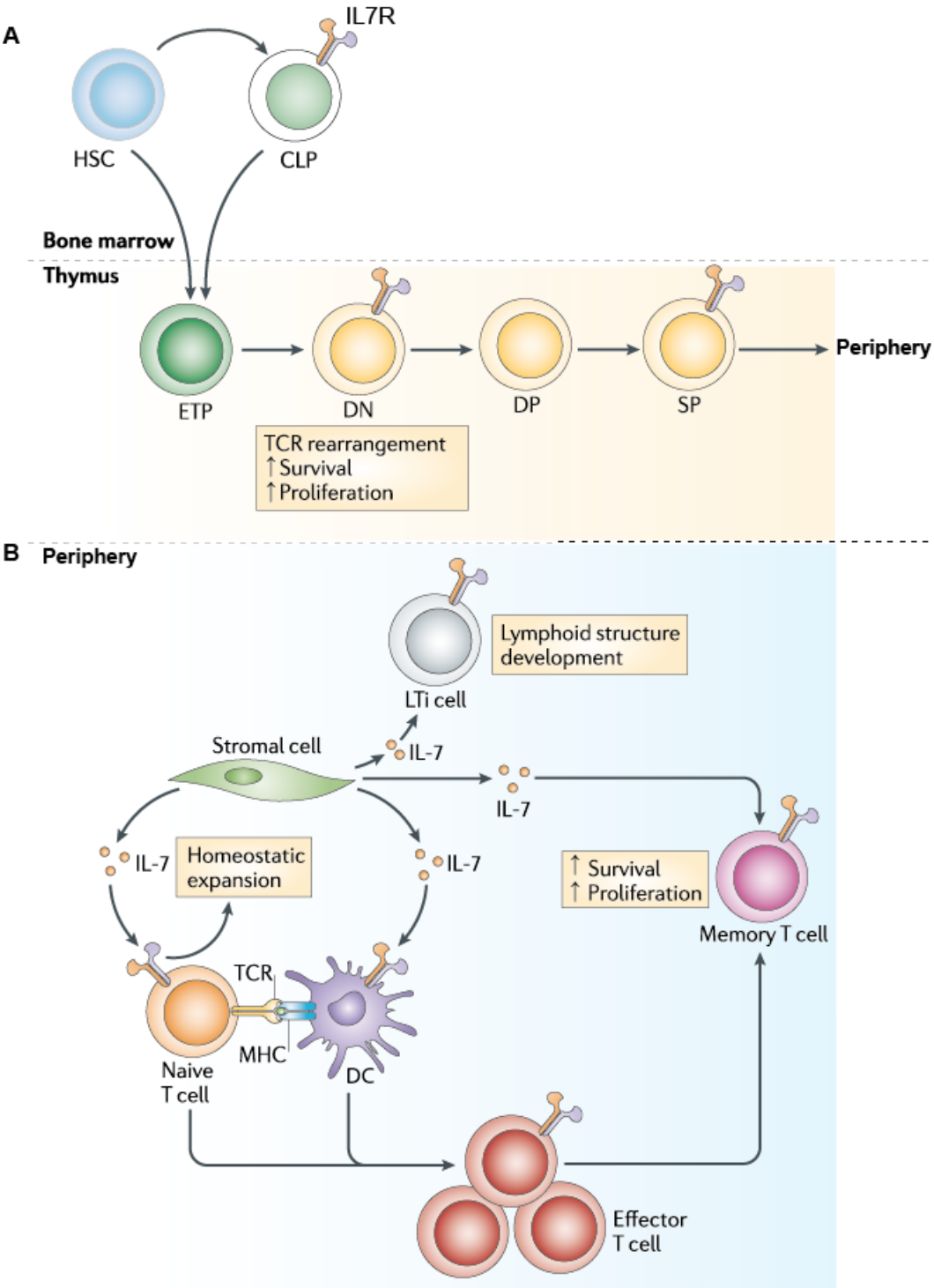

Figure 2.6: Regulation of IL-7R expression during T cell development and maturation. (A) Developing T cells modulate the expression of IL-7R at various stages. This has consequences on TCR rearrangement, T cell survival and proliferation, as IL-7 signaling promotes all of these events. (B) In the periphery, mature naive and memory T cells express the IL-7R, but it is lost on most cells upon activation and differentiation to effector T cells. Besides, some innate lymphoid cells (ILCs) and distinct DC subsets also express IL-7Rα. IL-7 is produced by stromal cells including fibroblasts, endothelial cells and epithelial cells. (Adapted from Mackall et al., 2011b)

2.3.3 IL-7R signaling pathway in T cells

On the molecular level, the IL-7R-associated signaling pathway involves two main signaling cascades, the PI3K (phosphoinositide 3-kinase) and the JAK-STAT (Janus kinase and signal transducer and activator of transcription) signaling cascade (Fig. 2.7A) (83, 92). The JAK-STAT signaling pathway features JAK1, JAK3 and predominantly STAT5. IL-7R-mediated signaling upregulates the expression of the antiapoptotic molecule B cell lymphoma-2 (Bcl-2) and leads to reduced expression of CD62L as well as cyclin-dependent kinase inhibitor 1B (P27KIP1) via the inactivation of forkhead box O1 (FOXO1). Accordingly, IL-7R-mediated signaling regulates survival, migration and proliferation of T cells, respectively (93–95). In addition, it affects metabolism by increasing glucose uptake and by activating the energy-sensitive kinase mammalian target of rapamycin (mTOR) which can induce proliferation and functional maturation during lymphopenia (96, 97).

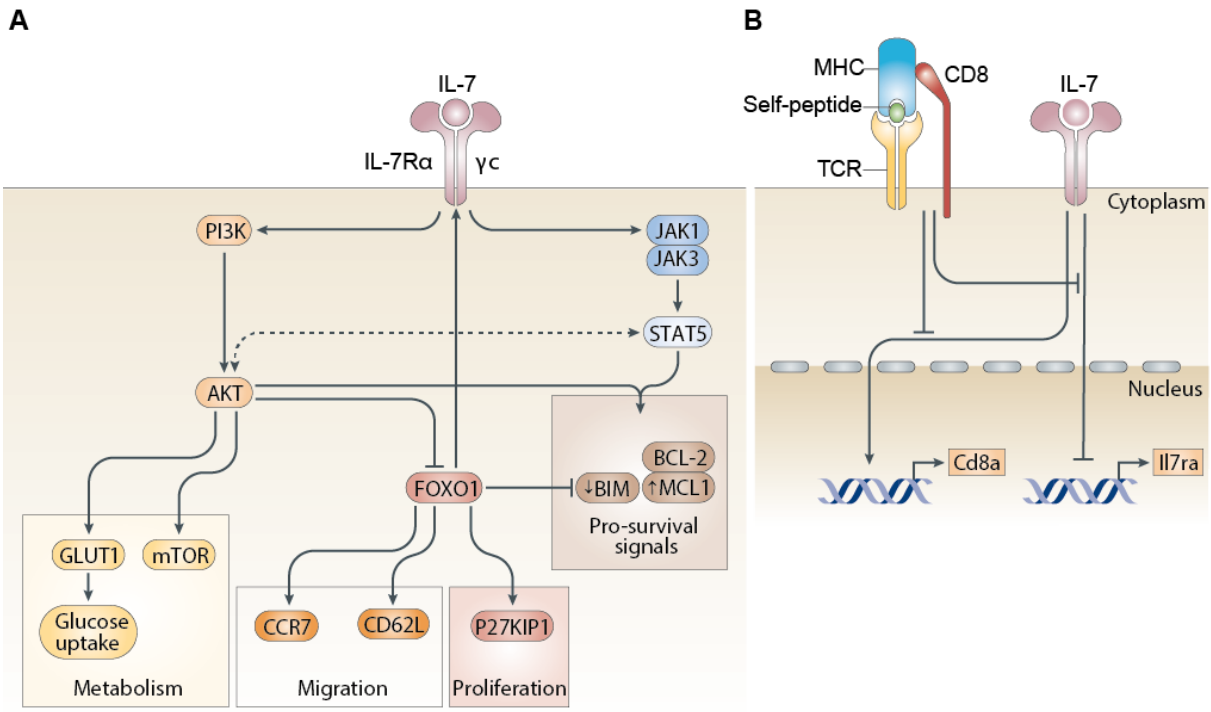

Figure 2.7: IL-7R signaling and its interplay with the TCR/CD8 complex.
(A) The main IL-7R-signaling pathways through JAK1/3 and STAT5 or alternatively through PI3K and protein kinase B (PKB or AKT) are depicted. These two signaling pathways intersect, but the exact mechanism for this is unclear (dashed line). IL-7R-mediated signaling can induce downregulation of its own receptor through the inactivation of FOXO1. Main downstream target proteins of IL-7R ligation are involved in metabolism such as glucose transporter 1 (GLUT1) and mTOR, but also in migration such as CCR7 and CD62L. Further downstream targets regulate proliferation such as P27KIP1 and Bcl-2, Bcl-2-interacting mediator of cell death (BIM) and myeloid cell leukemia sequence 1 (MCL1). (B) IL-7R signaling causes upregulation of CD8α, which can enhance TCR/CD8 signaling. This may in turn block some IL-7R-mediated signals in a negative feedback loop. (Adapted from Takada and Jameson, 2009)

Moreover, IL-7R signaling directly augments TCR-mediated signaling in at least two ways.

First, it causes reduced expression of the TCR signaling repressor Casitas B-lineage lymphoma B (Cbl-b) (98) and second, it leads to upregulation of the TCR-co-receptor CD8α (99). Together, this may increase TCR sensitivity, leading to stronger T cell responses against a threat or even self-Ag, thus inducing autoimmunity. In order to avoid excessive T cell activation, enhanced TCR signaling can in turn inhibit some IL-7R-mediated signals for maintaining TCR signaling thresholds. These include repression of CD8α and IL-7Rα upregulation (Fig. 2.7B). In another negative feedback loop, signaling through the IL-7R itself leads to IL-7Rα downmodulation directly by internalization and indirectly by transcriptional repression through the inactivation of FOXO1. This feedback may help to maximize the number of T cells that can survive with limiting amounts of IL-7 (81, 100, 101). However, recently is was shown that IL-7 signaling must be intermittent, not continuous, to promote $CD8^+$ T cell survival instead of cell death (102). Using IL-7R-tg T cells constantly expressing the IL-7Rα, it was observed that continuous IL-7 supply induced naive $CD8^+$ T cells to proliferate, acquire memory markers and produce IFN-γ, which finally lead to IFN-γ-triggered cell death. This indicates that downregulation of the IL-7R is not an altruistic feature of T cells to maximize overall T cell numbers, but rather helps T cells to adjust TCR stimulation thresholds. Also other cytokines have been shown to regulate IL-7Rα expression at least *in vitro.* IL-4, IL-6 and IL-15 decrease IL-7Rα expression on T cells, whereas TNF-α increases it (81). The mechanisms and *in vivo* relevance of these findings remain largely unclear, but may play crucial roles during T cell development and activation, where strong regulation of IL-7Rα expression can be observed (103). In summary, IL-7R-mediated signaling crucially regulates T cell survival and activation. Consequently therapeutic manipulation of this pathway may help to treat immunologic disorders.

2.4 Role of IL-7R signaling in non-T cells

Besides T cells, B-cell progenitors, ILCs, and DC subsets express the IL-7R (Fig. 2.6). While migratory DCs isolated from lymph nodes (LNs) express the IL-7R, it is absent from conventional and plasmacytoid DCs in spleen and LNs. Surprisingly, the frequency of migratory DCs remains unaffected by high amounts of IL-7 as found in IL-7tg mice. In contrast, the frequency of conventional and plasmacytoid DCs increased in those mice (104). With the help of mixed bone marrow (BM) transfer experiments, it has been shown that DC generation from $IL\text{-}7R^-$ BM is less efficient than from $IL\text{-}7R^+$ BM. DCs are generated from common lymphoid and myeloid progenitors. Since reduced numbers of CLPs are found in $IL\text{-}7^-$ mice, the authors concluded that lymphoid DC generation is affected by the lack of IL-7 early in development. The number of DCs is not only important for T cell activation but also for controlling T cell responsiveness to Ag (105). Hence, it remains to be determined whether exogenous IL-7 treatment may support T cell therapy indirectly via effects on DC numbers. IL-7 was also shown to act as chemoattractant factor on $IL\text{-}7R^+$ monocytes isolated from

patients with rheumatoid arthritis (106). However myeloid cell numbers are not affected in IL-7R$^-$ mice and lineage tracing experiments could only identify few granulocytes that expressed IL-7R during their ontogeny (104, 107). Hence, the role of IL-7R signaling in myeloid cells remains elusive. Another hematopoietic population expressing the IL-7R are lymphoid tissue inducer (LTi) cells. They initiate development of lymphoid tissues by instructing mesenchymal cells (108, 109). In the absence of IL-7R signaling, the numbers of LTi cells and their expression of lymphotoxin are reduced. This correlates with the lack of lymphoid structures called Peyer's patches in the intestine of IL-7R$^-$ mice (110, 111). Along this line, the majority of LNs are affected but present in IL-7R$^-$ animals (112). Concordantly, in mice overexpressing IL-7, the survival of LTi cells is prolonged and those mice have increased numbers of Peyer's patches and multiple ectopic LNs (113). As LTi cells are needed for SLO repair after infection with LN stroma-targeting pathogens, LTi cells can also exert immunoregulatory properties in adult hosts (114). LTi cells belong to the heterogeneous group of ILCs. Other IL-7R$^+$ members of this family can be found e.g. in the intestine, where they regulate the epithelial barrier function, thereby reducing microbe entry into the host and inflammatory responses (115–117). Since the inflammatory state can alter T cell responses, it is conceivable that IL-7 therapy modulates T cell responses indirectly via IL-7R$^+$ ILCs. Recent studies provide evidence that the IL-7R is also expressed on lymphoid endothelial cells (118). This may affect Ag-transport to LNs and hence initiation of immune responses. Notably, IL-7R expression has been identified on carcinoma samples from breast and lung tumors (119). Consequently, in case of cancer patients, the therapeutic benefit of IL-7 administration needs to be determined individually in order to exclude potential pro-survival effects on these tumor cells.

2.5 Therapeutic manipulation of IL-7R signaling

Recently, polymorphisms in the IL-7R gene have been identified as risk factor for a number of diseases that involve autoimmunity or excessive inflammatory responses including multiple sclerosis, type 1 diabetes, rheumatoid arthritis and inflammatory bowel disease (120). In mouse models, transgenic overexpression of *il-7* or exogenous IL-7 administration were shown to induce autoimmune diseases like dermatitis and colitis or aggravate arthritis and induce bone loss, respectively (121–123). Attempts to inhibit IL-7R signaling with Abs led to reduced progression of rheumatoid arthritis in mice (106) and could even reverse the autoimmune phenotype in diabetes-prone mice (124, 125). The therapeutic success of IL-7R blockade was associated with long-term inhibition of T cell function as shown by low IFN-γ production and high expression of the proapoptotic cell surface molecule PD-1 (Programmed Death-1). Besides, it was also suggested that the local reduction of IL-7 production from the liver attenuated systemic T cell responses (126). On the other hand, several preclinical trials studying syndromes of immunodeficiency demonstrated beneficial effects of exogenous IL-7

administration on T cell immunity. In more detail, IL-7 therapy accelerated immune reconstitution after BM transplantation in mice and humans (127, 128), which helps to prevent infections in the immunocompromised hosts. IL-7 therapy also improved survival of mice during sepsis by elevating T cell numbers and function, therefore preventing immunoparalysis (129). Furthermore, preclinical trials showed that IL-7 therapy leads to enhanced T cell responses against viral infections and tumors, hence prolonged survival of the affected hosts. In addition, IL-7 therapy promoted production of cytoprotective IL-22, which counterbalanced organ pathology during chronic viral infection (98, 130–133). These and other findings indicated that IL-7 administration can be applied in a multitude of therapeutic settings and paved the way to first phase-I clinical trials. Evaluation of toxicity and biological activity of recombinant human IL-7 did not reveal any major adverse effects of the 14-days treatment over the observation period of 60 days (134). This was only the first step towards broad clinical use. The optimal schedule for IL-7 therapy needs to be further defined. Since TCR signaling leads to a transient downregulation of IL-7Rα expression, it is assumed that T cells are insensitive to IL-7 during the expansion and effector phase but react to IL-7 in the contraction and memory phase (70). Indeed, IL-7 treatment during the contraction phase of an anti-viral immune response, but not in the effector phase, could increase the number of surviving pathogen-specific $CD8^+$ T cells for at least 2 months after infection (132). In current protocols for adoptive T cell therapy (ATT) of cancer, therapeutic T cells are genetically modified in order equip them with a tumor-specific TCR. Alternatively tumor-specific T cells are identified and expanded to large quantities *in vitro*. In both approaches, T cells are activated and cultivated for prolonged times *in vitro*, which can impair their long-term survival capacities (135). Here, IL-7 may be of use *in vitro* and *in vivo* to improve therapeutic T cell survival.

In light of the vast therapeutic potential of IL-7 administration for reconstitution of immunodeficiency states (caused by e.g. human immunodeficiency virus, radio- or chemotherapy) and enhancement of immune function (e.g. to pathogens or cancer), it is crucial to determine the appropriate conditions where manipulation of the IL-7R signaling improves immunity while minimizing side effects. Here we asked whether, under lymphopenic conditions, IL-7 therapy enhances the success of ATT and whether additional peptide vaccination improves therapeutic outcome. Furthermore, we aimed to determine which other host cell types that control $CD8^+$ T cell responses are responsive to IL-7 therapy. We asked whether IL-7 signaling in host cells affects $CD8^+$ T cell responses under physiologic conditions and after IL-7 therapy. Therefore, we compared the differentiation and function of adoptively transferred $CD8^+$ T cells in IL-7R signaling-competent and -deficient hosts. First evidence indicated that IL-7R signaling in host cells affects *il-7* expression (91).

Therefore, we studied which cells express *il-7* and whether IL-7 therapy can affect their *il-7* production.

3 Results

3.1 Distribution and regulation of *il-7* gene expression

Since the current methods to elucidate *il-7* gene regulation *in vivo* are limiting, a novel IL-7-reporter mouse was generated. It enables the non-invasive quantification of *il-7* gene activity and simultaneous targeting of genes in *il-7*-expressing cells (63). The generation of this mouse was based on the bacterial artificial chromosome (BAC) transgenic technology (136). The full length *il-7* promoter from the BAC RP23-446B12 was used to control the expression of the cDNAs encoding for enhanced green fluorescent protein (eGFP, G), improved Cre recombinase (C), human diphteria toxin receptor (D) and the click beetle green luciferase 99 (L). Hence, the construct was termed IL-7GCDL. In order to achieve comparable translation of the GCDL-cDNAs, they were linked by nucleotide sequences encoding the P2A peptide that dissociate by self-cleavage during translation (137). Two transgenic mouse lines were established, hereafter referred to as IL-7GCDL line A and line B. The levels of endogenous *il-7* mRNA expression correlate with luciferase signals determined by bioluminescence (BL) *in vivo* imaging, which strongly indicates that the transgenic luciferase signal serves as faithful reporter of *il-7* expression (63).

When both reporter mouse lines were compared for the intensity of luciferase expression by *in vivo* imaging, higher total body BL signals were detected from the IL-7GCDL line A compared to line B, but the pattern of the BL signal was similar (Fig. 3.1A left, 3.1B). This suggests that more copies of the IL-7GCDL transgene were incorporated into the genome of line A compared to line B. In line with this, BL imaging of the isolated tissues revealed higher BL signals from most organs of line A compared to line B, but again the pattern of BL expression was comparable in both lines and correlated with *il-7* expression by the respective tissues (Fig. 3.1A right, 3.1C) and (63). As expected, very high IL-7 reporter activity was detected in thymus. Surprisingly, similarly high BL levels were also recorded from the small and large intestine (SI and LI). Remarkably, the BL signal intensity reflects the total amount of IL-7 produced by the respective tissue. This implies that bigger sized tissues with a lower level of IL-7 expression per cell, such as the SI, can yield similar BL signals than small tissues with high levels of IL-7 expression per cell, such as the thymus or colon (Fig. 3.1A right, 3.1C). Hence, BL signals reflect the relative contribution of different tissues to the overall production of IL-7 by the organism. Moreover, strong BL signals were detected in skin and lung. Lymph nodes emitted lower BL signals, than thymus and gastrointestinal tract. Spleen, liver and kidney yielded low BL signals.

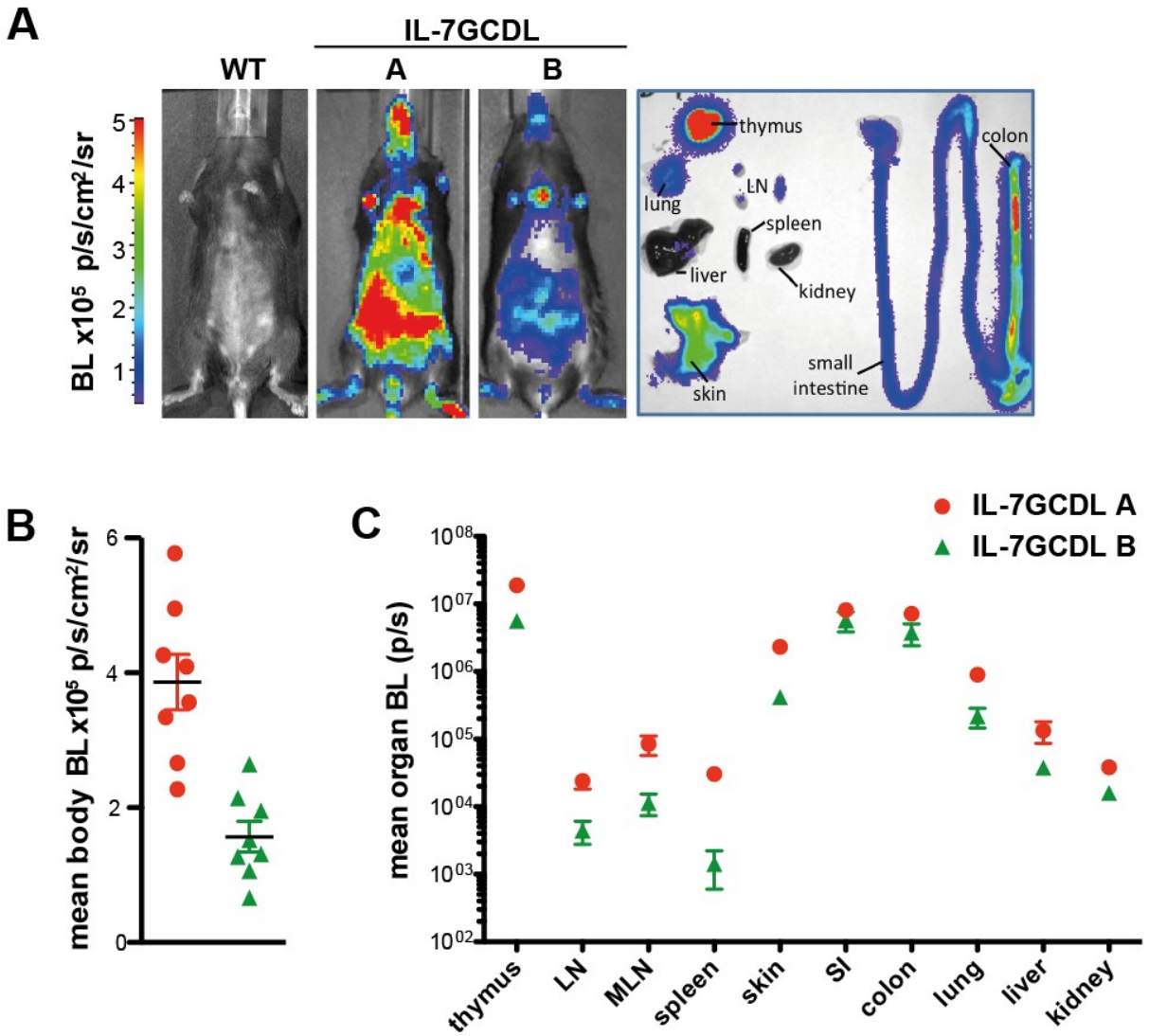

Figure 3.1: IL-7GCDL mouse line A shows higher IL-7 reporter activity than line B. Luciferase expression of the IL-7GCDL mouse serves as reporter for *il-7* gene expression. To determine luciferase transgene expression, B6 mice (WT) and IL-7GCDL mouse lines A and B were injected i.v. with 3 mg luciferin, anesthesized by isoflurane inhalation and (A left, B) mean body bioluminescence (BL) was measured. (A right, C) Tissues from these mice were collected, shortly incubated in PBS containing 1,5 mg/ml luciferin and organ BL was determined. Data are presented as (B) single dot/mouse and (C) mean of organs ± SEM from one representative experiment of 2 (n=4-8 reporter mice/group). Statistical analysis of data from body and organ BL intensities revealed significantly higher BL signals from IL-7GCDL line A than B ($p<0,01$; 1 and 2-way Anova).

The IL-7GCDL-transgene was integrated randomly into the genome and may therefore interfere with normal gene function. In order to test whether transgenesis affected immune cell development, splenic T and B cell numbers were determined for both IL-7GCDL lines. Splenic T and B cell numbers were not altered in IL-7GCDL line A and B compared to wild-type (WT) mice (Fig. 3.2).

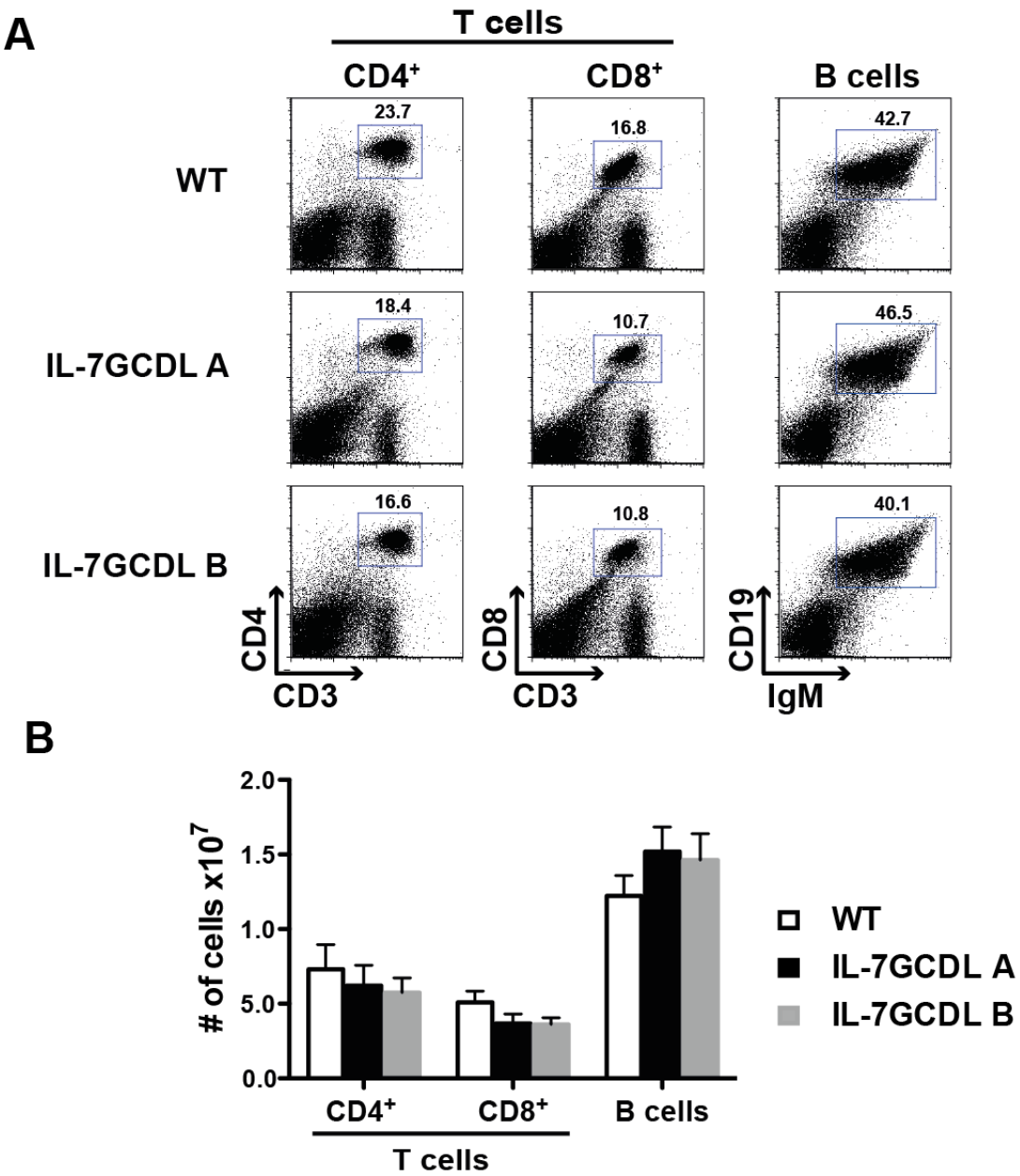

Figure 3.2: Peripheral T and B cell numbers are normal in IL-7GCDL mice.
Single cell suspensions from spleens of WT and both IL-7GCDL founder lines A and B were analyzed by flow cytometry. (A) Representative relative fluorescence intensities of the indicated markers to identify $CD3^+CD4^+$ and $CD3^+CD8^+$ T cells and $CD19^+IgM^+$ B cells are shown. Numbers indicate percentages of double positive cells. (B) Numbers are shown for the respective cell types in spleen as mean values ± SD (n=3 per group).

In addition, thymic T cell development in IL-7GCDL mice did not differ from WT mice as judged by a normal expression pattern of CD4 and CD8 T cell co-receptors (Fig. 3.3A, C). Moreover B and myeloid cell numbers were normal in the BM of IL-7GCDL compared to WT mice (Fig. 3.3B, D).

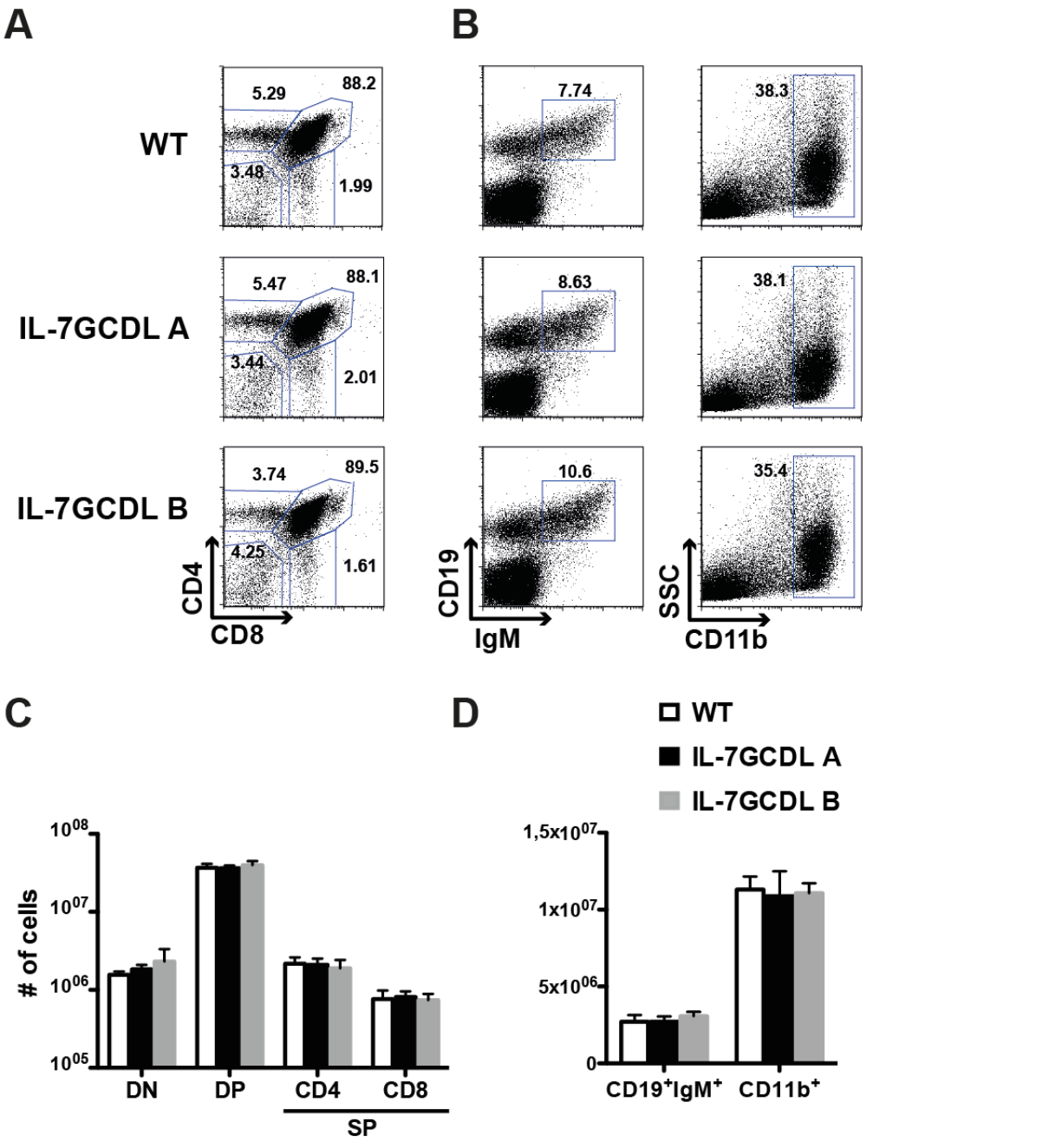

Figure 3.3: Thymocyte, B and myeloid cell development is normal in IL-7GCDL mice. Single cell suspensions from (A) thymi and (B) bone marrow of WT and both IL-7GCDL founder lines A and B were analyzed by flow cytometry. (A-B) Relative fluorescence intensities for the indicated markers are shown. Numbers indicate percentages of the respective populations. Cell numbers of (C) $CD4^{-}CD8^{-}$ double-negative (DN), $CD4^{+}CD8^{+}$ double-positive (DP), $CD4^{+}$ and $CD8^{+}$ single-positive (SP) cells per thymus as well as (D) $CD19^{+}IgM^{+}$ B cells and $CD11b^{+}$ myeloid cells in bone marrow are shown as mean values ± SD (n=3 per group).

Identification of IL-7-producing cells in tissues is impeded by the low level of IL-7 expression and the absence of reliable Abs for detecting it (64). In order to circumvent this issue, we made use of the *il-7* promoter-driven Cre-transgene expression of the IL-7CGDL mouse. We crossed it to the loxP-Tag mouse, which expresses the oncogenic simian virus 40 (SV40) large T antigen (Tag) after Cre-mediated excision of a loxP-site flanked DNA stop cassette (138). In IL-7GCDLxloxP-Tag (Tag^+) mice, Tag is detectable in *il-7*-expressing cells and leads to their expansion, facilitating the detection of these rare cell types.

Tag^+ mice were analyzed at 2-3 months of age. Necropsy revealed strongly enlarged thymi in 95 % of mice (n=20). Additionally, LNs were mildly enlarged and pancreas showed abnormal solid consistency in most Tag^+ animals, whereas other tissues including lung, liver, intestine, skin, heart and kidney showed no gross signs of transformation (data not shown). *In vivo* BL imaging revealed that BL signals were strongly increased in the thorax of Tag^+ mice (Fig. 3.4A) correlating with enlarged thymi (Fig. 3.4A inset). Flow cytometric analysis showed a more than 10-fold higher abundance of stroma cells ($CD45^-$) in thymi of Tag^+ mice, including epithelial cells ($CD45^-EpCam^+$) (Fig. 3.4B).

Tissue sections revealed the colocalization of Tag protein and EpCam in certain areas of thymi from Tag^+ mice. This demonstrates the expression of *il-7* by thymic epithelial cells (TECs, Fig. 3.4C left). Interestingly, Tag^+Epcam^+ cells formed ring-like structures, which is in line with the transforming potential of the oncogene. Notably, not all $Epcam^+$ cells expressed SV40 Tag, indicating that the *il-7* promoter is not equally active in all TECs. On the other hand, many Tag^+ cells did not express Epcam, indicating that non-epithelial cells also express *il-7*. These cells had a different morphology and some of them co-expressed gp38 (38 kDa glycoprotein, also known as podoplanin), a protein that is highly expressed by fibroblasts, subsets of endothelial and some epithelial cells (139, 140) (Fig. 3.4C right).

Tag expression is sufficient to immortalize cells for prolonged *in vitro* culture (141). To establish IL-7 reporter cell lines, tissues from Tag^+ mice were enzymatically digested and the single cell suspension was cultivated. Cell cultures were generated from thymus, LNs, lung, pancreas, tongue and kidney. However, long-term cultures from colon, BM and spleen could not be established. All of the long-term cultivated cells expressed Tag, indicating that they or their progenitors have expressed *il-7*. These cells did not express the leukocyte specific molecule CD45, but contained different amounts of gp38-expressing cells, which indicates that the cultures consisted of stromal cells. It also implies that stromal cells from various immune and non-immune system-related tissues like LN and pancreas can produce IL-7 (Fig. 3.4D).

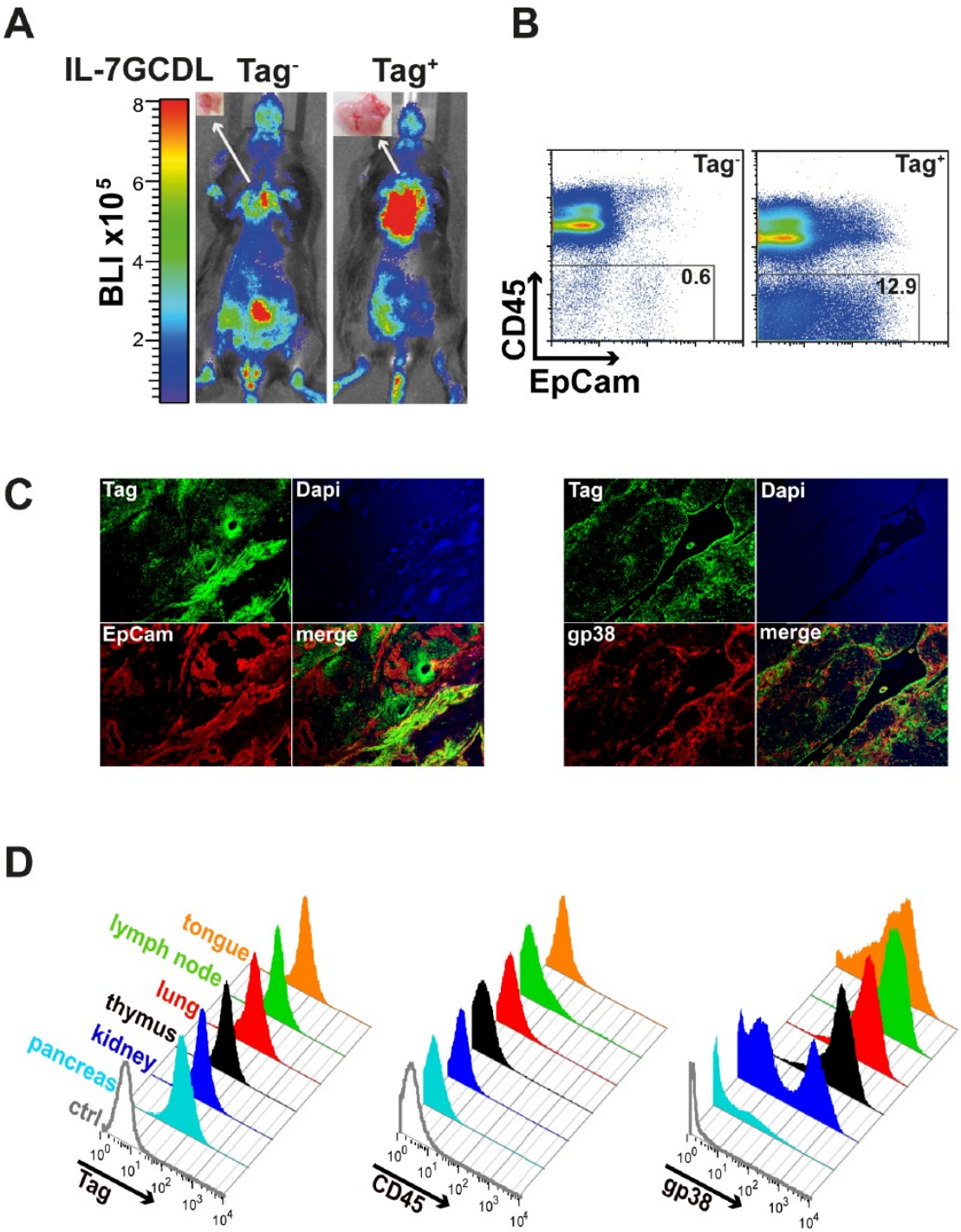

Figure 3.4: IL-7-Cre-mediated ongogene activation leads to expansion of thymic stromal cells.
(A) To assess luciferase transgene expression, IL-7GCDL and IL-7GCDLxloxP-Tag mice were injected i.v. with 3 mg luciferin and bioluminescence (BL) was measured. Representative BL intensities (BLI) for 6-8 week-old Tag^- and Tag^+ IL-7GCDL mice (Tag^+, n=10) are shown in photons/s/cm^2/steridian. Thymi of Tag^+ mice are hyperplastic (inset). (B) Thymi of WT (Tag^-) and Tag^+ mice were enzymatically digested and analyzed by flow cytometry for the relative abundance of $CD45^-$ thymic stroma containing epithelial cells ($CD45^-EpCam^+$). Representative plots of 3 independent experiments are shown. (C) Thymi of Tag^+ mice were analyzed by immunostaining for Tag, EpCam and gp38. Stainings of one out of 3 thymi are shown. (D) Cell cultures were established from the indicated organs of Tag^+ mice and analyzed for the expression of Tag, CD45 and gp38 by flow cytometry. Data from one experiment are shown.

To enable analysis of *il-7* gene regulation in distinct cell types, we aimed to generate epithelial and fibroblast-based IL-7 reporter lines. As our results (Fig. 3.4C) and previously published data indicate *il-7* expression by thymic fibroblasts and TECs (66, 142), thymic stroma from Tag^+ mice was chosen as source of both cell types. To enrich for epithelial cells over fibroblasts, epithelial cell growth factor, transferrin and insulin were added to the culture medium. Cells were cloned using limiting dilution. Flow cytometric analysis showed expression of Tag in all cultured cells (Fig. 3.5A). Furthermore, cells were labeled with Abs against CD44, Vcam-1 (vascular cell adhesion molecule-1, CD106) and gp38 to distinguish cultures of epithelial and fibroblast cell clones (Fig. 3.5A). Cells from several clones expressed high levels of CD44, Vcam-1 and gp38, well-established markers for fibroblasts (143). In contrast, other cultures of cloned cells expressed high levels of CD44, but were nearly devoid of Vcam-1 and gp38, indicative of epithelial cells. Their epithelial origin was confirmed by immunostainings for Keratin 5 and 8 (K5/8), established differentiation markers of TECs (Fig. 3.5B) (144). Thus, *il-7* reporter cell lines of pure thymic epithelial and fibroblastic origin were established from Tag^+ mice. IFN-γ upregulates *il-7* expression in keratinocytes (145). In order to test *il-7* gene regulation in Tag-immortalized thymic epithelial and fibroblast cell lines, cells were treated with recombinant murine IFN-γ (50 ng/ml). Upon IFN-γ stimulation, *il-7* and *luciferase* mRNA expression increased significantly compared to unstimulated cells indicating similar gene regulation for the *il-7* gene and the *luciferase* transgene in epithelial and fibroblastic cells, respectively (Fig. 3.5C-D). It also shows that the Tag^+ immortalized cells still retained their capacity to regulate *il-7* expression. In conclusion, the IL-7GCDL mouse seems to faithfully report *il-7* gene activity via *luciferase* expression and offers a new and simple way to study *il-7* gene regulation in isolated cells *in vitro* or the whole organism *in vivo*.

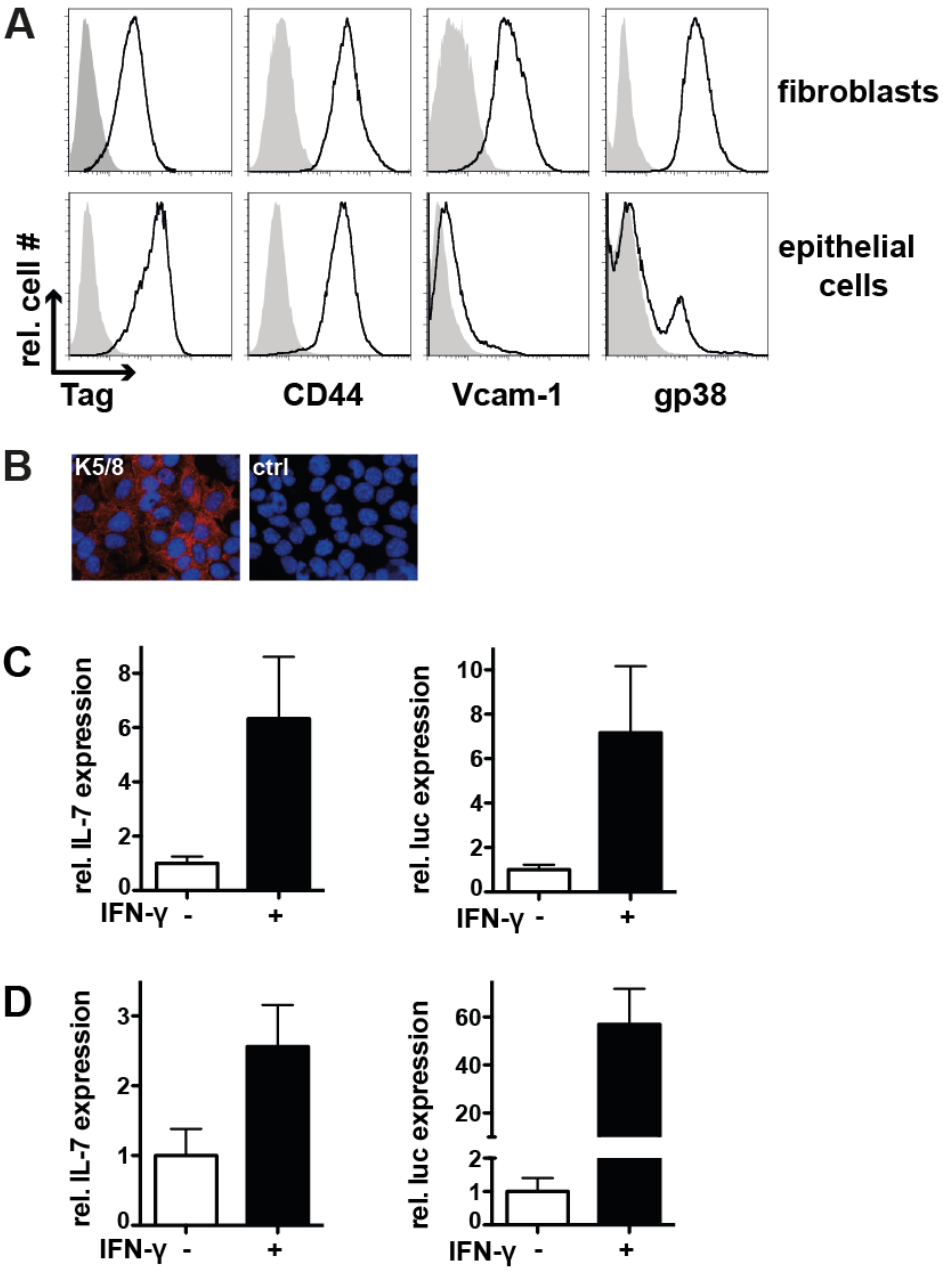

Figure 3.5: Thymic stromal cells express *il-7* and *luciferase in vitro.*
Cell cultures derived from the thymus of IL-7GCDLxloxP-Tag mice were cloned to obtain fibroblastic and epithelial cells. (A) These cultures were further analyzed for the expression of Tag, CD44, Vcam-1 and gp38 by flow cytometry. Relative expression of the indicated markers is shown for one representative of 3-4 cloned cell lines. (B) Cultured thymic epithelial cell clones were analyzed by immunostaining for the expression of cytokeratin 5/8 (K5/8). As a control (ctrl), the cells were stained with the secondary Ab only. Pictures are representative of 2 tested clones in 2 independent experiments. (C) Thymic epithelial cells or (D) fibroblasts were cultured in the presence or absence of recombinant murine IFN-γ (50 ng/ml) for 24 h. mRNA amounts for *il-7* and *luciferase* (luc) were determined by quantitative real-time PCR and normalized to *β-actin* or *hprt* and to amounts expressed by unstimulated cells. Graphs show representative data ± SD for 3-4 cloned cell lines.

3.2 Host IL-7R signaling and IL-7 therapy

IL-7 is a potent growth and survival factor for T cells but its amount is limited in the body (146). Exogenous IL-7 administration is currently studied as a novel therapy to overcome lymphopenia or to enhance the protective function of T cells against cancer or infectious diseases (for details see www.clinicaltrials.gov). Albeit IL-7 therapy has been shown to improve the function of anti-tumor $CD8^+$ T cells in preclinical models, tumor rejection has hardly been accomplished (147). Indeed, a negative feedback on endogenous *il-7* production by splenic stromal cells has been observed after IL-7 administration (91). This suggests that IL-7R signaling in host cells might limit the success of IL-7-supported T cell therapy. We hypothesize that several cell types, especially those producing IL-7, might be sensitive to IL-7 treatment thereby affecting the outcome of IL-7-supported T cell therapy. First, we asked whether stromal cells that are main sources of IL-7 in the body can integrate signals from IL-7. Since our data indicated that the intestine produces high amounts of IL-7 (Fig. 3.1C) and (63), we assessed the expression of the IL-7Rα-chain (CD127) on colonic epithelial cells (CECs). We detected the expression of CD127 on CECs, yet it was very weak in comparison to levels observed on splenic $CD8^+$ OT-I T cells (Fig. 3.6A). However, the expression was specific as validated by comparison of CECs from Rag-deficient (Rag^-) to CECs from IL-7Rα-deficient Rag^- mice ($IL\text{-}7R^-xRag^-$) (Fig. 3.6A). In support of our data, functional IL-7R expression has also been shown in human intestinal epithelial cells (148). This indicates that different stromal cell types in the body, such as splenic stromal and intestinal epithelial cells, can sense IL-7 availability. In order to test whether IL-7 therapy affects host *il-7* gene activity systemically, IL-7GCDL mice were treated with a mixture of recombinant murine IL-7 and stabilizing anti-IL-7 antibodies. These rIL-7/αIL-7 complexes improve/prolong the biological activity of IL-7 (149). Its use is termed “IL-7 therapy” hereafter. As shown in Figure 3.6B, BL signals were reduced by 25% 24 hours after IL-7 therapy. This shows that host cells respond to IL-7 therapy and that a single treatment with IL-7 lowers *il-7* gene activity systemically.

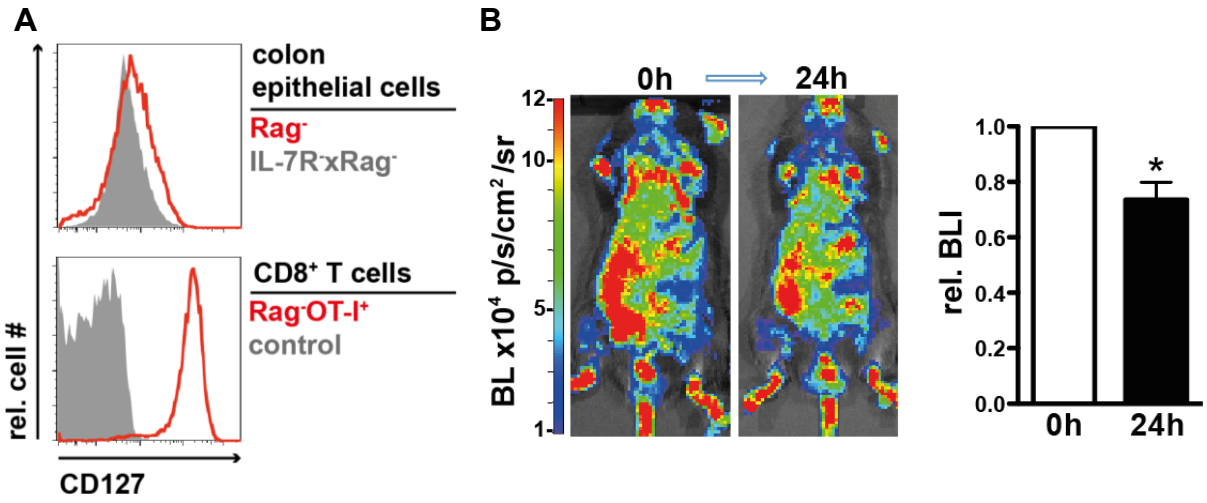

Figure 3.6: IL-7 administration decreases host *il-7* expression.
(A) To detect IL-7R expression, epithelial cells were isolated from the colon of Rag$^-$ and IL-7R$^-$xRag$^-$ mice (top). CD8$^+$ T cells were isolated from spleens of Rag$^-$OT-I$^+$ mice (bottom). The levels of IL-7Rα (CD127) expression were determined by flow cytometry. Shown are relative cell numbers and relative fluorescence intensities for CD127 after gating on 7AAD$^-$ CD45$^-$EpCam$^+$ epithelial cells (top) and after gating on 7AAD$^-$CD8$^+$Vα$^+$ OT-I T cells (bottom). As control, OT-I T cells were incubated with secondary antibodies only (bottom). Results are representative for 2 (bottom) and 3 (top) independent experiments. (B) To detect whether IL-7 administration alters *il-7* expression, luciferase activity in IL-7GCDL mice was determined by *in vivo* BL imaging before and 24 h after i.p. injection of IL-7/α-IL-7 mix (5 µg IL-7 mixed with 50 µg anti-IL-7 Ab M25). BLI signals of one representative mouse before and 24 h after IL-7 treatment are shown (left). BLI signals from mice 24 hours after IL-7 injection in relation to values obtained before treatment (rel. BLI) were determined (right). Shown are pooled data ± SEM of 2 experiments with a total of 6 mice. Statistical analysis was performed using Wilcoxon matched-pairs signed rank test.

To test whether host cells responding to IL-7 therapy affect the outcome of ATT (of cancer) we used Rag$^-$ and IL-7R$^-$xRag$^-$ mice and first analyzed the hematopoietic host cell population. We decided for animals on the T and B cell-deficient Rag$^-$ background since IL-7 therapy is mostly indicated in immunocompromised, lymphopenic patients. After 10-24 days of IL-7 therapy, splenic cellularity increased 5-fold in Rag$^-$ mice, which was not observed in IL-7R$^-$xRag$^-$ mice (Fig. 3.7A). In line with published results showing IL-7R-dependent development of immature B cells (150, 151), the frequency of CD19$^+$ pro-B cells was higher in Rag$^-$ compared to IL-7R$^-$xRag$^-$ mice. IL-7 therapy could raise the frequency of pro-B cells 30-fold in an IL-7R-dependent way (Fig. 3.7B). This confirms that IL-7 therapy is highly biologically active (149). We also determined the frequency of other cell types in spleen that have previously been shown to develop independently of IL-7R signals (104). The majority of splenic cells belonged to the myeloid CD11b$^+$ compartment which mainly consist of neutrophils, monocytes and macrophages (152). As expected, the number of CD11b$^+$ myeloid cells and of Gr-1 (granulocyte-differentiation antigen-1)-expressing myeloid cells was similar in both untreated hosts (Fig. 3.7C-D), affirming that IL-7R signaling is not important for the generation of these cells. After 10-24 days of IL-7 therapy, however, myeloid cell

numbers increased 3,5- to 4,8-fold in spleens of Rag$^-$ mice. Based on the expression pattern of Gr-1 the myeloid cell subsets accumulated equally strong after IL-7 therapy. This effect was not observed in spleens of IL-7R$^-$xRag$^-$ mice in which splenic cellularity remained unaltered (Fig. 3.7A, C-D). Since most myeloid cells do not express the IL-7R (107) the observed effect on those cells is presumably indirect.

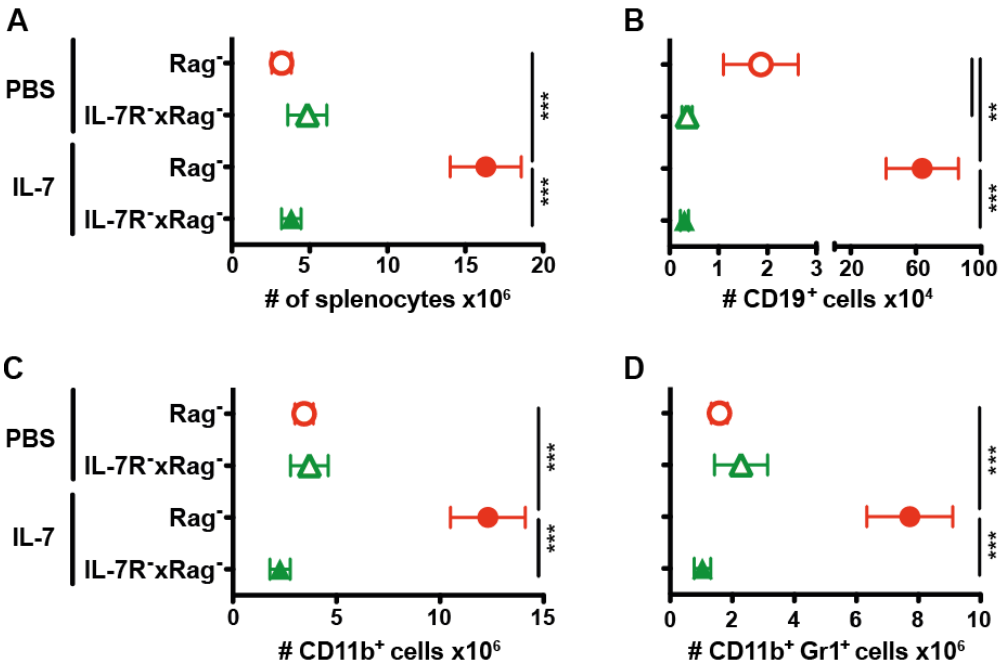

Figure 3.7: IL-7 therapy increases splenic cellularity.
Rag$^-$ and IL-7R$^-$xRag$^-$ mice received IL-7 therapy or PBS i.p. every 4 days for 10-24 days. (A) Total number of splenocytes and of (B) CD19$^+$ pro-B cells, (C) CD11b$^+$ myeloid cells and (D) CD11b$^+$Gr1$^+$ myeloid cells were determined by flow cytometry. Graphs show pooled data from 2 independent experiments with a total of 7-8 mice ±SEM per group.

Although conventional DCs in spleen do not express the IL-7R, IL-7R-mediated signaling was shown to promote DC generation at early stages of their development (104). The number of conventional DCs (defined as CD11c$^+$MHC-II$^+$) was similar in spleens of untreated Rag$^-$ and IL-7R$^-$xRag$^-$ mice and increased after IL-7 therapy in Rag$^-$ mice exclusively (Fig. 3.8A). We further assessed the composition of DC subsets with focus on CD8$^+$ DCs, since this subset is known for its high capacity to cross-present Ag to T cells (153) and thus might be of particular value during ATT of cancer. Absolute numbers of CD8$^+$ DCs were similar in spleens of PBS-treated Rag$^-$ and IL-7R$^-$xRag$^-$ (Fig. 3.8B). Remarkably, the number of CD8$^-$ DCs was 3-fold higher in spleens of PBS-treated Rag hosts (Fig. 3.8C). This indicates that the steady-state generation/accumulation of CD8$^-$ but not CD8$^+$ DCs in spleen is dependent on IL-7R-mediated signals. Splenic DC numbers increased after IL-7 therapy in Rag$^-$ mice exclusively (Fig. 3.8A-C).

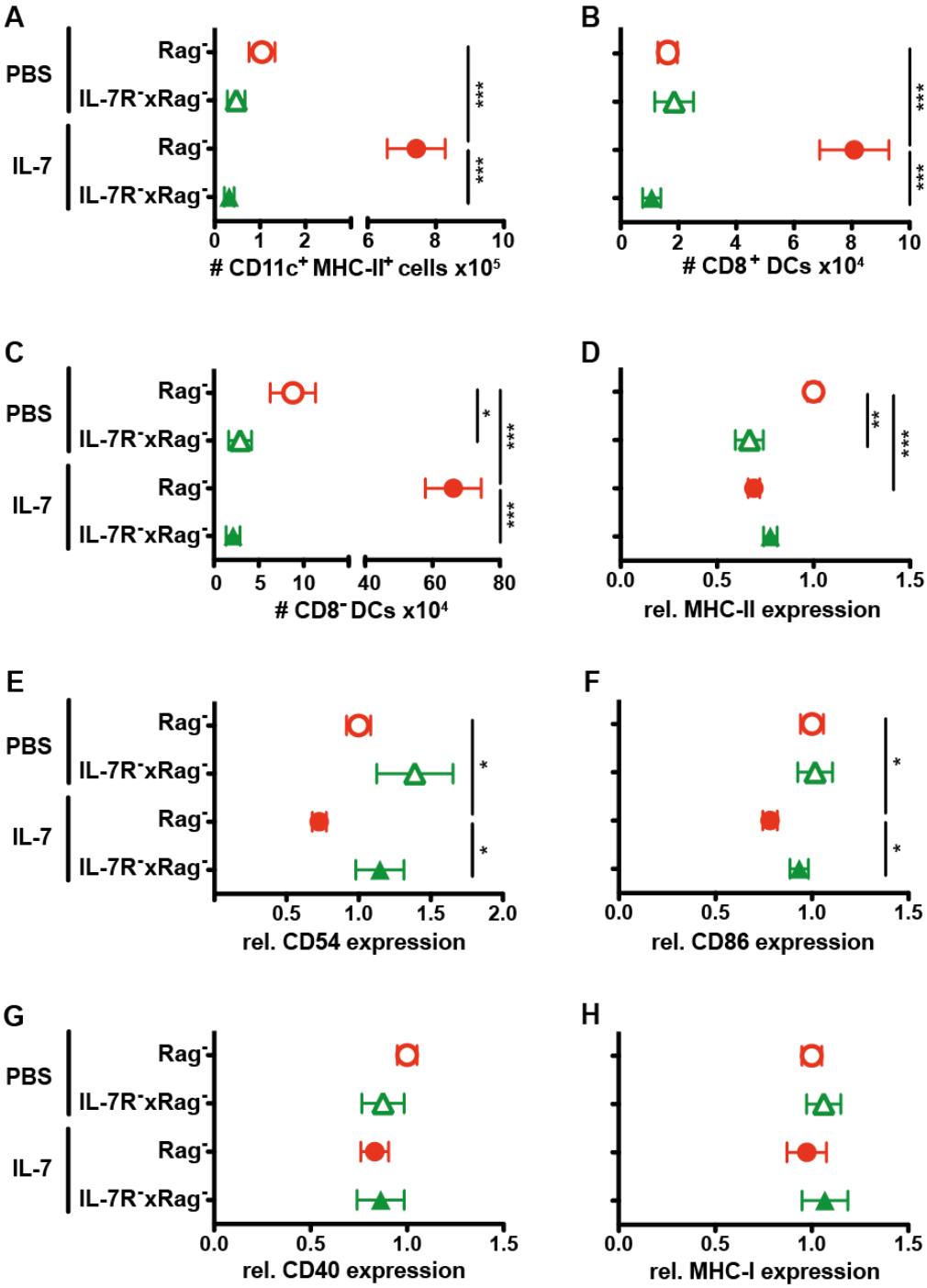

Figure 3.8: Host IL-7R signaling promotes DC expansion.
Rag$^-$ and IL-7R$^-$xRag$^-$ mice received IL-7 therapy or PBS i.p. every 4 days for 10-24 days. (A) Absolute numbers of CD11c$^+$MHC-II$^+$ cells (DCs) and its subset of (B) CD8$^+$ and (C) CD8$^-$ DCs in spleen were determined. The expression levels of (D) MHC-II, (E) CD54, (F) CD86, (G) CD40 and (H) MHC-I were analyzed by flow cytometry on splenic CD11c$^+$MHC-II$^+$ cells (B-D) or CD11c$^+$ cells (E-F). Data shown in (D-H) were normalized to the mean values obtained from PBS-treated Rag$^-$ mice. Pooled data of 2 independent experiments with a total of 7-8 mice ±SEM per group are shown.

We further investigated the phenotype of DCs to elucidate whether host IL-7R signals affect the expression of molecules implicated in T cell activation. Interestingly, the expression of MHC-II was higher on DCs from Rag$^-$ compared to IL-7R$^-$xRag$^-$ mice and decreased upon

IL-7 therapy to levels expressed by DCs from IL-7R$^-$xRag$^-$ mice (Fig. 3.8D). The expression of the T cell costimulatory molecules CD54 and CD86 was similar on DCs from Rag$^-$ and IL-7R$^-$xRag$^-$ mice. However, the levels of both molecules decreased after IL-7 therapy on DCs from Rag$^-$ animals (Fig. 3.8E-F). Yet, IL-7 therapy had no effect on DCs from IL-7R$^-$xRag$^-$ mice (Fig. 3.8A-F). Besides, the levels of the costimulatory molecule CD40 and MHC-I were not significantly regulated by IL-7R-mediated signaling in CD11c$^+$ cells (Fig. 3.8G-H), indicating that IL-7 therapy impairs the expression of distinct molecules by DCs, which are implicated in T cell activation.

In summary, steady state IL-7R signaling leads to increased frequencies of pro-B cells and CD8$^-$ DCs in spleen. Additionally, it regulates the expression of MHC-II on DCs. Strong IL-7R signaling induced by IL-7 therapy raises splenic cellularity, including pro-B cell, myeloid cell and DC numbers. Moreover, it affects the phenotype of DCs. Hence we showed that multiple host immune cells respond to IL-7 and could therefore affect the outcome of ATT. Especially DCs are important for CD8$^+$ T cell responses. Thus, their IL-7 therapy-induced expansion might promote the success of ATT. However, IL-7 therapy decreased the expression of T cell costimulatory molecules by DCs that in turn might impair the efficacy of ATT.

3.3 Effects of host IL-7R signaling on adoptive T cell therapy

To determine whether host IL-7R signaling affects the success of ATT, IL-7R-competent and -deficient hosts were reconstituted with mature CD8$^+$ T cells and their numbers and phenotype were followed. We aimed to use a T cell population with defined Ag-specificity. For this purpose, we performed adoptive transfer experiments with CD8$^+$ T cells from the well-characterized TCR-transgenic OT-I mouse. All CD8$^+$ OT-I T cells express a transgenic TCR that is specific for the SIINFEKL peptide derived from chicken-ovalbumin (154).

3.3.1 Effects of host IL-7R signaling on adoptive T cell therapy during LIP

The first question we addressed was whether host IL-7R signaling affects lymphopenia induced proliferation (LIP). LIP allows the generation of memory-like cells, which are similar to memory CD8$^+$ T cells that were generated in response to foreign Ag recognition (53, 155). Equal numbers of MACS-purified, TCR-transgenic CD90.1 congenic CD8$^+$ OT-I T cells (Fig. 3.9A) were adoptively transferred into Rag$^-$ and IL-7R$^-$xRag$^-$ mice. 3-4 weeks after transfer, CD8$^+$ OT-I T cells upregulated CD44 expression levels in Rag$^-$ and IL-7R$^-$xRag$^-$ but not WT mice, which indicated their successful development into memory-like cells in the lymphopenic environment (Fig. 3.9B). Only low numbers of transferred T cells were recovered from WT mice (Fig. 3.9C). In contrast, similar numbers of OT-I T cells were recovered from spleens of Rag$^-$ and IL-7R$^-$xRag$^-$ mice 3-4 weeks after T cell transfer (Fig. 3.9C). These data indicate that LIP occurs efficiently in IL-7R$^-$ hosts independently of the observed differences in DC differentiation. LIP is also dependent on intact SLO structure

(156). Hence, these results also prove that the SLOs in IL-7R$^-$ mice are able to support homeostatic proliferation including generation of memory-like CD8$^+$ T cell.

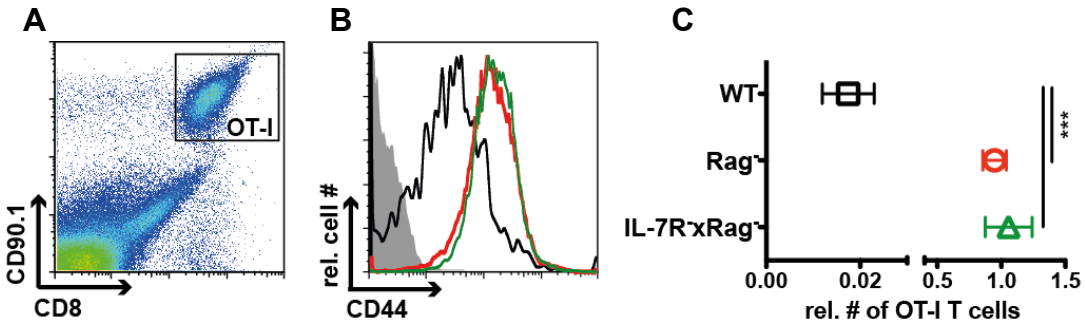

Figure 3.9: Lymphopenia-induced T cell proliferation (LIP) is independent of host IL-7R signaling.
Rag$^-$, IL-7R$^-$xRag$^-$ and WT mice were reconstituted with 1x10^6 MACS-purified CD8$^+$CD90.1$^+$ OT-I T cells. 21-27 days later, (A) splenic OT-I T cells were analyzed by flow cytometry after gating on CD8$^+$CD90.1$^+$ cells (representative dot plot). (B) CD44 expression levels were determined on splenic OT-I T cells from all 3 recipients (Rag$^-$, red; IL-7R$^-$xRag$^-$, green; WT, black line) and compared to CD44 isotype-matched control staining (ctrl, grey filled line; representative histogram). (C) Splenic OT-I T cell numbers were calculated for the different recipients and pooled data from 3 independent experiments with a total of 9-19 mice per group ±SEM are shown.

Next, we asked whether the observed effects of IL-7 therapy on host cells (Fig. 3.7-3.8) affect LIP. Mice received IL-7 therapy or PBS i.p. one day prior and 3 days post i.v. transfer of 1x10^6 MACS-purified OT-I T cells. To test whether the transferred OT-I T cells responded to IL-7 therapy, IL-7Rα (CD127) expression was measured, since it is downregulated in response to IL-7 binding (100). As depicted in Fig. 3.10A, 5 days after transfer, the expression of CD127 was higher on OT-I T cells transferred into Rag$^-$ hosts than into IL-7R$^-$xRag$^-$ recipients, presumably due to higher amounts of IL-7 in IL-7R$^-$ hosts (91). IL-7 therapy decreased the expression of CD127 on T cells transferred into both hosts to a similar level. This indicates that T cells responded to IL-7 therapy in both hosts. IL-7 administration was shown to increase peripheral T cell numbers by inducing proliferation and prolonging survival (149, 157). To distinguish proliferation from survival, T cells were labeled with the dye CFSE that allows visualization of T cell division. Within 5 days after transfer, T cells divided equally well in both hosts as determined by the CFSE profile of splenic OT-I T cells (Fig. 3.10B-C). These results support our findings that LIP of CD8$^+$ OT-I T cells is efficient in IL-7R$^-$ hosts. Upon IL-7 therapy, the frequency of OT-I T cells with more than 2 divisions increased similarly in both hosts compared to PBS-treated controls (Fig. 3.10B-C). Hence, it can be concluded that host IL-7R signaling does not affect IL-7-dependent CD8$^+$ T cell expansion in the first 5 days of LIP. These results also suggest, that our experimental system is suitable to discriminate between IL-7-therapy-mediated effects on host vs. T cells.

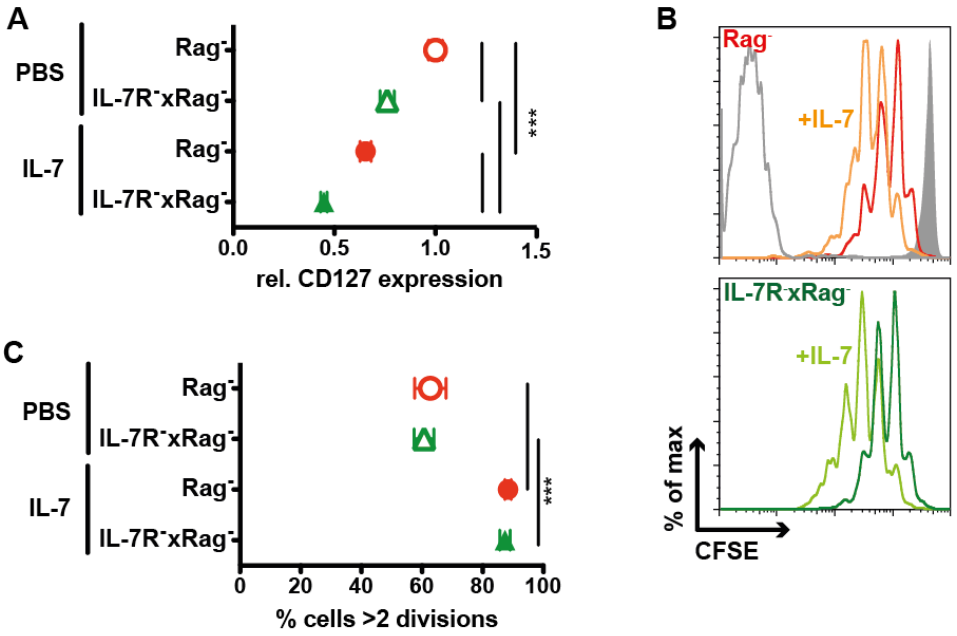

Figure 3.10: Host IL-7R signaling is not required for early T cell expansion after IL-7 therapy.
Rag$^-$ and IL-7R$^-$xRag$^-$ mice received IL-7 therapy or PBS i.p. 24 h prior and 72 h after i.v. transfer of 1x10^6 MACS-purified CFSE-labeled OT-I T cells. 5 days after transfer, splenic CD8$^+$ OT-I T cells were analyzed by flow cytometry for the intensity of (A) CD127 expression and (B-C) CFSE. Data shown in A were normalized to the mean values obtained from PBS-treated Rag$^-$ mice. (B) Representative histograms for CFSE intensities of OT-I T cells are shown. As controls, filled and open grey curves show undivided cells in WT hosts or CFSE-negative cells, respectively. (C) The number of OT-I T cell divisions was determined by CFSE intensity loss. Cells with more than 2 divisions are shown. Graphs show pooled data from 2 independent experiments with a total of 8 mice ±SEM per group.

T cell expansion was further analyzed after 2 and 3 weeks of LIP and IL-7 therapy. In accordance with Fig. 3.7A, splenic cellularity was similar in both PBS-treated hosts 11 and 21-25 days after T cell transfer (Fig. 3.11A, C). In the same period, IL-7 therapy increased splenic cell number in Rag$^-$ hosts but not in IL-7R$^-$xRag$^-$ hosts (Fig. 3.11A, C). 11 days after transfer, splenic OT-I T cell numbers were elevated in IL-7R$^-$xRag$^-$ compared to Rag$^-$ hosts (Fig. 3.11B). IL-7 therapy increased T cell numbers in both hosts, leading to highest T cells numbers in IL-7R$^-$xRag$^-$ mice (Fig. 3.11B). While IL-7 therapy continued to induce higher T cell numbers in spleen 21 days after transfer, splenic T cell numbers equaled in both hosts (Fig 3.11D). In conclusion, IL-7 therapy induces spleen enlargement exclusively in Rag$^-$ hosts. In contrast, it raises splenic T cell numbers efficiently in both, Rag$^-$ and IL-7R$^-$xRag$^-$ hosts.

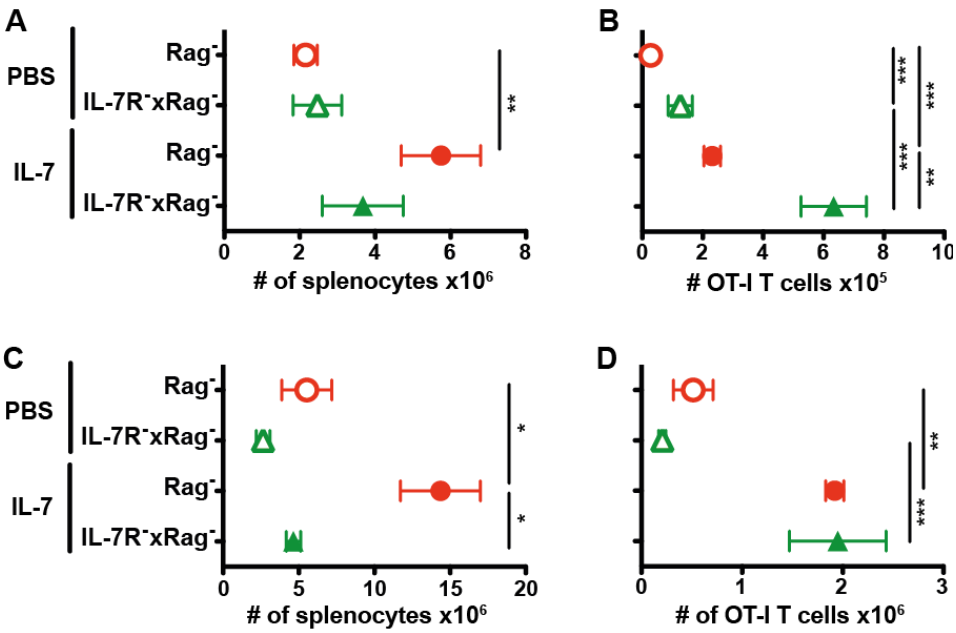

Figure 3.11: Host IL-7R signaling is not required for T cell expansion after IL-7 therapy. Rag$^-$ and IL-7R$^-$xRag$^-$ mice were treated i.p. with IL-7 therapy or PBS every 3-4 days starting one day prior to i.v. transfer of 1x10^6 MACS-purified OT-I T cells. 11 (A-B) and 21-25 (C-D) days post T cell transfer, splenic CD8$^+$ Thy1.1$^+$ OT-I T cells were analyzed. The number of (A, C) splenic cells and (B, D) splenic OT-I T cells was determined by flow cytometry. Graphs show pooled data from 2 independent experiments with 6-9 mice ±SEM per group.

In addition, the phenotype of the transferred OT-I T cells was analyzed after 21-25 days of LIP. As already shown in Fig. 3.9, high CD44 expression levels were observed on most OT-I T cells 3 weeks after transfer into Rag$^-$ and IL-7R$^-$xRag$^-$ hosts, indicating that they had developed into memory T cells (data not shown). The frequency of CD62L$^+$ T_{CM}, was higher in IL-7R$^-$xRag$^-$ compared to Rag$^-$ animals (Fig. 3.12A). Conversely, KLRG-1, a marker for short-lived effector T cells (T_{SLEC}) and T_{EM} cells, was expressed by fewer T cells in IL-7R$^-$xRag$^-$ mice (Fig. 3.12B). This suggests that T_{CM} differentiation was facilitated in IL-7R$^-$xRag$^-$ hosts. The levels of CD127 were similar on T cells in both hosts 21-25 days after transfer (Fig. 3.12C), which is in contrast to data obtained 5 days after T cell transfer (Fig. 3.10A). To determine the level of IL-7R signaling, we measured the expression of the anti-apoptotic molecule Bcl-2, which is induced by IL-7R signaling (81, 157). Interestingly, the levels of Bcl-2 were increased in T cells reisolated from IL-7R$^-$xRag$^-$ hosts, which is an indicator of higher IL-7-mediated signaling in those hosts. Furthermore, the effector function of the transferred T cells was assessed after short-term *in vitro* restimulation with the cognate peptide. A mildly decreased capacity to produce IFN-γ was detected in T cells reisolated from Rag$^-$ hosts. In summary, the differentiation towards T_{CM} is impaired in the host IL-7R-expressing host. This correlates with reduced levels of Bcl-2 and reduced capacity to produce the immunomodulatory cytokine IFN-γ.

When mice received IL-7 therapy concomitantly, increased frequencies of $CD62L^+$ OT-I T cells but decreased rates of KLRG-1^+ OT-I T cells were observed in both hosts, indicating that IL-7 therapy boosted T_{CM} differentiation (Fig. 3.12A-B). IL-7 therapy also augmented CD127 levels on T cells in both hosts (Fig. 3.12C), which is in contrast to the effects of IL-7 therapy observed early after application (Fig. 3.10A). Since most T cells after 5 days of LIP had not adopted a memory-like phenotype based on the expression of CD44 (data not shown), this suggests that the regulation of CD127 expression may depend on the differentiation state of a cell. As expected, IL-7 therapy elevated the levels of Bcl-2 in T cells from Rag^- mice, however the levels remained lower than in T cells from IL-7-treated IL-$7R^-$ xRag^- mice (Fig. 3.12D). We also compared the capacity of OT-I T cells to produce IFN-γ after IL-7 therapy. Yet, OT-I T cells recovered from Rag^- and IL-$7R^-$xRag^- mice produced IFN-γ equally well after short-term *in vitro* restimulation with the cognate peptide (Fig. 3.12E). In summary, the differentiation towards T_{CM} was facilitated by IL-7 therapy, especially in the IL-7R-deficient host. This correlated with elevated levels of the anti-apoptotic molecule Bcl-2. However, IL-7 therapy did not raise the effector function of T cells, as judged by the capacity to produce IFN-γ.

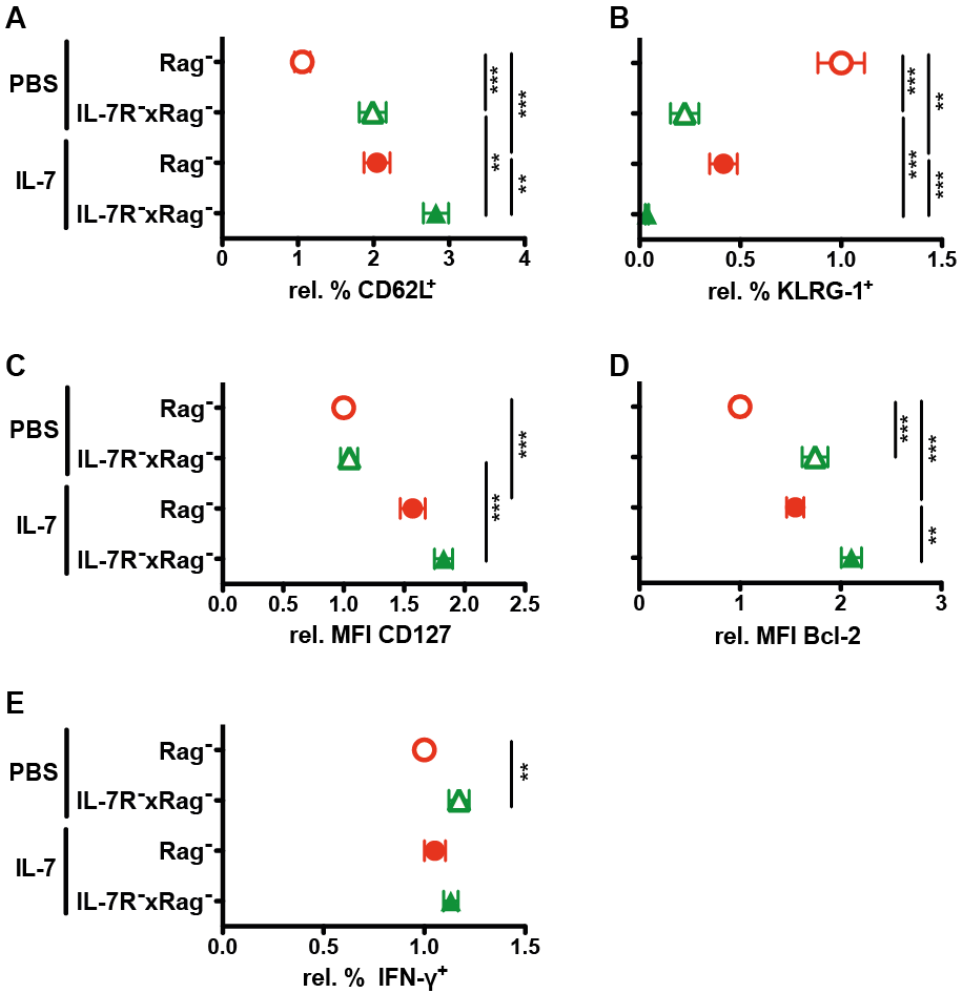

Figure 3.12: T_{CM} differentiation is increased after IL-7 therapy.
Rag$^-$ and IL-7R$^-$xRag$^-$ mice received IL-7 therapy or PBS i.p. every 4 days starting one day prior to i.v. transfer of 1x10^6 MACS-purified OT-I T cells. 21 days post T cell transfer, CD8$^+$ Thy1.1$^+$ OT-I T cells isolated from spleen were analyzed by flow cytometry for the expression of (A) CD62L, (B) KLRG-1, (C) CD127 and (D) Bcl-2. (E) The production of IFN-γ by OT-I T cells was determined after *in vitro* restimulation of splenocytes for 6 h with 1 mM SIINFEKL peptide in the presence of brefeldin A. Data shown in A-E were normalized to the mean values obtained from PBS-treated Rag$^-$ mice. Graphs show pooled data from 2-3 independent experiments with a total of 7-13 mice ±SEM per group.

In order to determine whether the observed effects of IL-7 therapy and host IL-7R signaling on adoptive T cell therapy modulate the T cell response towards Ag-expressing tumor cells, CD8$^+$ OT-I T cells were transferred into both Rag$^-$ and IL-7R$^-$xRag$^-$ hosts, which received IL-7 therapy or PBS for 22 days. This was followed by s. c. challenge with EG7 tumor cells. We excluded any impact of residual IL-7 therapy on the tumor or tumor microenvironment by simultaneously applying the tumor cell line and IL-7 therapy in separate groups of mice that had not received ATT. In these Rag$^-$ and IL-7R$^-$xRag$^-$ mice, tumor growth kinetics was unaffected by IL-7 therapy (Fig 3.13A). Yet, in some but not all experiments, tumors grew slightly slower in Rag$^-$ than in IL-7R$^-$xRag$^-$ mice. In comparison to untreated animals, ATT prolonged the tumor-free period or even prevented tumor outgrowth completely. Surprisingly,

IL-7 therapy in addition to ATT did not alter tumor incidence in IL-7R$^-$xRag$^-$ mice. There, tumor growth was prevented in 3/11 mice receiving PBS and 3/12 mice receiving IL-7 therapy (Fig. 3.13B). In Rag$^-$ mice that received ATT however, tumor growth was prevented in 1/11 mice receiving PBS but in 7/12 mice receiving IL-7 therapy (Fig. 3.13C). This suggests that IL-7 therapy promotes the anti-tumor response of CD8$^+$ T cells in IL-7R-competent but not in -deficient Rag$^-$ hosts.

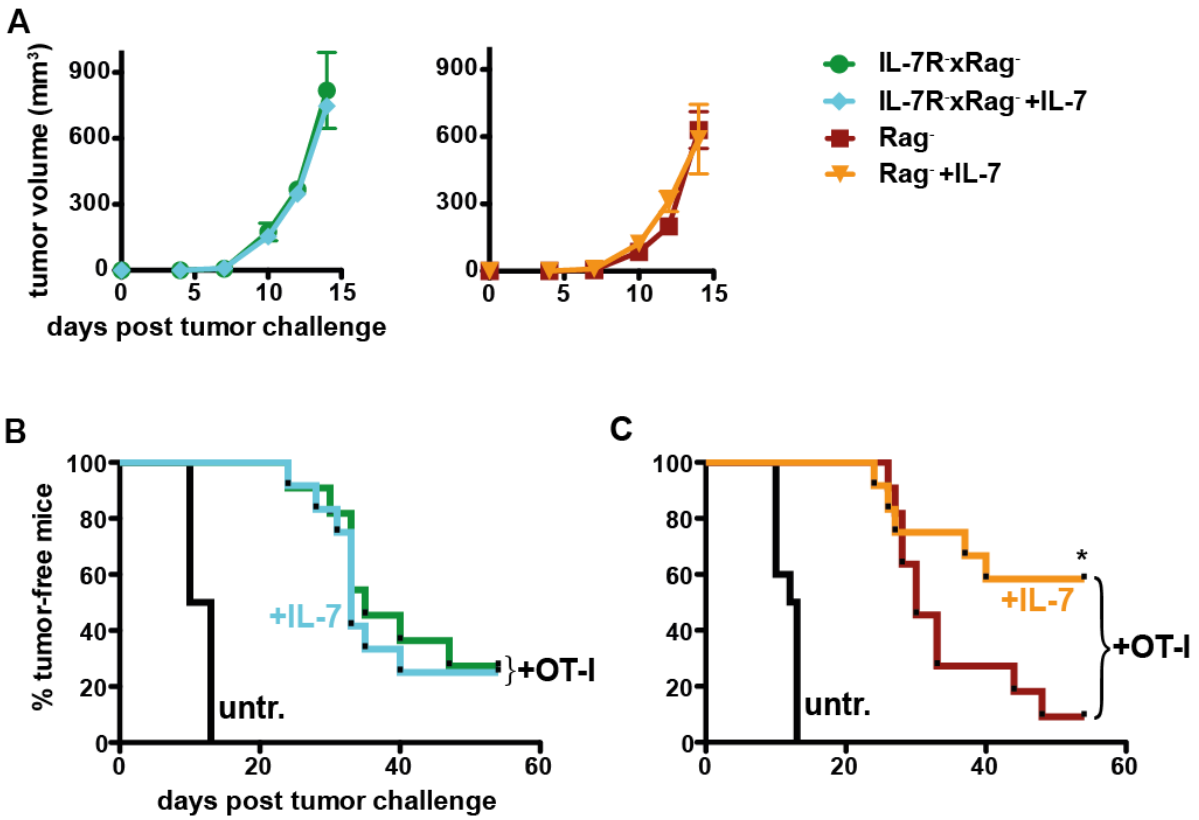

Figure 3.13: Host IL-7R expression is required for IL-7 therapy-assisted ATT.
(A) Mice were challenged s.c. with ova-expressing EG7 tumor cells and received IL-7 therapy or PBS i.p. every 3-4 days starting one day before tumor challenge. Tumor growth was determined every 2-4 days. Graphs show representative data from 1 out of 2 experiments with 4-5 mice/group ±SEM. (B) IL-7R$^-$xRag$^-$ and (C) Rag$^-$ mice were reconstituted with 7-10x10^5 MACS-purified CD8$^+$ OT-I T cells (+OT-I) and received (B, C) IL-7 therapy (+IL-7) or PBS every 4 days for 18 days starting one day before T cell transfer. 22-23 days after OT-I T cell transfer, these mice and untreated controls (untr.) were challenged s.c. with ova-expressing EG7 tumor cells. Mice with tumors >250mm^3 were scored as positive. Pooled data from 2 independent experiments with a total of 10-12 mice per group are shown. Statistical significance was calculated using the log-rank test.

The limited success of IL-7 treatment on adoptive T cell therapy against cancer in IL-7R-deficient Rag$^-$ mice was unexpected since IL-7 therapy-assisted CD8$^+$ OT-I T cell expansion occurred equally well in IL-7R-competent and -deficient animals (Fig. 3.11D). Although the IL-7 therapy-induced T cell numbers could not be fully sustained 4 weeks post tumor challenge and cessation of IL-7 treatment, OT-I T cell numbers ranged at similarly high

levels in spleens of tumor-bearing IL-7R$^-$xRag$^-$ compared to Rag$^-$ mice (Fig. 3.14A). At this stage, the T cell phenotype was still controlled by the host, as evidenced by slightly lower frequencies of CD62L$^+$ but higher rates of KLRG-1$^+$ cells within the OT-I T cells reisolated from Rag$^-$ hosts (Fig. 3.14B-C). However, the phenotypic changes caused by IL-7 therapy were no longer present, as judged by CD62L, KLRG-1 and CD127 expression pattern (Fig. 3.14B-D).

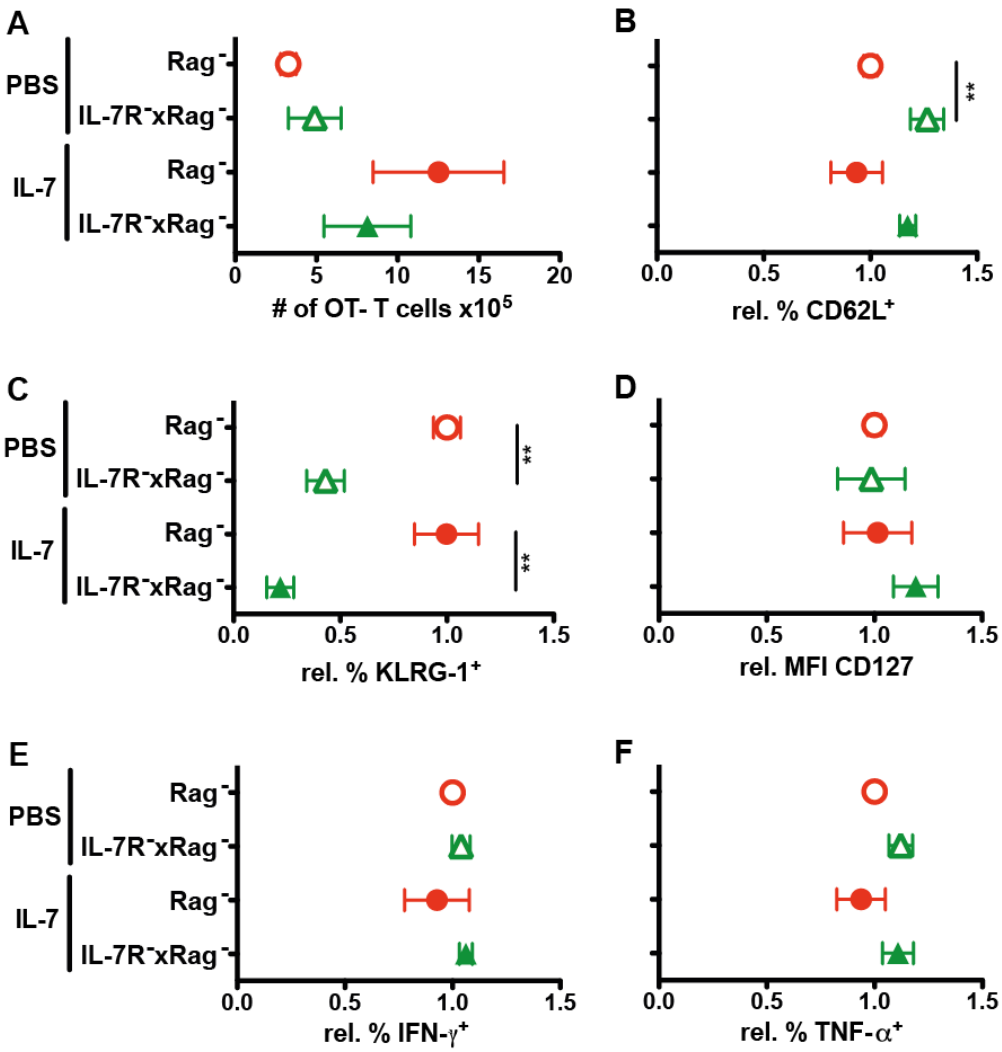

Figure 3.14: Host IL-7R signaling is not required for maintaining T cell numbers and effector functions 4 weeks post tumor challenge.
4-10x10^5 MACS-purified OT-I T cells were transferred into Rag$^-$ and IL-7R$^-$xRag$^-$ hosts. Mice received IL-7 therapy or PBS i.p. every 4 days for 19 days starting one day before T cell transfer. 3 weeks after T cell transfer, mice were challenged s.c. with 1x10^6 EG7 tumor cells. Splenic cells were analyzed from mice with large tumors 28-35 days after EG7 challenge. Frequencies of (A) T cells and (B) relative frequencies of CD62L$^+$ and (C) KLRG-1$^+$ cells as well as the relative expression of (D) CD127 within the OT-I T cell pool are shown. The production of (E) IFN-γ and (F) TNF-α by OT-I T cells was determined after *in vitro* restimulation of splenocytes for 6 h with 1 µM SIINFEKL peptide and brefeldin A. Data shown in B-F were normalized to the mean values obtained from PBS-treated Rag$^-$ mice. Shown are pooled data from 2 independent experiments with a total of 6-9 mice ±SEM per group.

To determine whether the large remaining population of tumor-specific T cells lost effector function and therefore allowed tumor outgrowth, their ability to produce IFN-γ and TNF-α was assessed after short *in vitro* restimulation with the cognate peptide. More than 50% of the OT-I T cells reisolated from spleen were still able to produce these cytokines indicating that they were not completely exhausted (raw data not shown). More importantly, these frequencies were similar in all tested groups (Fig. 3.14E-F). In conclusion, although T cell proliferation and effector function was similar in both hosts, IL-7 therapy exclusively promoted responses of tumor-specific T cells in the IL-7-responsive Rag^- hosts. This indicates that host IL-7R signaling is required for the success of IL-7 therapy-assisted ATT.

3.3.2 Effects of host IL-7R signaling on adoptive T cell therapy combined with immunization

As observed above, adoptive T cell therapy alone can be insufficient in mediating anti-tumor responses. In this condition, acute TCR stimulation can help to boost anti-cancer responses of therapeutic T cells (158). Hence it was recently suggested to include vaccinations into future clinical trials (135). In order to determine the effect of IL-7 therapy on T cell proliferation and function upon acute TCR stimulation, the experiments were extended by peptide vaccinations.

$CD8^+$ OT-I T cells were transferred into Rag^- and $IL\text{-}7R^-xRag^-$ hosts, which were immunized with 50 µg SIINFEKL peptide one day later. In addition the animals received IL-7 therapy or PBS every 4 days starting one day prior to T cell transfer. 3 weeks after T cell transfer, we did not observe any significant difference in splenic cellularity comparing both immunized hosts (Fig. 3.15A). Since peptide vaccination induces effector T cells and T_{SLEC} / T_{EM} that have the capacity to migrate from SLOs to the periphery (36), T cells circulating through the blood were also analyzed. Numbers of OT-I T cell were slightly higher in spleens and blood of immunized Rag^- compared to $IL\text{-}7R^-xRag^-$ hosts (Fig. 3.15B-C). Surprisingly, the combination of immunization and IL-7 therapy led to very high T cell frequencies in spleen and blood of Rag^- compared to $IL\text{-}7R^-xRag^-$ mice and animals, that did not receive IL-7 therapy (Fig. 3.15B-C). This indicates that IL-7R signaling in host cells is needed for strong T cell expansion upon TCR stimulation. In addition to T cell frequencies, the phenotype of the transferred OT-I T cells was analyzed. The frequency of $CD62L^+$ T_{CM} cells within the OT-I T cell pool was unchanged in spleen or blood of immunized Rag^- and $IL\text{-}7R^-xRag^-$ hosts and increased after IL-7 therapy to similar levels in both hosts (Fig. 3.15D-E). The expression of CD127 on T cells from spleen or blood was mildly elevated in Rag^- compared to $IL\text{-}7R^-xRag^-$ hosts (Fig. 3.15F-G). IL-7 therapy strongly increased CD127 levels on T cells exclusively in IL-7R-competent Rag^- mice (Fig. 3.15F-G). These results demonstrate that IL-7 therapy-induced T cell expansion and expression of the memory (precursor)-associated molecule CD127 (87) are dependent on an IL-7 responsive host environment.

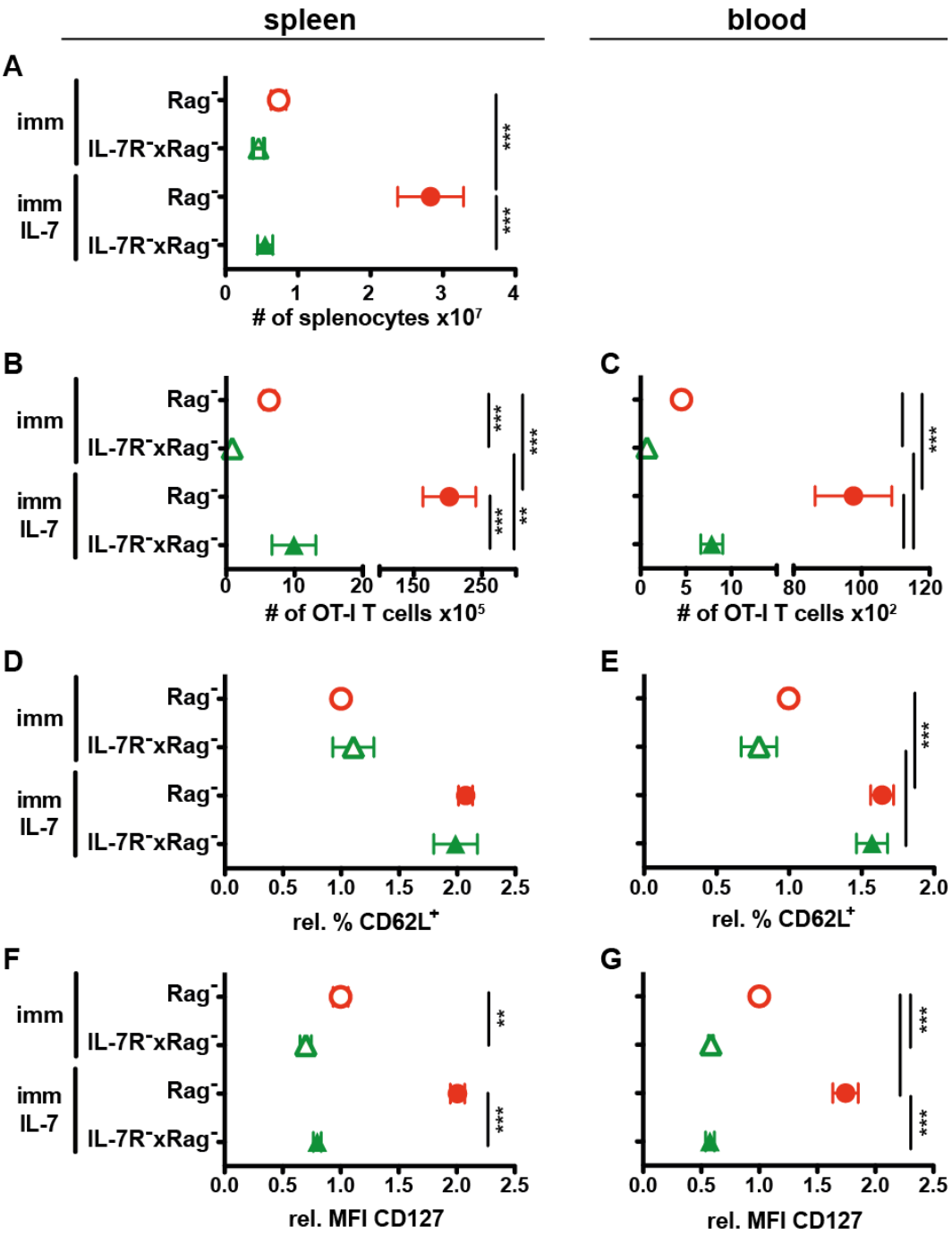

Figure 3.15: Enhanced T cell proliferation in response to peptide vaccination and IL-7 therapy depends on host IL-7R signaling.
Rag$^-$ and IL-7R$^-$xRag$^-$ mice received 1x10^6 MACS-purified OT-I T cells i.v. and were immunized with 50 µg SIINFEKL peptide one day after T cell transfer. Additionally, mice received IL-7 therapy (imm+IL-7) or PBS (imm) i.p. every 4 days starting one day prior to T cell transfer. 3 weeks later, (A) the number of splenic cells and number of CD8$^+$ Thy.1.1$^+$ OT-I T cells in (B) spleen and (C) blood was determined by flow cytometry. The frequency of (D-E) CD62L$^+$ cells within the OT-I T cell pool and the expression level of (F-G) CD127 on OT-I T cells from spleen and blood are shown, respectively. Data shown in D-G were normalized to the mean values obtained from PBS-treated (imm) Rag$^-$ mice. Shown are pooled data from 2-5 independent experiments with a total of 9-26 mice ±SEM per group.

The data presented in Fig. 3.15B-G also show that in our model, T cells have a similar phenotype and distribution in spleen and blood, suggesting that analysis of circulating T cells from peripheral blood is representative for splenic T cells. The T_{SLEC} / T_{EM} associated molecule KLRG-1 was expressed by more T cells in blood of immunized IL-7R$^-$xRag$^-$ mice (Fig. 3.16A). IL-7 therapy decreased the frequency of KLRG-1 expressing T cells in both hosts leading to almost undetectable KLRG-1 expression on T cells in IL-7R-competent hosts (Fig. 3.16A). Together with data showing that IL-7 therapy increased the frequency of CD62L$^+$ T cells (Fig. 3.15D-E), the results indicate more pronounced T_{CM} generation in the presence of IL-7 therapy. However, the so far observed inverse relation of CD62L and KLRG-1 expression on transferred T cells undergoing LIP (Fig. 3.12A-B) was not observed after vaccination. In vaccinated animals, the frequency of CD62L$^+$ T cells was similar, but the rate of KLRG-1$^+$ T cells was elevated in IL-7R$^-$xRag$^-$ mice (Fig. 3.15E vs. 3.16A). Hence, it was difficult to infer the differentiation to T_{CM} (CD62L$^+$KLRG-1^{low}) or $T_{EM/SLEC}$ (CD62L$^-$ KLRG-1$^+$) from this analysis. In order to conclude whether host IL-7R expression alters the memory differentiation after peptide vaccination, we included the analysis of T-bet and Eomes. The balanced expression of these transcription factors determines effector vs. long-lived T_M cell differentiation (97, 159–161). T-bet was expressed at similar levels by T cells in both hosts and decreased after IL-7 therapy (Fig. 3.16B). The expression pattern of T-bet correlated negatively with CD62L (Fig. 3.15E, 3.16B). Eomes was expressed at similar levels by T cells in both hosts (Fig. 3.16C). After IL-7 therapy, T cells in Rag$^-$ hosts retained these levels, whereas T cells transferred into IL-7R$^-$xRag$^-$ hosts increased Eomes expression (Fig. 3.16B). While T-bet is expressed by effector T cells but declines during memory formation, Eomes expression increases (162). Thus, we suggest that IL-7-responsive host cells affected the generation of T_{SLEC} vs. T_M cells after vaccination and IL-7 therapy. Additionally, we determined the expression levels of the anti-apoptotic and IL-7-inducible T_M-precursor and T_M-associated molecule Bcl-2 (163). T cells isolated from immunized IL-7R-competent and -deficient hosts expressed similar levels of Bcl-2 (Fig. 3.16D). After IL-7 therapy, Bcl-2 expression remained stable in T cells in Rag$^-$ hosts, but increased in T cells transferred into IL-7R$^-$xRag$^-$ mice. This expression pattern correlates with Eomes and indicates high survival capacities of the few T cells in IL-7-treated immunized IL-7R$^-$xRag$^-$ hosts. Besides this survival-promoting factor, we also assessed the proliferative state of the transferred T cells. T cells in Rag$^-$ mice exhibited a lower basic proliferation rate than T cells in IL-7R$^-$xRag$^-$ mice as assessed by the marker Ki-67 (Fig. 3.16E). However IL-7 therapy raised those rates to levels observed in IL-7R-deficient hosts. These data indicate that host IL-7R signaling does not improve the survival or proliferation of the OT-I T cells 3 weeks after transfer, suggesting that IL-7-responsive host cells facilitate IL-7 therapy-induced T cell expansion early after vaccination.

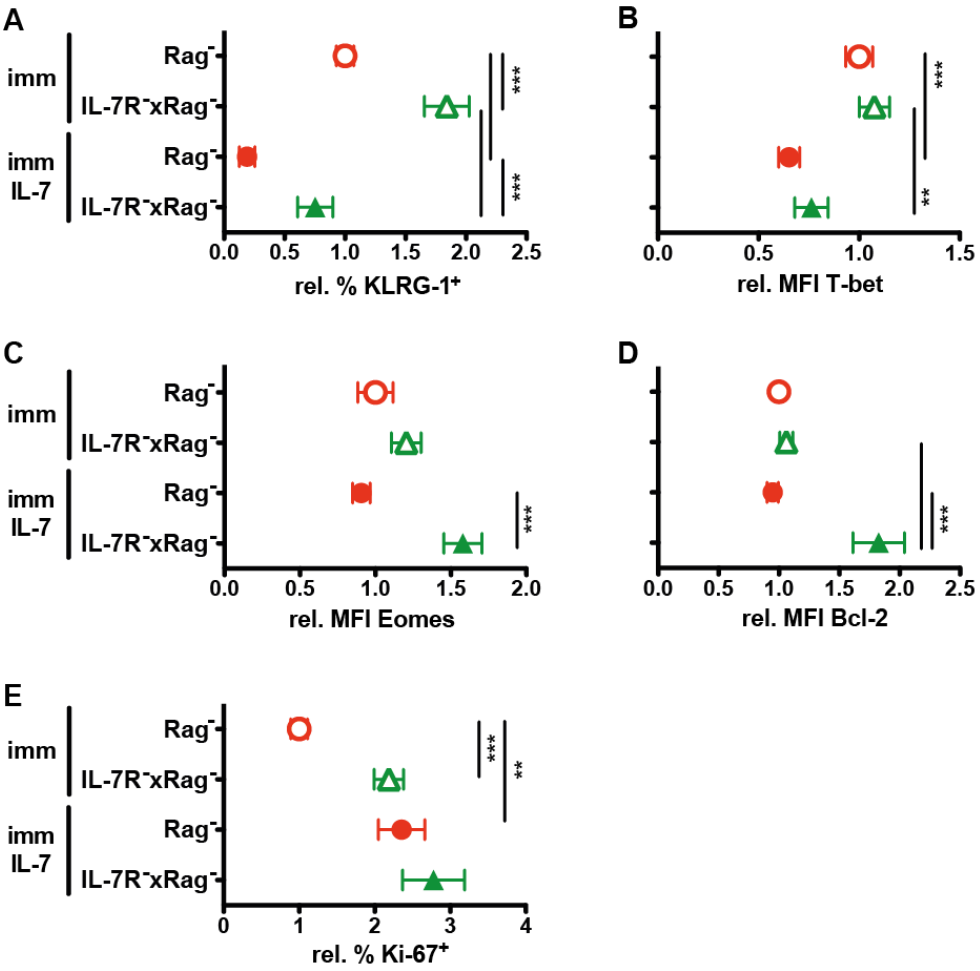

Figure 3.16: Eomes and Bcl-2 expression by T cells in response to peptide vaccination and IL-7 therapy is regulated by host IL-7R signaling.
Rag$^-$ and IL-7R$^-$xRag$^-$ mice received 1x10^6 MACS-purified OT-I T cells i.v. and were immunized with 50 µg SIINFEKL peptide one day after T cell transfer. Additionally, mice received IL-7 therapy (imm+IL-7) or PBS (imm) i.p. every 4 days starting one day prior to T cell transfer. 3 weeks later, peripheral blood CD8$^+$ OT-I T cells were analyzed for (A) the frequency of KLRG-1$^+$ and (E) Ki-67$^+$ cells and for the MFI of (B) T-bet, (C) Eomes and (D) Bcl-2 by flow cytometry. Data shown in A-E were normalized to the mean values obtained from PBS-treated (imm) Rag$^-$ mice. Shown are pooled data from 3 independent experiments with a total of 16-18 mice ±SEM per group.

We continued to assess phenotypic markers implicated in T cell responsiveness. The intensity of TCR and CD8 co-receptor expression sets the Ag responsiveness of T cells (164, 165). As the TCR is expressed on the cell surface in a complex with CD3, which is needed for TCR signal transduction, we determined CD3ε surface expression to determine TCR expression (166). 3 weeks after transfer, CD3ε levels did not differ on T cells reisolated from immunized IL-7R$^-$xRag$^-$ and Rag$^-$ hosts (Fig. 3.17A). However, CD3ε levels increased after additional IL-7 therapy exclusively on T cells transferred into IL-7R$^-$xRag$^-$ mice. In line with the expression pattern of CD3, CD8 levels were similar on T cells from immunized IL-7R$^-$xRag$^-$ and Rag$^-$ mice and increased after IL-7 therapy in IL-7R$^-$xRag$^-$ mice (Fig. 3.17B). In contrast, CD8 levels decreased on T cells in Rag$^-$ mice after IL-7 therapy. Together, this

indicates that IL-7 therapy decreased TCR-mediated T cell responsiveness in immunized Rag^- mice while increasing it in IL-$7R^-$xRag^- mice. To determine whether host IL-7R signaling affects TCR-mediated signaling, we measured the levels of CD5, which correlates with the intensity of homeostatic TCR engagement (167). The expression of CD5 was lower on T cells from immunized IL-$7R^-$xRag^- compared to Rag^- mice (Fig. 3.17C). When immunization was combined with IL-7 therapy, the expression of CD5 equaled in both hosts. This indicates that Ag-experienced OT-I T cells have less intense contact to self-peptide MHC-complexes in the IL-$7R^-$ hosts. Yet, IL-7 therapy-induced upregulation of TCR and coreceptor expression may have restored the defect. Tonic TCR engagement is important for maintaining responsiveness to foreign Ag (105). Moreover T cell responses are impaired by PD-1 (168, 169). Interestingly PD-1 was expressed at similar levels on OT-I T cells in IL-$7R^-$xRag^- and Rag^- mice (Fig. 3.17D). IL-7 therapy selectively reduced PD-1 levels on T cells in Rag^- mice. However, the low PD-1 level after IL-7 therapy did not substantially improve effector function of those OT-I T cells, which was assayed after short-term *in vitro* restimulation of PBMCs with the peptide SIINFEKL (Fig. 3.17E-G). TNF-α was produced by about 40% of the OT-I T cells in both hosts (data not shown and Fig. 3.17F). The percentage of TNF-α producers was slightly enhanced after IL-7 therapy, irrespective of host IL-7R signaling. Approximately 50% of the T cells were able to produce IFN-γ (data not shown). The percentage of IFN-γ-producing T cells was slightly decreased in immunized IL-$7R^-$xRag^- (Fig. 3.17E). Yet this reduction was recovered by IL-7 therapy. Furthermore, the T cell's ability to release cytotoxic substances by degranulation was estimated by measurement of CD107a on the T cell's surface. 60-70% of the T cells were $CD107a^+$ (data not shown). We observed a very mild decrease of this frequency in IL-7R-deficient hosts (Fig. 3.17G). IL-7 therapy did not alter these frequencies, indicating that the majority of T cells exhibited cytotoxic function irrespective of IL-7 therapy and host IL-7R signaling.

In conclusion, T cell effector functions as determined by the production of the cytokines IFN-γ and TNF-α and the capacity to release cytotoxic substances from vesicles were not majorly affected by host IL-7R signaling. However, since IL-7 therapy induced a more than 10-fold increase in the number of T cells selectively in immunized Rag^- mice (Fig. 3.15B-C), we conclude that the absolute number of T cells with immediate effector function is highest in IL-7R competent hosts. Moreover, IL-7 therapy and host IL-7R signaling were able to modulate Ag-driven memory T cell differentiation in immunized IL-$7R^-$xRag^- and Rag^- mice. IL-7 therapy increased the number of T_{CM} largely independent of host IL-7R expression, as assessed by the expression of CD62L, KLRG-1 and T-bet.

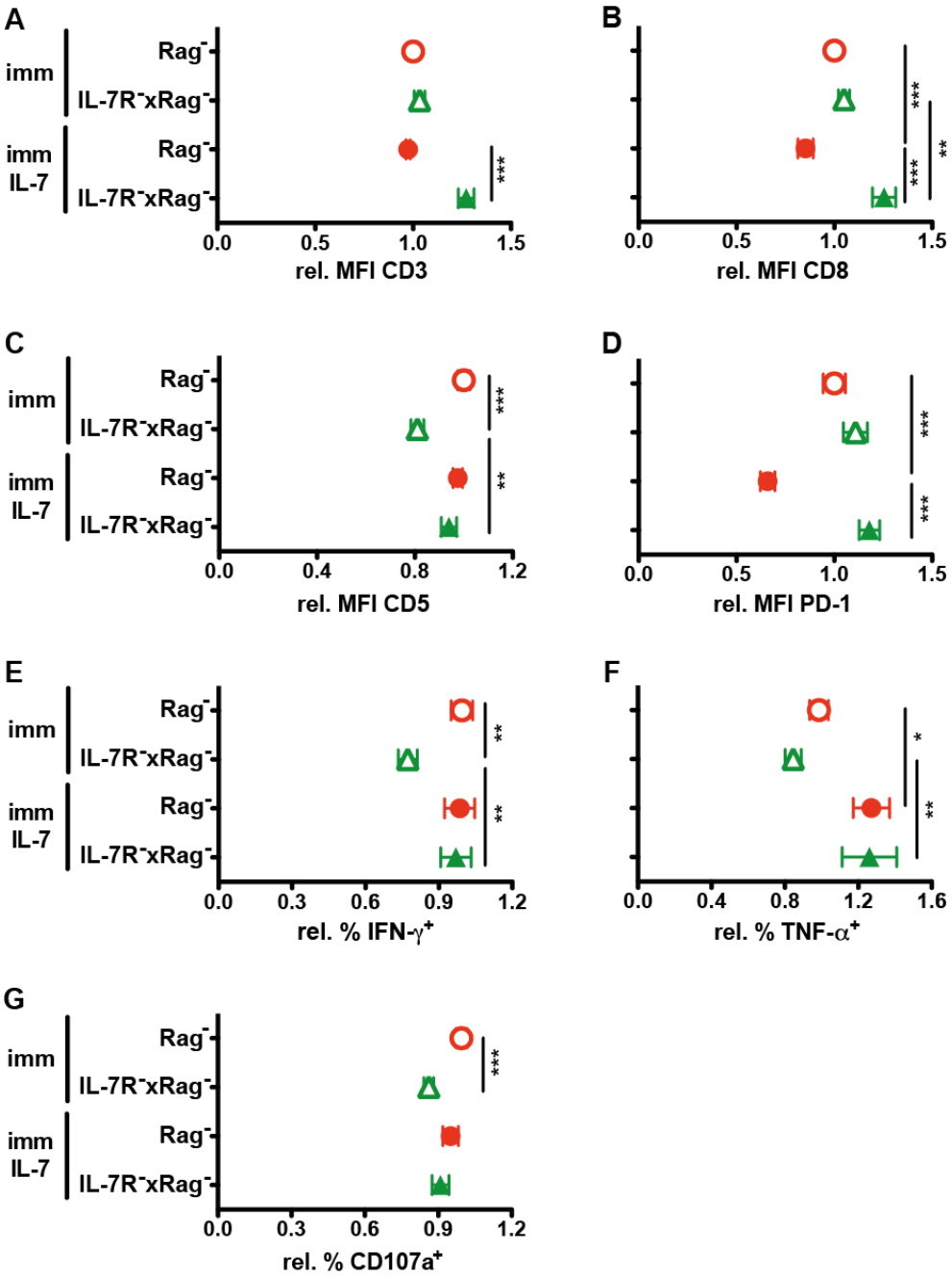

Figure 3.17: T cell effector functions in response to peptide vaccination and IL-7 therapy are independent of host IL-7R signaling.
Rag$^-$ and IL-7R$^-$xRag$^-$ mice received 1x10^6 MACS-purified OT-I T cells i.v. and were immunized with 50 µg SIINFEKL peptide one day after T cell transfer. Additionally, mice received IL-7 therapy (imm+IL-7) or PBS (imm) i.p. every 4 days starting one day prior to T cell transfer. 3 weeks later, OT-I T cells from peripheral blood were analyzed for the relative expression of (A) CD3, (B) CD8, (C) CD5 and (D) PD-1 by flow cytometry. The production of (E) IFN-γ, (F) TNF-α by OT-I T cells and surface levels of (G) CD107a on OT-I T cells were determined after *in vitro* restimulation of PBMCs cocultured with splenocytes from Rag$^-$ mice for 6 h in the presence of 1 µM SIINFEKL peptide, brefeldin A and monensin. Data shown in A-G were normalized to the mean values obtained from PBS-treated (imm) Rag$^-$ mice. Shown are pooled data from (A) 2 independent experiments with a total of 12-13 mice and (B-G) 3 independent experiments with a total of 15-18 mice ±SEM per group.

Additionally, molecules involved in the survival of T cells (IL-7R and Bcl-2) were modulated. Surprisingly, IL-7R expression by host cells is required to induce high IL-7R levels on T cells upon IL-7 therapy. Conversely, increased expression of Bcl-2 and Eomes in OT-I T cells was only observed in IL-7R-deficient hosts after IL-7 therapy. These results suggest that the IL-7R$^+$ host environment together with IL-7 therapy change the memory differentiation and the size of the memory pool.

In a first attempt to identify those host cells involved in the regulation of T cell responses by IL-7, the contribution of the hematopoietic vs. non-hematopoietic host cells was analyzed. Mice were lethally irradiated to replace their hematopoietic system by reconstitution with donor BM cells. As a result, IL-7R expression was restricted either to hematopoietic cells (BM transfer from Rag$^-$ into irradiated IL-7R$^-$xRag$^-$ hosts) or non-hematopoietic cells (BM transfer from IL-7R$^-$xRag$^-$ into irradiated Rag$^-$ hosts). At least 6 weeks post hematopoietic cell reconstitution, MACS-purified OT-I T cells were transferred into BM-chimeric Rag$^-$ and IL-7R$^-$xRag$^-$ animals. One day later, mice were immunized i.v. with SIINFEKL peptide. In addition, they received IL-7 therapy every 4 days starting one day prior to T cell transfer. 3 weeks after transfer, the degree of BM engraftment and the number of CD11b$^+$ myeloid cells, DCs and OT-I T cells were analyzed in spleen. By use of CD45.1 and CD45.2 congenic mice, we were able to discriminate hematopoietic cells from the donor vs. recipient. The pattern of CD45.1 vs. CD45.2 expression by CD11b$^+$ cells showed that the rate of BM engraftment ranged at 97%, demonstrating that the hematopoietic system was replaced efficiently (Fig. 3.18A). We analyzed the splenic cell composition for CD11b$^+$ myeloid cells and DCs, since both cell types regulate T cell responses and their numbers were altered after IL-7 therapy in the absence of ATT (Fig. 3.7C and 3.8A). Splenic CD11b$^+$ myeloid cell and CD11c$^+$MHC-II$^+$ DC numbers were lower in spleens of IL-7R$^-$ BM-reconstituted animals (BM transfer from IL-7R$^-$xRag$^-$ into IL-7R$^-$xRag$^-$ recipients; IL-7R$^-$xRag$^-$→IL-7R$^-$xRag$^-$) compared to all other chimeras (Fig. 3.18B-C). These results show that IL-7R expression by either hematopoietic or stromal cells was sufficient to reach myeloid cell and DC numbers observed in IL-7R-competent mice. OT-I T cell numbers were 15x higher in IL-7R-competent BM-reconstituted mice (Rag$^-$→Rag$^-$) than in IL-7R$^-$ hosts (IL-7R$^-$xRag$^-$→IL-7R$^-$xRag$^-$) (Fig. 3.18D). This finding is also in line with data obtained in non-chimeric mice (Fig. 3.15B). When IL-7R signaling was restricted to non-hematopoietic cells (IL-7R$^-$xRag$^-$→Rag$^-$) T cell numbers were 14x higher compared to the IL-7R-deficient mice. However, when IL-7R signaling was restricted to hematopoietic cells (Rag$^-$→IL-7R$^-$xRag$^-$), T cell numbers were only 5x higher compared to the IL-7R-deficient animals. This indicates that the main mediators of IL-7 therapy-induced T cell expansion are non-hematopoietic cells. Yet, there is also a small but significant influence of IL-7R-expressing hematopoietic cells.

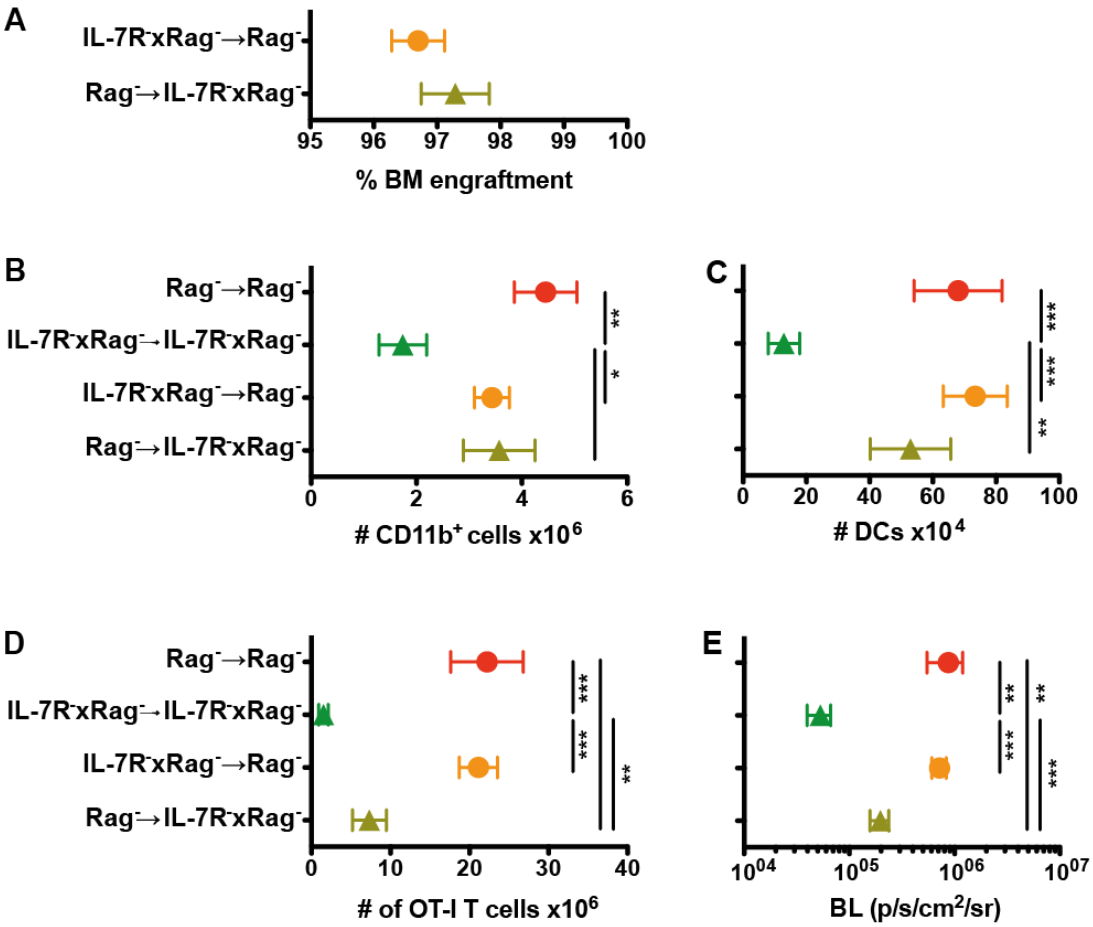

Figure 3.18: IL-7R signaling in non-hematopoietic cells is sufficient for high T cell expansion in response to peptide vaccination and IL-7 therapy.
Lethally irradiated CD45.1$^+$ Rag$^-$ and CD45.2$^+$ IL-7R$^-$xRag$^-$ mice were reconstituted with the indicated bone marrow (BM) cells (BM donor → recipient). At least 6 weeks later, 1x10^6 WT or luciferase-tg MACS-purified CD8$^+$ OT-I T cells were transferred into these BM-chimeras. One day later, mice were immunized i.v. with 50 µg SIINFEKL peptide. IL-7 therapy was applied i.p. every 4 days starting one day prior to T cell transfer. (A-D) The BM-chimeric mice were analyzed 3 weeks after T cell transfer. (A) The degree of BM engraftment was evaluated by determining the frequency of splenic CD11b$^+$ cells expressing donor-specific CD45.1 or CD45.2 by flow cytometry. The numbers of (B) CD11b$^+$ cells, (C) CD11c$^+$MHC-II$^+$ DCs and (D) CD8$^+$ OT-I T cells in spleen were determined. (E) To detect T cell numbers systemically, hosts were treated as described above and 100 µg colenterazine was injected i.v. 6 days after transfer of luciferase$^+$ T cell and total body BL imaging was performed. Shown are pooled data ±SEM of (A-D) 3 or (E) 2 independent experiments with a total of (A-D) 10-17 or (E) 5-10 mice/group.

Furthermore, we wanted to know whether T cell numbers in spleen reflect T cell expansion systemically or whether lymphocytes migrated differently. Therefore, luciferase$^+$ OT-I T cells were transferred into BM-chimeric mice and treated as described above. BL intensities reflecting T cell abundance in the entire body were acquired by *in vivo* imaging 6 days after T cell transfer (Fig. 3.18E). Indeed, splenic T cell numbers correlated with systemic BL intensities from luciferase$^+$ OT-I T cells. These data further underline that non-hematopoietic IL-7-responsive host cells predominantly regulate T cell expansion in response to peptide

vaccination and IL-7 therapy. These results also show that this process is set in the first week after immunization.

Next, the phenotypic changes of the OT-I T cells in spleen were analyzed. Surprisingly, the frequency of $CD62L^+$ T cells was strongly impaired when IL-7R signaling was restricted to the hematopoietic compartment only (Fig. 3.19A). This reveals an unexpected interactive role of IL-7-expressing host cells on CD62L regulation by T cells. The $CD62L^{low}$ phenotype correlated with highest frequencies of KLRG-1^+ OT-I T cell in this group, indicating that memory differentiation and not only CD62L regulation was affected (Fig. 3.19B). Furthermore, the expression of CD127 on OT-I T cells was 2x higher in IL-7R-competent compared to IL-7R-deficient BM-chimeric hosts (Fig. 3.19C). This observation is in line with previous results in non-chimeric animals (Fig. 3.15F). When IL-7R expression was restricted to non-hematopoietic host cells ($IL\text{-}7R^-xRag^-\rightarrow Rag^-$), CD127 expression reached similarly high levels as in IL-7R-competent hosts, indicating that IL-7R-expression by non-hematopoietic cells was sufficient to induce the observed regulation of CD127 on OT-I T cells. Yet, hematopoietic cell-restricted IL-7R expression ($Rag^-\rightarrow IL\text{-}7R^-xRag^-$) also increased CD127 expression on T cells compared to values observed in $IL\text{-}7R^-$ mice, but did not reach levels observed in IL-7R-competent hosts (Fig. 3.19C). Since IL-7R signaling can directly promote Bcl-2 expression (170), its abundance was analyzed next. The expression of anti-apoptotic Bcl-2 by OT-I T cells was lower in hosts, which contained IL-7R-expressing hematopoietic or non-hematopoietic cells compared to $IL\text{-}7R^-$ hosts (Fig. 3.19D). Interestingly, Bcl-2 expression correlated inversely with CD127 expression on T cells, as already shown (Fig. 3.16D). This suggests that IL-7R-signaling in T cells may not be responsible for the observed Bcl-2 regulation. Since Bcl-2 can also be induced by other cytokines binding to receptors of the γ_c-chain family (81, 171), we determined the expression of the γ_c-chain. Indeed we observed a similar pattern of γ_c-chain (CD132) expression as observed for Bcl-2 (Fig. 3.19E). Hence, we suggest that Bcl-2 might be regulated by other γ_c-chain-cytokines than IL-7. Since T_M homeostasis is regulated by IL-7 and IL-15 (69), we speculate that γ_c-chain-dependent IL-15R-signaling might regulate the Bcl-2 levels of the OT-I T cells. Similar to the regulation of Bcl-2, Eomes expression by OT-I T cells was lower in hosts, which contain IL-7R-expressing hematopoietic or non-hematopoietic cells compared to $IL\text{-}7R^-$ animals (Fig. 3.19F). Furthermore, the levels of CD8 and PD-1 were largely dependent on IL-7R expression by non-hematopoietic hosts cells, although hematopoietic cell-expressed IL-7R could also partially downmodulate their expression (Fig. 3.19G-H). These data indicate that non-hematopoietic host cells are the main regulators of OT-I T cell expansion and differentiation after vaccination and IL-7 therapy.

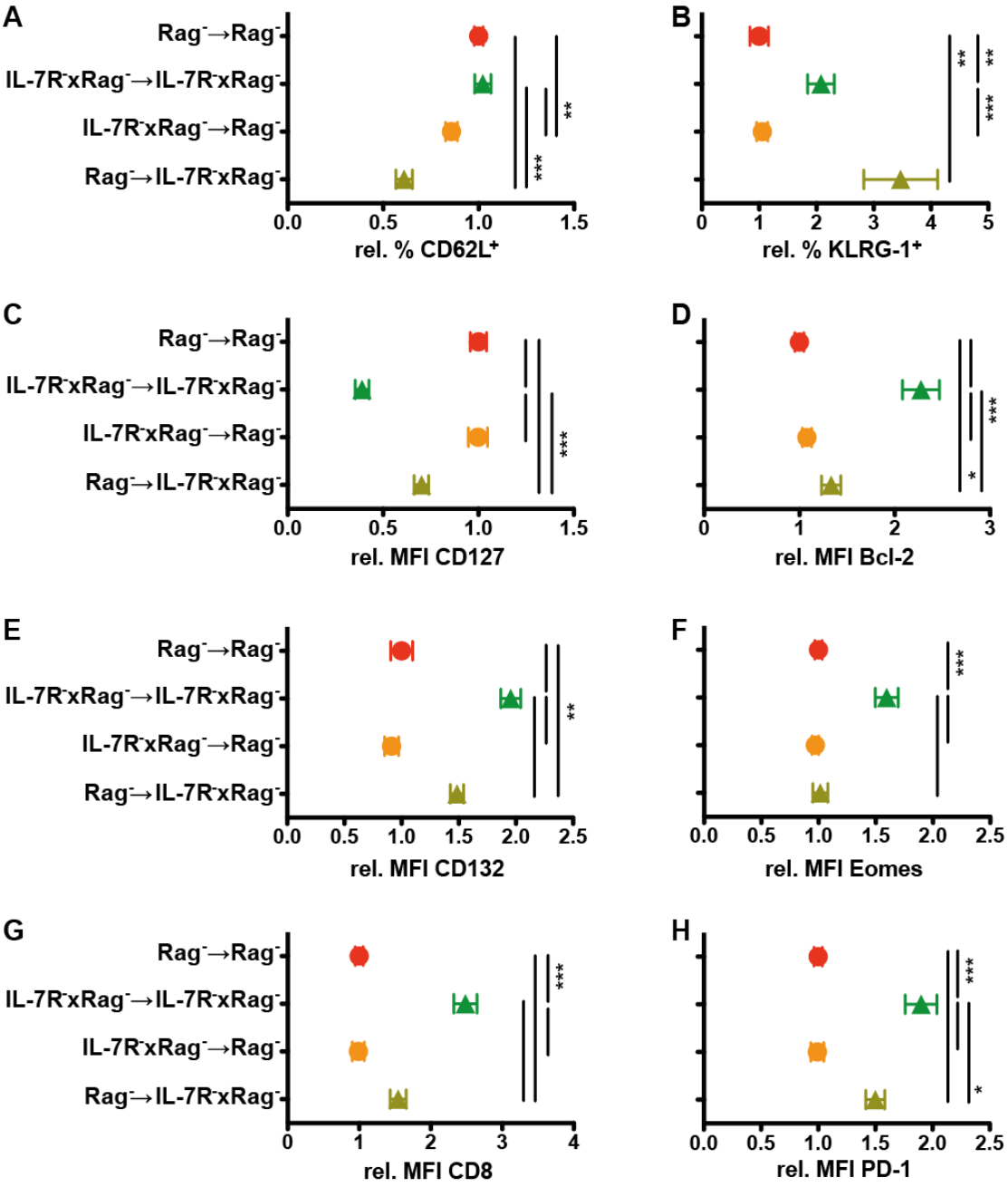

Figure 3.19: IL-7R signaling in non-hematopoietic host cells regulates the memory differentiation of T cell in response to peptide vaccination and IL-7 therapy.
Lethally irradiated Rag$^-$ and IL-7R$^-$xRag$^-$ mice were reconstituted with the indicated bone marrow (BM) cells (BM donor → recipient). At least 6 weeks later, 1x10^6 WT or luciferase-tg OT-I T cells were transferred into these BM-chimeras. One day later, mice were immunized i.v. with 50 µg SIINFEKL peptide. IL-7 therapy was applied i.p. every 4 days starting one day prior to T cell transfer. 3 weeks after T cell transfer, the phenotype of the CD8$^+$ OT-I T cells was analyzed in spleen. The frequency of (A) CD62L$^+$ and (B) KLRG-1$^+$ cells and the expression of (C) CD127, (D) Bcl-2, (E) CD132, (F) Eomes, (G) CD8 and (H) PD-1 were determined by flow cytometry. Data shown in A-H were normalized to mean values obtained from Rag$^-$→Rag$^-$ mice. Shown are pooled data ±SEM of (A-D, F-H) 3 or (E) 2 independent experiments with a total of (A-D, F-H) 10-17 or (E) 4-10 mice/group.

Next we aimed to determine whether the striking differences in OT-I T cell expansion and phenotype after peptide vaccination and IL-7 therapy in IL-7R signaling-competent

vs. -deficient mice affected the response towards tumor cells. Hence, $CD8^+$ OT-I T cells were transferred into both (Rag^- and $IL\text{-}7R^-xRag^-$) hosts and treated as described above. 22 days after transfer, these mice and untreated control groups were challenged s.c. with EG7 tumor cells and tumor outgrowth was monitored. ATT delayed/inhibited tumor outgrowth in comparison to untreated controls (Fig. 3.20A-B). IL-7 therapy did not alter tumor growth in immunized T cell transferred $IL\text{-}7R^-xRag^-$ mice, where tumor growth was prevented in 1/12 and 2/12 mice receiving IL-7 therapy or PBS, respectively (Fig. 3.20A). In contrast, in immunized T cell transferred Rag^- mice, tumor growth was prevented in 6/12 mice receiving PBS, but only in 2/12 mice receiving IL-7 therapy (Fig. 3.20B).

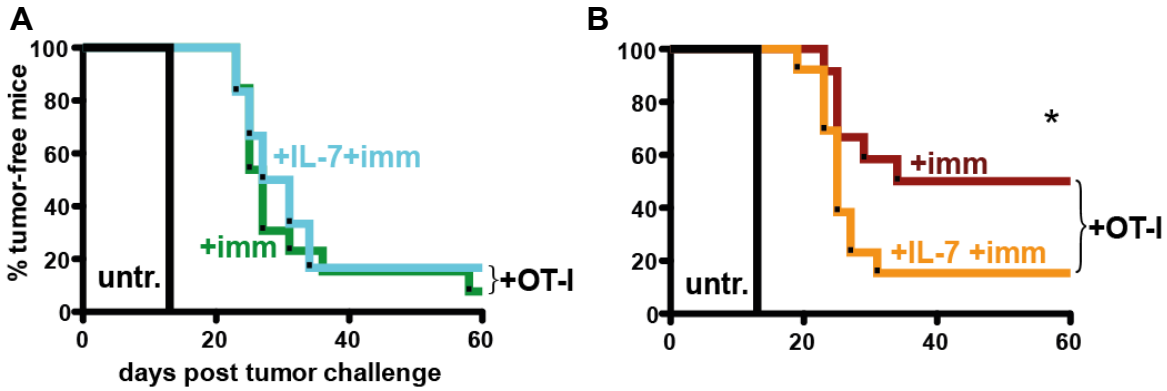

Figure 3.20: IL-7 therapy impairs T cell-dependent tumor rejection in peptide vaccinated Rag^- mice.
$1x10^6$ MACS-purified $CD8^+$ OT-I T cells were transferred into (A) $IL\text{-}7R^-xRag^-$ and (B) Rag^- mice. Hosts were immunized with 50 µg SIINFEKL peptide one day after T cell transfer. Mice received IL-7 therapy (+IL-7+imm) or PBS (+imm) for 19 days every 3-4 days starting one day prior to T cell transfer. Mice were challenged s.c. with $1x10^6$ EG7 tumor cells 22 days after T cell transfer. Mice with tumors larger than 250 mm^3 were scored as tumor positive. Shown are pooled data from 2 independent experiments with a total of 12-13 T cell-reconstituted mice. Primary tumor growth was analyzed in untreated (untr.) $IL\text{-}7R^-xRag^-$ and Rag^- mice (n=3). Statistical significance was calculated using the log-rank test.

Unexpectedly, IL-7 therapy impaired the anti-tumor response in immunized IL-7R-competent mice, reducing the protective effect of T cell therapy from 50% to only 17%. When mice with large tumors were analyzed 4 weeks after tumor challenge, OT-I T cells were still most abundant in previously IL-7-treated, immunized Rag^- mice (Fig. 3.21A). The frequency of $CD62L^+KLRG\text{-}1^-$ T_{CM} and the level of CD127 expression were still higher in IL-7-treated compared to only immunized Rag^- mice (Fig. 3.21B-D). The observed phenotype may suggest that T cells were not able to adopt a secondary effector phenotype in previously IL-7-treated, immunized Rag^- hosts. This would explain the impaired success of ATT in Rag^- mice after immunization and IL-7 therapy.

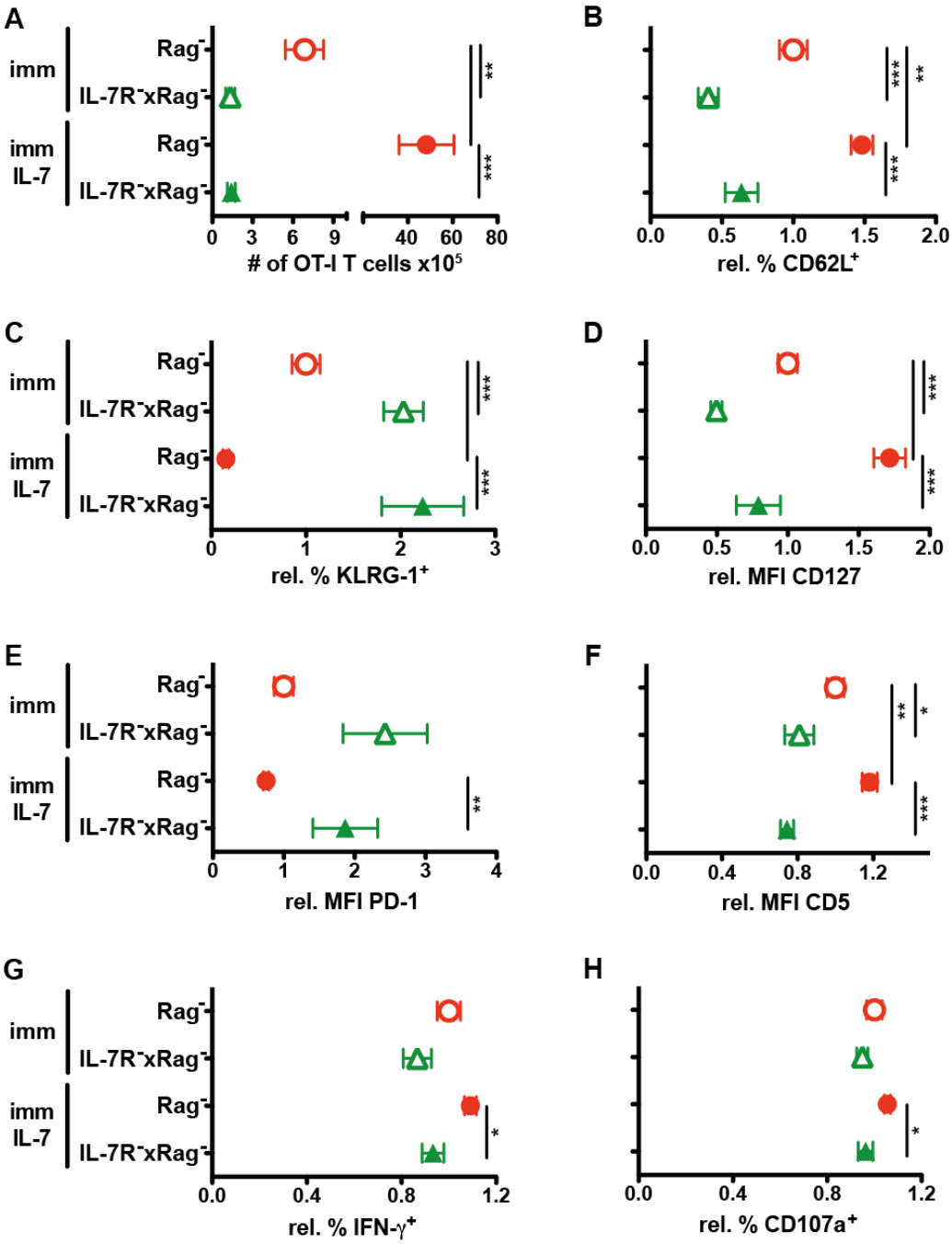

Figure 3.21: IL-7 therapy-induced T cell expanison persists 4 weeks post tumor challenge.
1x10^6 MACS-purified OT-I T cells were transferred into Rag$^-$ and IL-7R$^-$xRag$^-$ hosts. Mice were immunized with 50 µg SIINFEKL peptide i.v. one day after T cell transfer. Additionally, mice received IL-7 therapy or PBS i.p. every 4 days for 19 days starting one day prior to T cell transfer. 3 weeks later, mice were challenged s.c. with 1x10^6 EG7 tumor cells. Splenic cells of tumor-bearing mice were analyzed 28-37 days after tumor cell injection.
Shown are (A) absolute numbers of CD8$^+$ OT-I T cells and frequencies of (B) CD62L$^+$, (C) KLRG-1$^+$ cells within the CD8$^+$ OT-I T cell pool and the relative expression of (D) CD127, (E) PD-1 and (F) CD5 by these OT-I T cells as determined by flow cytometry. The (G) production of IFN-γ and (H) capacity to release cytotoxic granules (as assessed by the surrogate marker CD107a) was determined in OT-I T cells after *in vitro* restimulation of splenocytes for 6 h with 1 µM SIINFEKL peptide in the presence of brefeldin A and monensin. Data shown in B-H were normalized to the mean values obtained from PBS-treated (imm) Rag$^-$ mice. Shown are pooled data from two 2 independent experiments with a total of 6-11 mice ±SEM per group.

Moreover, the level of PD-1 equalized and CD5 expression even increased in previously IL-7-treated compared to only immunized Rag$^-$ hosts (Fig. 3.21E-F). Since CD5 acts as negative regulator of TCR signaling, these results indicate that IL-7 therapy reduced TCR responsiveness in Rag$^-$ hosts. This could also help to explain why IL-7 therapy impaired anti-tumor responses of OT-I T cells in immunized Rag$^-$ hosts. However, after short-term *in vitro* restimulation with the cognate peptide SIINFEKL, more than 80% of OT-I T cells from Rag$^-$ mice were able to produce IFN-γ and degranulate (based on the frequency of CD107a$^+$ cells) (Fig. 3.21G-H). Yet, it is unclear whether those cells efficiently reached the tumor, since they did not readopt an effector phenotype.

In conclusion, the detrimental effect of IL-7 therapy in immunized mice is in stark contrast to the situation in unimmunized hosts, where T cells underwent LIP and were activated by very weak TCR stimuli through self-peptides (Fig. 3.13C). Here, tumor growth was prevented by IL-7 therapy in 58% of the IL-7R-competent hosts but only in 10% of the group receiving T cells only. These data suggest that IL-7 therapy can act like a “double-edged sword” either promoting or impairing the anti-tumor function of adoptively transferred T cells in an IL-7-responsive lymphopenic environment. More importantly, the data presented in Figure 3.10-21 also strongly suggest that IL-7 influences host cells that critically modulate the numbers and differentiation of adoptively transferred CD8$^+$ OT-I T cells in lymphopenic conditions.

In summary, the data obtained for this thesis show that next to direct effects of IL-7 therapy on adoptively transferred T cells, IL-7-responsive non-hematopoietic host cells mainly regulate the expansion and the memory differentiation of the therapeutic CD8$^+$ OT-I T cells after peptide vaccination. IL-7-responsive host cells are needed for successful ATT against cancer after peptide immunization. However, the therapeutic success of peptide immunization and ATT is impaired by concomitant IL-7 therapy, despite highly efficient T cell expansion. Yet, in the absence of peptide vaccination, IL-7 therapy promotes the success of ATT against cancer exclusively in IL-7-responsive hosts. In conclusion, the IL-7-responsive host environment and the availability of Ag crucially affect the success of IL-7-assisted ATT against cancer. We show that IL-7 therapy affects DCs, myeloid and *il-7*-expressing stromal cells. Since non-hematopoietic host cells mainly regulate the expansion and the memory differentiation of the therapeutic CD8$^+$ OT-I T cells after peptide vaccination, we suggest that *il-7*-expressing stromal cells modulate the success of ATT.

4 Discussion

IL-7 is an essential cytokine for development and maintenance of lymphocytes (60). IL-7 levels must be balanced tightly, on the one hand, to transmit sufficient survival signals to the T cell pool in order to eliminate pathogens and malignant cells and, on the other hand, to limit unwanted T cell activation and subsequent tissue damage. Despite its non-redundant role in T cell homeostasis, only a limited set of data describes the sites of IL-7 production, how IL-7 expression is regulated and which other host cells are affected by IL-7 signaling. Most importantly, it remained completely unknown whether the success of IL-7-assisted adoptive T cell therapy against cancer is dependent on IL-7-mediated signals in host cells.

4.1 The IL-7GCDL mouse - powerful tool to understand the regulation of *il-7* gene expression and to manipulate *il-7*-expressing cells

In order to determine which cells produce IL-7, immunohistochemistry for IL-7 in various organs, gene expression analysis of purified cell subsets or generation of IL-7 reporters is required. Since *il-7* is only expressed at a low level and high-quality antibodies are not available for murine IL-7, immunohistochemical identification of IL-7 producing cells is not reliable (64). From experiments using BM-chimeric IL-7^{-} mice, it was deducted that most IL-7-producing cells belong to the non-hematopoietic compartment (70). The purification of non-hematopoietic cells from tissues is a tedious, time-consuming process involving enzymatic digestion steps. Thus this method is accompanied by loss of sensitive cell subsets, and may alter gene expression profiles in the remaining cells. Therefore, it is not the preferred way to analyze IL-7 production. To overcome these obstacles, the IL-7GCDL reporter mouse was generated, in which expression of eGFP, DNA recombinase Cre, DTR and luciferase are controlled by the IL-7 promoter. Although eGFP mRNA expression was detectable, the fluorescent eGFP reporter protein could not be visualized by flow cytometry or immunostaining (63). We hypothesize that eGFP expression does not cross the detection limit due to low *il-7* promoter activity. In fact, low sensitivity of fluorescing BAC-transgenic IL-7 reporter mice was also reported by others, where only cells expressing *il-7* at high levels were fluorescing strong enough to allow direct or anti-fluorophore-antibody-mediated detection (64, 66). In contrast to eGFP, the activity of the reporter protein luciferase was well detectable by BL imaging *in vivo*. Since a single luciferase molecule can catalyze many reactions leading to light emission, it amplifies the reporter signal and hence leads to high reporter sensitivity. However, BL imaging has some caveats. The availability of cofactors such as Magnesium ions, oxygen and adenosintriphosphate can affect the reporter accuracy *in vivo* (172). Besides, the imaging procedure needs to be standardized precisely, since substrate distribution and metabolism restrict the time window when luciferase-catalyzed light emission is stable. In addition, the light signal cannot penetrate all tissues and gets quenched by hemoglobin (173). This means that the same organs from different mice can be

compared well. Yet, direct comparison of e.g. the dark-red spleen and light lymph node is inaccurate. Despite these limitations, luciferase activity proved to be a reliable reporter for *il-7* expression in organs, as we showed that it closely mimicked endogenous *il-7* gene expression (63). Two independently generated mouse lines were analyzed and compared. Both lines showed a similar pattern of reporter activity comparing different organs, but one mouse line had overall stronger BL activity, most likely due to higher copy number of the transgenic reporter (Fig. 3.1). With help of the *il-7* promoter-driven luciferase activity of the IL-7GCDL mouse, we identified various distinct tissues that contain *il-7* expressing cells. We detected high expression of *il-7* in the thymus and thereby confirmed data obtained by use of other IL-7 reporter mice and RNA *in-situ* hybridization (64–66, 142, 174). Moreover, we showed that due to its size, the intestine is a large source of IL-7 in the body. Additionally, we also affirmed *il-7* expression from LNs and skin, and detected *il-7* expressing cells in lung, which has hardly been described as source of IL-7 (Fig. 3.4) (63, 65, 174, 175). Next to the very high sensitivity of BL imaging, its major advantage lays in the fact that BL intensities reflect the expression from a region of interest such as the lung, which contains rather immobile *il-7* producing stromal cells. When, for instance during an infection, leukocytes infiltrate the organ, these infiltrates can lead to falsely low relative *il-7* RNA levels, since they lead to an increase of the RNA amount per organ. However, infiltrating cells do not interfere with the level of BL detected from the whole organ. This example emphasizes the benefits of the luciferase reporter, especially for analyzing the regulation of stromal cell-derived molecules like IL-7. Moreover, the mildly invasive *in vivo* imaging procedure (as substrate injection, short anesthesia) of the luciferase reporter mice allows observing *il-7* gene regulation during the course of an experiment, such as drug treatment or an immune response against an infection and will thus facilitate studies on organ-specific regulation of *il-7* gene expression.

Moreover, *il-7* promoter-controlled expression of the DNA-recombinase Cre allowed tracking of *il-7* producers on the single cell level. We crossed the IL-7GCDL mouse to the loxP-Tag mouse (138) to label and amplify rare *il-7* producing cells. Hence, with help of the IL-7GCDLxloxPTag mouse, identification and long-term culture of the rare *il-7* producing cells was facilitated. We established Tag^+ cell cultures from primary and secondary lymphoid organs but also from non-lymphoid tissues like lung and pancreas, indicating that these tissues contain *il-7* producing non-hematopoietic cells (Fig. 3.4). Interestingly, to my knowledge, *il-7* production from the pancreatic tissue has not been deeply investigated so far. However, recently published data show that blockade of IL-7R signaling by administration of IL-7R-specific Abs can ameliorate the phenotype of autoimmune diabetes in mice (125). Such systemically active therapeutic interventions impair T cell function in general and can therefore not be applied to patients. Since we detected *il-7* expressing cells

in the pancreas, we propose to test more specific therapies in order to inhibit local *il-7* production by pancreatic cells. To identify selective inhibitors of *il-7* production, the newly generated cell lines from IL-7GCDLxloxPTag mice might be particularly useful (Fig. 3.4).

Since *il-7* promoter-driven Cre expression was highly effective in thymic stroma, we focused on the analysis of these cells. Several studies showed high *il-7* expression from thymic epithelium by use of IL-7 reporter mice or gene expression studies (64–66, 142). In our model, we additionally detected *il-7* promoter-driven Cre-activity in thymic fibroblasts (Fig. 3.5). Furthermore, we detected reporter-expressing fibroblasts in lymph nodes but not in spleen, indicating that *il-7* expression may vary in different SLOs or fibroblast subsets (Fig. 3.4). These data are similar to results from a second BAC-tg mouse in which IL-7 regulatory elements drive expression of Cre (65). Our results indicating *il-7* expression by fibroblasts from thymus and lymph nodes are further supported by recent reports. These reports include gene expression profiles from sorted stromal subpopulations and studies based on two newly generated knock-in mice, where the endogenous *il-7* promoter drives *gfp* expression (174–177).

Comparing the novel IL-7 reporter GFP knock-in mice to the IL-7GCDL mouse, the data indicate that the knock-in mice provide higher reporter sensitivity than the IL-7GCDL mouse. Besides differential reporter protein stability, it cannot be excluded that the BAC-derived promoter region does not contain all *il-7* regulatory elements or that structures around the unknown genomic integration sites affect reporter activity. These concerns are largely excluded by the knock-in technology. However, the knock-in disrupts *il-7* gene function and hence leads to lower amounts of IL-7 in these mice. This results in partial lymphopenia and limits the usability of these mice especially in studies involving IL-7-dependent cells like T cells (175). In contrast, the BAC-transgenic IL-7GCDL mouse shows normal development of the immune system (Fig. 3.2-3.3) and normal *il-7* expression (63) emphasizing that these mice allow studies on the interplay of immune cells and their environment.

In conclusion, the IL-7GCDL mouse allows identification, tracing and manipulation of *il-7*-expressing cells and will subsequently help to further unravel the function of IL-7 and of its producers. Better understanding of these processes will help to develop therapies to ameliorate progression of autoimmune disorders by e.g. inhibition of IL-7 signaling. Alternatively, therapies increasing IL-7 availability or triggering of its downstream molecules may help to drive immune reconstitution in lymphocyte-depleted patients and improve immune responses against chronic infections or even cancer.

4.2 IL-7-expressing host cells decrease *il-7* gene activity in response to IL-7 therapy

One possibility to increase IL-7 availability is certainly to administer exogenous recombinant IL-7. However, it has been suggested that IL-7 signaling regulates IL-7 production by lymphoid stromal cells *in vivo* (91). The hypothesis is based on measurements of *il-7* gene

activity in splenic stroma after IL-7 treatment or ablation. It implicates that the host counterbalances high IL-7 availability by decreasing *il-7* gene expression. Since we detected IL-7R expression on the anatomically and developmentally very distinct intestinal epithelial cells (Fig. 3.6), we wanted to extend the analysis to all putatively involved tissues. Therefore we decided to study the effect of IL-7 application on *il-7* gene activity systemically by determining the luciferase activity in IL-7GCDL mice. Indeed, a single injection of IL-7 downmodulated *il-7* reporter expression by 25% within 24 h (Fig. 3.6). This decline does not decisively interfere with systemic IL-7 levels since therapeutic doses still cause supraphysiological IL-7 serum levels, as shown in a human preclinical trial (134). However, since it was suggested that the protein mainly binds locally to extracellular matrix proteins (178), IL-7 therapy may alter local gradients of IL-7 availability. Whether this affects the homeostasis of IL-7-responsive cells has not been investigated so far. A second open question is whether IL-7 signaling regulates the expression of other molecules besides IL-7 in *il-7*-producing stromal cells that in turn influence T cell homeostasis.

So far, only few studies addressed the effect of IL-7 on *il-7*-expressing cells, partially because their identity has remained largely unknown. Since it was demonstrated that fibroblastic reticular cells in lymph nodes, (175, 176, 179), thymic fibroblasts (Fig. 3.5) and bone marrow mesenchymal stem cells (180) can produce *il-7* mRNA, it is conceivable that fibroblasts from many organs have this capacity. As essential and frequent components of tissue structure throughout the entire body, fibroblasts constitute a vital target for IL-7 therapy. Indeed, first reports described that IL-7 treatment inhibited transforming growth factor-beta (TGF-β)-induced collagen synthesis from pulmonary fibrosis fibroblasts *in vitro* and *in vivo* (181, 182). Under physiologic conditions, collagen can bind chemokines and thus create a chemokine gradient, that may affect migration of leukocytes (183) and hence T cell homoestasis. Besides fibroblasts, endothelial cells can likewise produce and respond to IL-7 *in vitro* (184–186). Treatment of human aortic endothelial cells with IL-7 increased expression of monocyte chemoattractant protein-1 (MCP-1), intercellular adhesion molecule-1 (ICAM-1) and VCAM-1, which enhanced recruitment of monocytes (185). Recently published data also show that IL-7 is produced by lymphatic endothelial cells (LECs) and supports their growth and function (118). Lymphatic drainage was suggested to contribute to peripheral tolerance by delivering self-Ag to lymph node–resident leukocytes in the steady state. However, LECs can also directly act as APCs by scavenging and cross-presenting exogenous Ags. This causes dysfunctional activation of $CD8^+$ T cells and thereby contributes to peripheral tolerance (187, 188). So far, it has not been investigated whether IL-7 therapy can alter immune responses by affecting LEC growth and function. Yet, it is well-accepted that lymphatic drainage of soluble Ags and migration of APCs via lymphatics are pivotal for initiation of protective immune responses (189, 190).

In conclusion, our results show that IL-7-producing cells react to IL-7 treatment, which leads to decreased *il-7* expression *in vivo.* So far, we have not analyzed in detail which cell types react to IL-7 and which other molecules are affected by IL-7 therapy. However, fibroblasts, blood and lymphatic endothelial cells have already been described as putative cell types producing and responding to IL-7. All of these stromal cells interact with leukocytes. Hence IL-7 therapy may affect T cell homeostasis indirectly via its action on stromal cells.

4.3 IL-7 therapy induces T cell-independent enlargement of the spleen

The effect of IL-7 therapy on leukocytes was first tested in spleens of T cell-deficient hosts. IL-7 therapy led to an IL-7R-dependent enlargement of the spleen, which mostly consisted of myeloid cells (Fig. 3.7). Since myeloid cells develop independently of IL-7 in the steady state and myeloid cell counts do not increase in blood of IL-7-treated patients, the increased numbers of myeloid cells in spleen is presumably indirect and might involve processes like chemoattraction (104, 134, 185). Enlargement of the spleen after IL-7 therapy has also been detected in other studies involving T cell-competent mice and humans (134, 149). Since LIP and Ag-induced activation of T cells is controlled by DCs (105, 191), we also wanted to study whether they reacted to IL-7 therapy. DC numbers increased upon IL-7 therapy in spleens of Rag^- mice (Fig. 3.8A). Since most mature DCs do not express the IL-7R, it is assumed that they do not respond to IL-7. Yet, IL-7 signaling was shown to increase DC numbers by driving the development of DC subsets, presumably from IL-7-dependent common lymphoid progenitors (104). Interestingly, the proportion of $CD8^-$ cells within the DC pool was elevated in PBS-treated Rag^- compared to $IL\text{-}7R^-xRag^-$ animals (Fig. 3.8C). This small but significant effect of steady-state IL-7 signaling has, to my knowledge, not been described before. It suggests that basal host IL-7 signaling affects the generation of these cells. In contrast, it was already shown that IL-7 signaling downmodulates MHC-II on DCs and this observation correlated with reduced LIP of $CD4^+$ T cells (91). We extended these findings from IL-7 signaling-deficient mice to the clinically relevant setting of IL-7 therapy (Fig. 3.8D). The fact that DCs from $IL\text{-}7R^-xRag^-$ inherently express lower levels of MHC-II shows that other factors regulate its expression. Since the IL-7Rα chain is utilized by the IL-7R and the TSLPR (thymic stromal lymphopoietin receptor) (192), the lack of TSLPR-signaling may contribute to the observed phenotype. Indeed, it has already been shown that treatment of isolated DCs with TSLP causes MHC-II upregulation *in vitro* (193, 194). Thus, absence of TSLPR-signaling in $IL\text{-}7R\alpha^-$ animals might be causal for the low MHC-II expression by DCs. Yet other indirect mechanisms cannot be excluded. Besides MHC-II expression, CD54 and CD86 were also downmodulated on DCs from Rag^- mice after IL-7 therapy (Fig. 3.8E-F), while expression of CD40 and MHC-I remained unaffected (Fig. 3.8G-H). The decreased expression of important molecules for T cell stimulation by IL-7-treated DCs may affect their capacity to efficiently elicit T cell responses. On the other hand, increased DC numbers in

spleens of IL-7-treated Rag$^-$ mice may counterbalance the phenotypic changes and increase homeostatic proliferation and responsiveness to foreign Ag (105, 195). Therefore, it was tested whether IL-7 therapy mediates its effects on T cells via host cells including DCs.

4.4 IL-7-responsive host cells and IL-7 therapy affect the memory formation of adoptively transferred T cells

IL-7 signals in CD8$^+$ T cells are essential for LIP (70). However, it was unknown whether IL-7 signaling in non-T cells contributes to the modulation of LIP. To answer this question, OT-I T cells were transferred into Rag$^-$ and IL-7R$^-$xRag$^-$ hosts. Based on the recovered cell number 3 weeks after transfer and traced frequency of divisions 5 days after transfer, OT-I T cells underwent LIP similarly well in both hosts, indicating that IL-7R$^-$xRag$^-$ mice are suitable to separate the effects of IL-7 therapy on T cells exclusively from effects on the host and T cells (Fig. 3.9-3.10). IL-7 therapy increased the rate of division in both hosts equally well (Fig. 3.10B-C), indicating that proliferation is independent of host IL-7R-mediated signals and hence also independent of the DC phenotype and numbers. Interestingly, 11 days after transfer, OT-I T cells accumulated more in spleens of IL-7R$^-$xRag$^-$ recipients and IL-7 therapy enhanced this difference (Fig. 3.11B). This host IL-7R-regulated effect was transient and not observed 3 weeks after transfer (Fig. 3.11D). Since some lymph nodes in IL-7R$^-$xRag$^-$ mice are smaller sized or even absent (110, 112), it is possible that limited space in LNs alters distribution and increases OT-I T cell frequencies in spleen early after transfer. When we analyzed the phenotype of the OT-I T cells 3 weeks after transfer, we observed lower frequencies of CD62L$^+$ T_{CM} cells in spleens of IL-7R-competent Rag$^-$ recipients (Fig. 3.12A). Together with higher frequencies of KLRG-1$^+$ T_{EM} / T_{SLEC} cells (Fig. 3.12B), our data indicate that homing or differentiation of adoptively transferred T cells is regulated by IL-7-responsive host cells. IL-7 therapy increased not only the number of T cells but also the frequency of T_{CM} cells in IL-7R-competent and -deficient recipients, suggesting that IL-7 therapy enhances T_{CM} cell differentiation and/or proliferation. Higher T_M cell numbers were also observed in other studies applying IL-7 to mice and humans, but a shift towards T_{CM} has only been observed in some studies (132, 133, 149, 157, 196). However, the involved signaling pathways have largely remained unclear. It was shown that IL-7 signaling can lead to AKT activation that is able to decrease FOXO1 activity and thus lower CD62L expression in T cells (94, 95, 101). Accordingly, strong AKT activation by high-dose IL-7 treatment leads to low CD62L levels (197). Remarkably, it was demonstrated that the IL-7 therapy regime used in this study consisting of IL-7 in a complex with an IL-7-neuralizing Ab is highly potent *in vivo* because it decreases rapid consumption of IL-7 (198). Thus, it can be considered as weak but persistent signal. Indeed, it was shown that this treatment actually increases FOXO1 activity (197). In consequence, the tightly balanced contact to IL-7 can explain why we detected higher frequencies of CD62L$^+$ T cells after IL-7 therapy and why results are inconsistent in

this field. Similar to CD62L, also the expression of CD127 is regulated by FOXO1 (101). Therefore it is not surprising that CD127 expression was also elevated after 3 weeks of IL-7 therapy (Fig. 3.12C). Yet, in contrast to CD62L, the regulation of CD127 was not affected by IL-7-responsive host cells. Bcl-2 expression is induced by IL-7R-signaling in T cells (81). Indeed, others and we detected higher Bcl-2 levels in T cells after IL-7 therapy (Fig. 3.12D) (133, 157). Interestingly, Bcl-2 levels were also controlled by IL-7R-competent host cells, as its levels were lower in T cells transferred into IL-7R^{+} recipients. This could be due to lower IL-7 levels in these mice (91). However, since host IL-7R signaling affected Bcl-2 levels even in the presence of IL-7 therapy, we suggest that IL-7 availability is not the main environmental factor controlling Bcl-2 expression. In summary, we showed that over a period of 3 weeks, the number and phenotype of adoptively transferred T cells was modulated by IL-7 therapy, which promoted the accumulation of or differentiation to T_{CM} cells in lymphopenic conditions. Remarkably, this development was partially compromised in IL-7R-competent hosts, indicating that host IL-7R signaling may counteract IL-7 signaling-induced processes in T cells.

4.5 IL-7 therapy-assisted anti-tumor ATT depends on IL-7-responsive host cells

Since the memory phenotype of T cells was influenced by host IL-7R signaling and IL-7 therapy, we aimed to determine the T cell effector function. After short-term *in vitro* stimulation with cognate peptide, the capacity to produce IFN-γ was mildy increased in T cells that were transferred into IL-7R^{-}xRag^{-} mice (Fig. 3.12E). In IL-7-treated animals however, this difference was not observed. In contrast, other groups observed stronger IFN-γ production upon IL-7-mediated signaling both, *in vitro* and *in vivo* (102, 122, 199, 200). One possible explanation for this discrepancy is that in our study, the T cells were stimulated with high doses of Ag to determine the total response capacity. This might have masked differences in T cell responsiveness. Moreover, T cells were transferred into lymphopenic mice that already contain elevated amounts of IL-7 (91). Thus the threshold for enhancing IFN-γ production might have already been reached. Furthermore, long-term cytotoxic function of the transferred T cells was assessed by challenge of the previously IL-7-treated or untreated T cell recipients with the Ag-expressing tumor cell line EG7. Tumor growth was delayed in all therapeutic T cell-containing animals. However, the group that received IL-7 therapy and expressed the IL-7R on host cells was significantly better protected than all other groups (Fig. 3.13B-C). We anticipated that IL-7 therapy would improve anti-tumor responses, as it promoted T_{CM} generation which was shown to mediate protection from tumor growth (58, 59) and increased T cell numbers that persisted for 4 weeks in tumor-bearing hosts (Fig. 3.14A). Other groups also reported a beneficial effect of IL-7 administration on anti-tumor and anti-viral responses in preclinical models (130, 131, 201). Unexpectedly, our results showed that IL-7 therapy did only improve anti-tumor responses in IL-7R-competent

hosts, indicating that IL-7-assisted anti-tumor therapy is dependent on the IL-7-responsive environment. This observation is surprising because T cell numbers and phenotype ($CD62L^{+}KLRG\text{-}1^{-}Bcl\text{-}2^{high}CD127^{high}$) pointed to at least equally strong anti-tumor responses in $IL\text{-}7R^{-}xRag^{-}$ compared to Rag^{-} hosts (Fig. 3.11D, 3.12). However, only the IL-7R signaling-competent Rag^{-} mice profited from IL-7 therapy with significantly decreased tumor incidence. The question emerges whether T cell responses are in general impaired in $IL\text{-}7R^{-}xRag^{-}$ compared to Rag^{-} animals, e.g. due to developmental defects in some SLOs needed for initiating immune responses (117). However, tumor growth was delayed/inhibited to a similar extent in PBS-treated Rag^{-} and $IL\text{-}7R^{-}xRag^{-}$ mice compared to animals that had not received T cells (Fig. 3.13B-C), suggesting that T cell functionality was retained in $IL\text{-}7R^{-}$ hosts. Yet, it cannot be excluded that the $IL\text{-}7R^{-}$ environment altered tumor cell settling, growth or persistence. Notably, IL-7 was reported to induce proangiogenic factors, which in turn could facilitate nutrient supply but also entry of immune cells modulating tumor growth (202, 203). However, IL-7 administration during the growth phase of the EG7 tumor did not reveal any influence of IL-7 availability on tumor growth in our experimental system (Fig. 3.13A). Despite that, careful analysis of tumor growth kinetics revealed a slightly faster tumor growth rate in most experiments involving $IL\text{-}7R^{-}xRag^{-}$ compared to Rag^{-} hosts that had not received OT-I T cells (Fig. 3.13A). This suggests that the absence of IL-7R-signaling in host cells enhances tumor cell settling or growth. In conclusion, the presented data strongly indicate that the beneficial effect of IL-7 therapy on anti-tumor ATT is dependent on an IL-7R-competent host environment.

4.6 IL-7-responsive host cells and IL-7 therapy affect the memory differentiation of adoptively transferred T cells after peptide vaccination

Using a model of pancreatic cancer, it was shown that IL-7 therapy only promotes anti-tumor T cell responses when the animals were vaccinated with the cancer Ag (98). Thus, in order to further improve anti-tumor T cell responses, we tested the combination of IL-7 treatment with peptide vaccination. The model also provided the opportunity to compare the potency of IL-7 cytokine stimulation after strong TCR stimulation to results obtained from weakly self-peptide-stimulated T cells undergoing LIP.

When mice were vaccinated with the cognate peptide of OT-I T cells one day after transfer, higher T cell numbers were recovered from spleens and blood of Rag^{-} compared to $IL\text{-}7R^{-}xRag^{-}$ hosts 3 weeks after immunization. Concomitant IL-7 therapy massively enhanced T cell accumulation in immunized Rag^{-} animals, but surprisingly, did only mildly raise T cell numbers in $IL\text{-}7R^{-}xRag^{-}$ hosts (Fig. 3.15B-C). This observation is in contrast to data obtained during LIP, were T cells expanded equally well in both hosts in response to weak self-peptide-MHC contacts (Fig. 3.11D). These data suggest that T cell priming with a strongly stimulating dose of Ag is impaired in $IL\text{-}7R^{-}$ mice. This constraint becomes more prominent in

the presence of IL-7 therapy, indicating that IL-7 signaling in T cells cannot compensate for impaired Ag-mediated priming.

Moreover, we analyzed the phenotypic changes that occurred in transferred T cells 3 weeks after peptide vaccination in the early memory phase. IL-7 therapy increased the frequency of $CD62L^+$ T cells while it decreased the percentage of KLRG-1^+ OT-I T cells in both hosts, indicating that IL-7 therapy promoted T_{CM} cell survival / differentiation directly (Fig. 3.15D-E, 3.16A). This effect of IL-7 therapy on Ag-experienced T cells was also reported in non-lymphopenic mice after viral infection (133, 196). In contrast to observations from unimmunized mice (Fig. 3.12A), the IL-7-responsive host environment did not modulate the frequency of Ag-experienced $CD62L^+$ T_{CM} cells (Fig. 3.15D-E). Yet, it lowered the percentage of KLRG-1^+ T_{SLEC} / T_{EM} cells (Fig. 3.16A). Opposing results on the regulation of KLRG-1 were obtained in unimmunized hosts (Fig. 3.12B), which indicates that signals mediated by weak vs. strong TCR stimulation together with signals from the IL-7-responsive host drive distinct differentiation or survival processes in T cells. Another example for the stimulation- and host-modulated effects on T cell differentiation is the regulation of the T_M-development-associated molecule CD127. Its levels increased on OT-I T cells in immunized IL-7-treated Rag^- recipients (Fig. 3.15F-G), but remained low in IL-$7R^-$xRag^- mice. These data differ from results obtained in unimmunized animals, where CD127 regulation was independent of host IL-7R expression (Fig. 3.12C). Moreover, we detected decreased levels of the inhibitory receptor PD-1 on OT-I T cells in IL-7-treated, vaccinated Rag^- hosts (Fig. 3.17D). This finding is supported by previously published reports (98, 204). However, IL-7 therapy did not cause decreased PD-1 levels on T cells in IL-$7R^-$xRag^- recipients, affirming that the IL-7-responsive host modulates effects of therapeutic IL-7 on T cells. In conclusion, we show that for the generation of therapeutic T_M cells with a long-lived $CD127^{high}KLRG\text{-}1^{low}PD\text{-}1^{low}CD62L^{high}$ phenotype, IL-7 therapy has to engage host cells. This unexpected and to my knowledge novel finding implies that some aspects of T cell differentiation or survival are controlled by the IL-7-responsive host environment. This hypothesis is supported by other observations, for instance: IL-7 therapy decreased T-bet levels in T cells in immunized IL-7R-competent and -deficient animals equally well (Fig. 3.16B). The decreased expression of T-bet together with increased frequency of $CD62L^+$ cells indicates that IL-7 therapy activated FOXO1 in the transferred T cells (197, 205), irrespective of IL-7-responsive host cells. However, in the same conditions, IL-7 therapy increased Bcl-2 expression exclusively in IL-$7R^-$ hosts (Fig. 3.16D). Together, we conclude that signals from the IL-7-responsive host environment, together with TCR signaling intensity, cause divergent T cell differentiation.

4.7 IL-7-responsive non-hematopoietic host cells are the main regulators of memory differentiation after peptide vaccination and IL-7 therapy

To determine which IL-7-responsive host cells mediate the distinct effects on T cell expansion and differentiation, BM-chimeras were generated using Rag^- and $IL\text{-}7R^-xRag^-$ mice. To achieve highest resolution for the effects of host cells on T cells, the treatment with strongest differences in T cell numbers was chosen. Therefore chimeric mice were treated with peptide vaccination and IL-7 therapy. Equally to non-chimeric animals, higher T cell numbers were detected when hematopoietic and non-hematopoietic host cells were $IL\text{-}7R^+$ than when both host cell populations were $IL\text{-}7R^-$ (Fig. 3.18D-E). IL-7R-expression by the non-hematopoietic compartment was sufficient to reconstitute T cell numbers. Furthermore, IL-7R expression restricted to the hematopoietic compartment resulted in low, but significantly higher T cell numbers than in the $IL\text{-}7R^-$ host. In conclusion, non-hematopoietic cells critically affect T cell expansion. To a lesser extent, hematopoietic host cells are also involved. Additionally, we showed that the effect on T cell accumulation is occurring systemically and already very prominent 6 days after immunization, indicating that the early Ag-driven expansion is affected by IL-7 responsive host cells (Fig. 3.18E).

Moreover, the T cell phenotype was analyzed. CD127 expression was enhanced in presence of $IL\text{-}7R^+$ host cells, weakly in hosts with hematopoietic cell-restricted IL-7R, and strongly in hosts with non-hematopoietic cell-restricted IL-7R expression (Fig. 3.19C). This indicates that mainly non-hematopoietic IL-7-responsive host cells regulate the level of CD127 expression on transferred T cells or their survival. We also analyzed the expression of the γ_c-chain (CD132), which pairs with CD127 to form the IL-7R heterodimer (79). Although described as stable or ubiquitous (75, 80), it was shown that CD132 surface levels can be modulated, for instance after T cell stimulation (206). We detected an inverse relationship of CD132 to CD127 expression (Fig. 3.19C, E) and again observed that IL-7-responsive non-hematopoietic host cells act as main regulators of CD132 expression. What could drive this differential expression? IL-15 is a main regulator of memory T cell survival and self-renewal and its receptor contains the γ_c-chain (69). Hence high CD132 levels on T cells might facilitate IL-15 signaling. IL-15 was shown to decrease CD127 levels but increase expression of the anti-apoptotic molecule Bcl-2 (81, 207). Interestingly Bcl-2 expression was highest in T cells with lowest CD127 levels, indicating that IL-15 signaling could causally link our observations (Fig. 3.19C, D). Furthermore, high Bcl-2 levels correlated with high Eomes expression (Fig. 3.19D, F). As Eomes induces the IL-2/15Rβ-chain, CD122 (160, 208), it might have contributed to the suggested sensitivity of the OT-I T cells for IL-15 in $IL\text{-}7R^-$ animals.

In conclusion, the data presented so far strongly indicate that IL-7 therapy acts not only on T cells but also on host cells. IL-7-responsive non-hematopoietic host cells majorly affect the

expansion and differentiation of adoptively transferred T cells that proliferated strongly in response to peptide vaccination and IL-7 therapy in lymphopenic conditions.

4.8 Vaccination-assisted anti-tumor ATT depends on IL-7 responsive host cells

We evaluated the therapeutic potential of OT-I T cells expanded in vaccinated and IL-7-treated IL-7R$^+$ animals and compared them to cohorts that did not receive IL-7 therapy or were transferred into IL-7R$^-$ recipients. In line with data obtained in unimmunized animals (Fig. 3.13B), the transferred T cells delayed tumor outgrowth compared to untreated control mice, but the majority of immunized T cell-transferred IL-7R$^-$xRag$^-$ mice did not control tumor outgrowth, irrespective of IL-7 therapy (Fig. 3.20A). In contrast, the transferred OT-I T cells blocked tumor growth in 50% of immunized Rag$^-$ mice, indicating that IL-7-responsive host cells support T cell-mediated tumor cell rejection (Fig. 3.20B). Surprisingly, the group of immunized, T cell transferred Rag$^-$ hosts that additionally received IL-7 therapy was less well protected against tumor outgrowth. These data are in contrast to results obtained with unimmunized mice (Fig. 3.20B vs. 3.13C), indicating that the success of IL-7 therapy-assisted anti-tumor treatment is modulated by TCR-mediated T cell differentiation. Despite strong accumulation of T cells in the IL-7-treated, immunized Rag$^-$ group, these T cells did not sufficiently eliminate tumor cells. The reason for the impaired function is unclear, as T cells reisolated from spleens of mice with large tumor burden were still functional (Fig. 3.21G-H). T cells were also initially able to migrate to the site of tumor growth, recognize and kill tumor cells, as they delayed tumor outgrowth in all groups compared to non-T cell-transferred cohorts. Subsequently, T cells in the tumor microenvironment might have lost functionality or died. Alternatively, certain T cell subsets were shown to promote tumor growth by affecting host or tumor cells (209, 210). Hence, it is possible that immunization combined with IL-7 therapy led to a distinct differentiation and cytokine release that fostered growth of the remaining tumor cells. When comparing the phenotype of these T cells, we detected very low frequencies of KLRG-1$^+$ T cells in IL-7-treated vaccinated Rag$^-$ hosts (Fig. 3.21C). Since KLRG-1$^+$ cells belong to the T_{SLEC} / T_{EM} subset, which migrate more efficiently to non-lymphoid organs, they may have an advantage in detecting the s.c. injected tumor cells. Thus, when combined with immunization, IL-7 therapy might restrict T cell plasticity and inhibit conversion of memory cells to secondary, cytotoxic effector T cells that would eradicate tumor burden. These results show that IL-7 therapy is like a mixed blessing, but also demonstrate that the success of ATT against cancer is dependent on IL-7-responsive host cells.

4.9 Conclusions

To summarize, this study demonstrates that IL-7-responsive host cells can affect the numbers, the phenotype and anti-tumor function of adoptively transferred T cells in Rag$^-$

mice. The regulatory capacity of IL-7-responsive host cells is dependent on the mode of T cell activation. When T cells differentiate by contact to homeostatic cytokines and self-peptides during LIP, the IL-7R$^+$ host does not regulate T cell numbers, but impedes differentiation to long-lived T_{CM}. In this situation, IL-7 therapy promotes T_{CM} generation and expands the T cells largely independent of host IL-7R engagement. When T cells differentiate in response to strong Ag-stimulation by peptide vaccination in lymphopenic conditions, T cell expansion is promoted better in the IL-7-responsive host than in IL-7R$^-$ T cell recipients. Additional IL-7 therapy increases T cell numbers strongest in the IL-7-responsive environment. This host-mediated effect correlates with highly increased CD127 expression and low frequencies of terminally differentiated KLRG-1$^+$ cells among the therapeutic T cell population. In mice receiving peptide vaccination combined with IL-7 therapy, IL-7-responsive non-hematopoietic cells mainly regulated T cell expansion and differentiation. To a lesser extent, hematopoietic cells also contributed. Long-term function of the therapeutic T cells was assessed by challenge with an Ag-expressing tumor cell line. It revealed that protection from tumor growth is dependent on IL-7-responsive host cells. Surprisingly, IL-7 therapy promoted survival of mice when the transferred T cells had only received weak self-Ag-mediated TCR signals, but impaired survival when mice were vaccinated early after transfer and T cells thereby had received strong TCR signals. In conclusion differential TCR signaling combined with IL-7R-mediated signals in T cells regulated divergent memory differentiation. Surprisingly, IL-7-responsive host cells crucially affected these processes and in consequence, therapeutic efficacy of the adoptively transferred T cells. This study extends the current knowledge of how IL-7 therapy influences the success of adoptive T cell therapy against cancer. It proposes to focus investigations on the involved non-hematopoietic host cell types and mechanisms to develop more selective strategies of immune modulation via host cells and thereby improving therapeutic success. Our knowledge about non-hematopoietic host cell - T cell interactions and their role in regulation of immune responses is very limited. It was recently shown that lymph node stromal cells inhibit proliferation of activated T cell by mechanisms involving direct cell contact (211). The immune-regulatory stromal cells were identified as fibroblastic reticular cells (FRCs) and LECs. Both cell types produce IL-7 and can also respond to it (118, 181, 182). FRCs expand after vaccination. This process is mainly dependent on DC-induced trapping of naive lymphocytes (212), indicating that stromal cell - T cell interactions are bidirectional. We link DC frequency to IL-7 signaling as we showed that DC numbers in spleen are regulated by both hematopoietic and non-hematopoietic IL-7 responsive host cells. Interestingly, it was also shown that IL-7 therapy-induced homeostatic T cell proliferation was sufficient for FRC expansion (212). In light of these data and results

obtained in this work, we propose that IL-7 signaling links T cell to stromal cell homeostasis and thereby critically regulates T cell responses and the success of ATT against cancer.

5 Materials and methods

5.1 Materials

5.1.1 Equipment and software

Equipment	Company
Centrifuge Megafuge 1S-R	Heraeus-Thermo Scientific
Centrifuge Pico 17	Heraeus-Thermo Scientific
Flow Cytometer FACSCalibur	BD Biosciences
Flow Cytometer Canto II	BD Biosciences
Flow Cytometer LSR Fortessa	BD Biosciences
Gel Dokumentation Herolab E.A.S.Y	Herolab
IVIS Imaging System Series 200	Xenogen
Magnetic Cell Sorter AutoMACS	Miltenyi Biotech
Mastercycler Gradient	Eppendorf
Microscope Axioplan 200	Zeiss
Microscope Leica DM-RE	Leica
Microwave	Severin
PCR Machine T3000 Thermocycler	Biometra
qPCR Machine iCycler	Biorad
Thermal shaker Thermomix Compact	Eppendorff

Software	Company
Adobe CS6	Adobe Systems Software
AxioVision Release 4.5	Zeiss
FlowJo 8	TreeStar
Living Image 2.6	Xenogen
Prism	GraphPad Software Inc.
SPOT Advanced	SPOT Imaging Solutions

5.1.2 Reagents

Substance	Company
7-AAD Viability Staining Solution	BD Biosciences / Biolegend
Agarose peqGold	PeqLab
Biocoll	Biochrom
Borgal	Virbac Tiergesundheit
Colenterazine	Biosynth
Collagen G	Biochrom

Collagenase D	Roche
Collagenase P	Roche
Crystal 5x DNA loading buffer blue	Bioline
CFSE	Invitrogen
D-luciferin	Synchem OHG
DMSO	Sigma-Aldrich
DAPI (4,6-Diamidino-2-Phenylindole)	Carl Roth
DNase I	Roche / Sigma-Aldrich
dNTP	Applied Biosystems / Carl Roth
Dispase II	Roche
Dimitridazole	Sigma-Aldrich
Doxocyclin	Sigma-Aldrich
DMEM	Gibco
Easy Ladder I	Bioline
Easycoll	Biochrom
Epithelial growth factor	BioVision
Ethidium Bromide	Carl Roth
Fetal calf serum (FCS)	PAN Biotech
G418	Carl Roth
Gelatine 45% from cold water fish skin	Sigma-Aldrich
Golgi Plug	BD Biosciences
Golgi Stop	BD Biosciences
Glycerol for molecular biology	Sigma-Aldrich
Heparin Sodium Salt	Applichem
Hexanucleotide mix	Roche
Hydrocortisone	Sigma-Aldrich
Insulin, human	Sigma-Aldrich
Interleukin-7, murine, carrier-free	eBioscience
Ketamin (Ketavet)	Pharmacia
LPS from E.coli serotype 0111:B4	Sigma-Aldrich
Lymphoprep	Axis-Shield
NaCl 0,9%	Delta Pharma
Non-essential amino acids 100x	Gibco
Orange G	Sigma-Aldrich / Applichem
Platinum Taq DNA Polymerase	Invitrogen
Penicillin / streptomycin	Gibco
Primocin	Amaxa

Proteinase K	Sigma-Aldrich
Recombinant mouse IFNγ	R&D Systems / Biolegend
Rompun	Bayer Health Care
RPMI 1640	Gibco/Millipore
SIINFEKL (95%)	Biosynthan
Sugar	supermarket
Superscript II reverse transcriptase	Invitrogen
TaqMan Universal PCR Master Mix	Applied Biosystems
Tissue Tek OCT compound	Sakura Finetek
Transferrin	Gibco
Vectashield Mounting Medium	Vector Laboratories
Whatman 3MM paper	Sigma-Aldrich

Kit	**Company**
Cytofix/Cytoperm Fixation/Permeabilization Solution Kit	BD Biosciences / Biolegend
FASER Kit-APC	Miltenyi Biotech
Foxp3 / Transcription Factor Staining Buffer Set	eBioscience
Rnase-Free DNase Set	Qiagen
Rneasy Mini Kit	Qiagen

Antibody	**Clone**	**Company**
B220	RA3-6B2	BD Biosciences
Bcl-2	10C4	Biolegend
CD106	429	BD Biosciences
CD107a	1D4B	BD Biosciences / Biolegend
CD11b	MI70	Biolegend/ BD
CD11c	N418	BD Biosciences / Biolegend
CD127	A7R34	BD Biosciences / Biolegend
CD132	TUGm2	BD Biosciences
CD16/CD32 Fc block	2.4G2	BD Biosciences / own production
CD19	1D3	eBioscience
CD19	6D5	Biolegend
CD326	G8.8	BD Biosciences / Biolegend
CD4	GK1.5	BD Biosciences
CD4	RM4-5	Biolegend
CD40	HM40-3	Biolegend
CD44	IM7	BD Biosciences / eBioscience / Biolegend
CD45	30-F11	BD Biosciences / Biolegend
CD45.2	104	BD Biosciences / Biolegend

CD49b	DX5	Biolegend
CD5	53-7.3	BD Biosciences / eBioscience
CD54	3E2	BD Biosciences
CD62L	MEL-14	BD Biosciences / Biolegend
CD69	H1.2F3	BD Biosciences / Biolegend
CD71	R17217	eBioscience
CD71	R17217	Biolegend
CD80	16-10A1	BD Biosciences / Biolegend
CD86	GL-1	BD Biosciences / Biolegend
CD8a	53-6.7	BD Biosciences / eBioscience / Biolegend
CD90.1	OX7	BD Biosciences / Biolegend
CD90.2	30H12	BD Biosciences / Biolegend
CD90.2	53-2.1	BD Biosciences / Biolegend
DX5	DX5	BD Biosciences
Eomes	Dan11Mag	eBioscience
gp38	8.1.1	Biolegend
Gr1	RB6-8-C5	Biolegend
H2kb	AF6-88.5	Biolegend
I-Ab	AF6-120.1	Biolegend
IFN-γ	XMG1.2	eBioscience
Ki-67	SolA15	eBioscience
KLRG1	2F1	eBioscience
IL-7	M25	BioXCell
Ly51	BP-1	BD Biosciences
PD1 (CD279)	J43	eBioscience
SV40 Ag	Pab 108	BD Biosciences
T-bet	4B10	Biolegend
TER119	TER119	Biolegend
TNF-α	MP6-XT22	BD Biosciences
Vα2	B20.1	BD Biosciences
Cytokeratin 5/8	RCK102	BD Biosciences
anti-hamster IgG		Southern Biotech / Invitrogen
anti-rabbit IgG		Invitrogen
anti-rat IgG		Invitrogen
anti-rat IgG2a		Southern Biotech

Microbeads	**Clone**	**Isotype**	**Company**
α-mouse CD8α	53-6.7	Rat IgG2a, κ	Miltenyi Biotech

PCR primers for genotyping	**Sequence**
Rag1 oIMR1746 WT Forward	5'-GAG GTT CCG CTA CGA CTC TG-3'
Rag1 oIMR3104 WT Reverse	5'-CCG GAC AAG TTT TTC ATC GT-3'
Rag1 oIMR8162 MT Forward	5'-TGG ATG TGG AAT GTG TGC GAG-3'
IL-7R 119 WT Forward	5'-CTT TTA CGA GTG AAA TGC CTA ACT C-3'
IL-7R 120 WT Reverse	5'-CAG GTA TGA TTC AAG AAT GCA ATA CA-3'
IL-7R 121 MT Reverse	5'-CAC GGC TAG CCA ACG CTA TGT C-3'
Luciferase Forward	5'-GGC CTT TGA TAC ACA GCT CG-3'
Luciferase Reverse	5'-ACC GTC TTG GTC TAC T TG CCT-3'

Primer and probes for RNA expression analysis

Luciferase Forward	5'-GGC CTT TGA TAC ACA GCT CG-3'
Luciferase Reverse	5'-ACC GTC TTG GTC TAC T TG CCT-3'
Luciferase-TaqMan probe	6-FAM-CCAAGATTATGAAGTCCGCAGTGTCATCAA-TMR

TaqMan primer and probes for RNA expression analysis

IL-7	Mm 00434291_m1	Applied Biosystems
HPRT	Mm 00446968_m1	Applied Biosystems
Actb	Mm 00607939_s1	Applied Biosystems

5.1.3 Mouse strains

Strain name	Common name	Provider / Breeding facility
B6.SJL-Ptprca Pep3b/BoyJ	CD45.1 / WT	Charles Rivers
B6.129S7-Rag1^{tm1Mom}	Rag^{-}	JAX
B6.129S7-Rag1^{tm1Mom}/JxB6.SJL-Ptprca Pep3b/BoyJ	CD45.1xRag^{-}/ Rag^{-}	FEM Berlin
B6.129S7-Il7r^{tm1Imx}/J	IL-7R^{-}	JAX
B6.129S7-Rag1^{tm1Mom}/JxB6.129S7-Il7r^{tm1Imx}/J	IL-7R^{-}xRag^{-}	FEM Berlin
IL-7GCDL	IL-7GCDL	DKFZ Heidelberg
OT-IxB6.PL-Thy1a/Cy	OT-I	DKFZ Heidelberg
OT-IxB6.PL-Thy1a/CyxB6.129S7-Rag1^{tm1Mom}/J	RagOT-I	FEM Berlin
OT-IxChRLuc	ChRLuc-OT-I	T. Blankenstein MDC Berlin
LoxP-Tag	LoxP-Tag	G. Willimsky MDC Berlin

All mouse strains were on a C57BL/6 background. Mice were bred under specific pathogen-free conditions at Charite Berlin, Campus Benjamin Franklin in the Research Institute for Experimental Medicine (FEM), at Max-Delbrueck-Center Berlin-Buch (MDC) or at Otto-von-Guericke University Magdeburg in the Central Animal Laboratory (ZTL).

5.1.4 Buffers and media

<u>(Ammonium-Chloride-Potassium) ACK solution</u>

0,1 mM Na_2EDTA
10 mM $KHCO_3$
155 mM NH_4Cl
pH: 7,2-7,4

<u>Anesthetic Ketamin/Rompun</u>

Ketamin 34 mg/ml
Rompun 2,4 mg/ml
NaCl 0,9%

Antibiotics mix 1

4 g Dimitridazole

0,012% Borgal

15 g sugar

1 l of drinking water

Antibiotics mix 2

0,2 g Doxycycline

50 g sugar

1 l of drinking water

pH: 2,8-3,0

Coelenterazine

Coelenterazine ampulla (0,5mg powder in controlled atmosphere at -20°C)

150µl DMSO solvent

450µl PBS diluent

Prepared freshly and used within 10 min

D-luciferine

15 mg/ml D-luciferin

1x PBS

Stored as 1,5ml aliquots at -20°C

Epithelial cell medium

DMEM

10% FCS

2 mM L-Glutamine

1 mM Na-Pyruvate

1x non-essential amino acids

20 ng/ml epithelial growth factor

6 ng/ml transferrin

6 ng/ml insulin

1 µg/ml hydrocortisone

50 µM ß-Mercaptoethanol

100 µg/ml Primocin or 100 U/ml Penicillin / 100 µg/ml Streptomycin

Loading buffer for PCR reactions

0,2% w/v Orange G (practical grade)

30% v/v Glycerol

70% v/v H_20

1x PBS

1,7 mM NaH_2PO_4

6,5 mM Na_2HPO_4

154 mM NaCl

pH: 7,2-7,4

1x PBS + 2 mM EDTA

1x PBS

2 mM EDTA

pH: 7,2-7,4

1x PBS + 2 mM EDTA + 0,5% BSA

1x PBS + 2 mM EDTA

0,5% BSA w/v

pH: 7,2-7,4

PBS-Heparin solution

1x PBS

5000 U/l Heparin

0,03% NaN_3

Standard medium

RPMI 1640

10% FCS

100 U/ml Penicillin / 100 µg/ml Streptomycin

T cell medium

Standard medium

2 mM L-Glutamine

1 mM Na-Pyruvate

50 µM β-Mercaptoethanol

T cell stimulation medium

T cell medium

1 µg/ml SIINFEKL

1/1000 dilution of GolgiPlug for IFN-γ and TNF-α detection

1/1000 dilution of GolgiStop for CD107a detection (in addition to GolgiPlug)

Tail Buffer

200 mM NaCl

100 mM Tris/HCl pH: 8,5

5 mM EDTA

0,2% SDS

50x TAE buffer

242 g Tris

57 ml Acetic Acid

100 ml 0,5 M EDTA pH: 8,0

TE buffer

10 mM Tris/HCl pH 8

1 mM EDTA pH: 8,0

Tissue digestion medium I

RPMI 1640

10% FCS

100 U/ml Penicillin / 100 µg/ml Streptomycin

1 mg/ml Collagenase D

1 mg/ml Dispase II

100 µg/ml DNAse I

Tissue digestion medium II

RPMI 1640

10% FCS

100 U/ml Penicillin / 100 µg/ml Streptomycin

0,2 mg/ml Collagenase D

0,2 mg/ml Dispase II

10 µg/ml DNAse I

5.2 Methods

5.2.1 Molecular biology methods

5.2.1.1 Isolation of genomic DNA from mouse-tail biopsies

Tail (or ear) biopsies were taken from 3-6 week old mice and frozen at -20°C until DNA extraction. Biopsies were digested with 5 µl of Proteinase K (20 mg/ml) in 600 µl Tail Buffer for at least 4 hours at 56°C and 350 rpm in a thermal shaker. Digested tails were then centrifuged at 13800 g for 5 min. In order to precipitate the DNA, the supernatant was transferred into a new tube containing 600 µl of 2-propanol. The sample was inverted for at least 10x before the sample was centrifuged at 13800 g for 10 min. The supernatant was removed and then, 600 µl of 70% ethanol was added to the tube. The sample was again centrifuged at 13800 g for 10 min. After removal of the supernatant, the DNA pellet was allowed to air-dry before it was dissolved in 50-300 µl TE buffer for 1hour at 68°C and 350 rpm using a thermal cycler.

5.2.1.2 Genotyping of mice by polymerase chain reaction

Transgenic and knockout mice were genotyped by polymerase chain reaction (PCR). In order to amplify a segment of DNA, it is first heated to denature, and separate the DNA into two pieces of single-stranded DNA. Next, complementary short DNA sequences called primers, bind to the DNA region of interest allowing the enzyme Taq polymerase to synthesize two new strands of DNA. The cycle of denaturing and synthesizing new DNA is repeated as many as 40 times, leading to more than one billion exact copies of the DNA segment of interest, making it easy to e.g. determine the genotype of mice.

IL-7R^{-} mice were generated by insertion of a neomycin resistance cassette into exon 3 of the IL-7Rα-chain creating a non-functional gene (151). PCR was performed using a mix of 3 primers amplifying an 850 bp fragment from wild-type (WT) DNA and a 950 bp fragment from mutant DNA allowing the discrimination of IL-7R WT, heterozygous or knockout mice. The Rag^{-} mouse was developed by replacement of a genomic fragment of the Rag1 gene by a neomycin cassette leading to a non-functional gene (213). The presence of the mutant allele was confirmed by PCR using 3 primers amplifying a 474 bp fragment from WT DNA and a 530 bp fragment from mutant DNA allowing the discrimination of Rag WT, heterozygous or knockout mice. IL-7GCDL mice were analyzed for the presence of luciferase cDNA using 2 transgene-specific primers amplifying a 478 bp fragment. The described fragments were generated from approximately 100 ng of DNA using the components and conditions described below:

PCR Mix	Luciferase	Rag	IL-7R
Component	Volume (µl)	Volume (µl)	Volume (µl)
H_2O	9,95	9,95	9,35
10x-Puffer	2	2	2
$MgCl_2$ (50 mM)	2	2	2
dNTPs (2,5 mM)	2	1	1,6
Primer 1 (10 µM)	1	1	1
Primer 2 (10 µM)	1	1	1
Primer 3 (10 µM)		1	1
Loading buffer	1	1	1
Taq polymerase	0,05	0,05	0,05
DNA	1	1	1

Table 5.1: PCR master mix reagents used to amplify transgenic luciferase cDNA as well as wild-type and mutant Rag1 and IL-7Rα gene segments.

PCR	Luciferase		Rag		IL-7R		
Steps	T (°C)	time (s)	T (°C)	time (s)	T (°C)	time (s)	
Polymerase activation	94	120	94	120	95	180	
DNA denaturation	94	30	94	30	95	30	⎫
Primer annealing to DNA	69,2	30	58	45	66	30	⎬ 35x
DNA extension	72	60	72	45	72	60	⎭
Final DNA elongation	72	300	72	120	72	300	
Final hold	10	unlimited	10	unlimited	10	unlimited	

Table 5.2: Thermal cycler settings used to amplify transgenic luciferase cDNA as well as wild-type and mutant Rag1 and IL-7Rα gene segments.

5.2.1.3 Agarose gel electrophoresis

1,5%-3% w/v agarose gels were prepared by boiling agarose with 100 ml 1x TAE buffer in a microwave. After cooling the agarose solution to ca. 55°C, 0,5 µg/ml Ethidium Bromide was added and the gel was casted. Alternatively, the gel was stained with 1 µg/ml Ethidium Bromide for 20 min after electrophoresis was completed. The gel was transferred to an electrophoresis apparatus prefilled with 1x TAE buffer. As a DNA size indicator, 5 µl of “DNA Ladder” (100-2000 bp range) was loaded into a lane. The gel was run at 120 V for 45 min. Then, the gel was analyzed under UV light.

5.2.1.4 Preparation of total RNA and cDNA

Cultured cells were lysed with 600 µl RLT buffer (Qiagen). The samples were homogenized using a 1ml syringe and a 20G needle. Total RNA was isolated by use of the Qiagen RNeasy Mini Kit according to the manufacturers recommendations. Genomic DNA was removed on-column using the RNase-free DNase Set. RNA was eluted in RNase-free water and its concentration as well as purity was measured. For cDNA synthesis, 1 µg RNA was incubated

in 10 µl RNase-free water at 70°C for 10 min in a thermal cycler before addition of the cDNA master mix as described below:

Component	**Volume (µl)**
5x RT (first strand) buffer	4
20 mM dNTPs	1
0,1 M DTT	2
10x Random Hexamers	2
Superscript II RT	1

Table 5.3: Master mix reagents used to transcribe 1 µg RNA in 10 µl H_20 into cDNA.

cDNA synthesis		
Steps	**T (°C)**	**time (min)**
RNA denaturation (1 µg RNA in 10 µl H_20)	70	10
Addition of master mix	4	1-2
Primer annealing to RNA	25	10
cDNA synthesis	42	45
Polymerase inactivation	99	3
Final hold	4	unlimited

Table 5.4: Thermal cycler temperature settings used to transcribe RNA into cDNA.

5.2.1.5 Quantification of mRNA expression

Quantitative PCR (qPCR) is used to analyze the amount of RNA expressed in tissues or cells in comparison to stably expressed RNA from a so-called housekeeping gene, whose expression should not change upon e.g. a treatment of interest. In principle, the same techniques are applied as mentioned above, however, the template is reverse transcribed mRNA, so-called cDNA. In this work, TaqMan-probe-based assays were used to analyze specific amplification products. The oligonucleotide probe contains a reporter fluorescent dye on the 5' end and a quencher dye on the 3' end. While the probe is intact, the proximal quencher dye inhibits the emission of fluorescence by the reporter dye by fluorescence resonance energy transfer. Since the probe is designed to bind downstream of the primer site, it is cleaved by the 5' nuclease activity of Taq polymerase as the primer is extended. The cleavage leads to the separation of the reporter dye from the quencher dye, increasing the reporter dye signal, which is detected in every PCR cycle. Additional reporter dye molecules are cleaved from their probes with each cycle, resulting in an increase in fluorescence intensity proportional to the amount of amplicon produced. Relative expression of the gene of interest was normalized to *hprt* or *Actb* (*β-actin*). The fold difference (as relative mRNA expression) was calculated by the comparative CT (cycle threshold) method, where the CT value is determined as the number of cycles needed to detect the first fluorescence signal over threshold in the logarithmic phase of fluorescence intensity growth.

Relative expression level: $2^{\Delta CT}$

$\Delta CT = CT_{\text{housekeeping gene}} - CT_{\text{gene of interest}}$

The TaqMan assay for *il-7* and the housekeeping gene *hprt* or *β-actin* were obtained from Applied Biosystems. TIB MOLBIOL customized the qPCR assay for Luciferase mRNA quantification. The master mixes were distributed in triplicates into 96-well RT-PCR plates and 1µl of the cDNA sample was added per well. The qPCR components and cycle conditions are described below:

Component	**Volume (µl)**
2x TaqMan universal PCR master mix	12,5
DNase & Rnase-free water	10,25
20x primers and probe mix	1,25

Table 5.5: QPCR master mix reagents used to amplify *hprt, β-actin* or *il-7* cDNA segments.

RNA denaturation	**T (°C)**	**time (s)**	
Polymerase activation	95	600	
cDNA denaturation	95	15	] 40x
DNA extention	60	60	
Final hold	4	unlimited	

Table 5.6: Thermal cycler temperature settings used to amplify *hprt, β-actin* or *il-7* cDNA segments.

Component	Volume (µl)
H_2O	10,3
10x-Puffer	2
$MgCl_2$ (50 mM)	2
dNTPs (2 mM)	1
Primer 1 (10 µM)	1
Primer 2 (10 µM)	1
Probe (10 µM)	1
BSA 10 µg/ml)	1
Taq polymerase	0,2
cDNA	1

Table 5.7: QPCR master mix reagents used to amplify *luciferase* cDNA segments.

Temperature (°C)	Time (s)	
94	300	
94	30	] 40x
66,6	30	
72	30	
4	unlimited	

Table 5.8: Thermal cycler temperature settings used to amplify *luciferase* cDNA segments.

5.2.2 Cell biological methods

5.2.2.1 Preparation of cells from different tissues

Preparation of leukocytes from blood

Blood was taken from the facial vein of mice, mixed with 100 µl PBS-heparin or 6 µl of 0,5 M EDTA solution and RPMI 1640 before layering it onto Lymphoprep or Biocoll solution. The blood samples were then centrifuged at 600 g for 20 min at room temperature (RT) and without brake. Since peripheral blood mononuclear cells (PBMCs) have a lower density than erythrocytes, they can be separated by centrifugation on appropriate density gradient medium. More dense erythrocytes sediment through the medium while less dense mononuclear cells are retained on top. PBMCs were then collected in new tubes, washed with 1x PBS containing 2 mM EDTA and centrifuged at 2400 g for 5 min and used for labeling with Ab. Alternatively, 50-100 µl of blood mixed with EDTA was directly used for labeling with 50 µl of Ab mix and then erythrocytes were lysed by adding 1-2 ml of red blood cell lysis solution from BD Biosciences for 20 min at RT in the dark. Then cells were washed once with 2ml of PBS containing 2 mM EDTA and used for flow cytometric analysis.

Preparation of single cell suspensions from spleen and lymph nodes

The spleen as well as brachial and inguinal lymph nodes were removed and stored in 2 ml PBS containing 2 mM EDTA on ice. The spleen or the 4 LNs together were forced through metal sieves with a plunger of a 10 ml plastic syringe. With the help of a 20G needle on a 10 ml syringe, the visible tissue lumps were further disaggregated by repeated aspiration and release of the suspension. The tools were washed with PBS containing 2 mM EDTA in order to retrieve all cells from the respective tissues. Then, the single cell suspension was transferred into a 15 ml tube and centrifuged at 468 g for 5 min at 4°C before resuspending them in 1x PBS containing 2 mM EDTA for cells from lymph nodes or lysis of erythrocyte for splenic cells.

Preparation of single cell suspension from bone marrow

The femurs of mice were removed and stored in 2 ml 1x PBS containing 2 mM EDTA on ice. Then, the bones were cleaned from muscle tissue and both ends were cut off in order to insert a 22G needle and flush out the bone marrow with 1x PBS containing 2 mM EDTA. Then, the cell suspension was transferred into a 15 ml tube and centrifuged at 468 g for 5 min at 4°C before erythrocytes were lysed.

Isolation of thymic fibroblasts and epithelial cells

The thymus was removed from individual mice, minced and incubated in RPMI 1640 for 20 min at RT under gentle agitation. Remaining tissue fragments were incubated with tissue digestion medium at 37ºC for 45 min per cycle under gentle agitation. The tissue digestion

medium containing the released single cells was collected in 15 ml PBS containing 5 mM EDTA and replaced with fresh tissue digestion medium for up to 3 cycles until no fragments were visible anymore. The cell fractions from the digestion cycles were pooled and used for flow cytometric analysis or cell culture experiments. The concentration of Collagenase D and Dispase II was tested and 0,2-0,5 mg enzyme per ml medium (dependent on the tissue size) was used to isolate stroma cells with good yield, high viability and retained cell surface antigen expression. For the generation of cultures of fibroblasts, single cell suspensions were cultured in standard medium, whereas for the enrichment of epithelial cells, single cell suspensions were cultured in epithelial cell medium on Collagenase G-coated plates. Medium was replaced every 3-4 days, and cells were grown to 70-90% confluency per passage.

Isolation of colonic epithelial cells

Freshly isolated colons were cut in 3 pieces and incised longitudinally for feces removal. Then, colons were shortly washed in 20 ml PBS containing 2 mM EDTA and subsequently incubated for 30 min at 37°C in 2 ml/colon tissue digestion medium II. The incubation was stopped by addition of 30 ml PBS containing 5 mM EDTA. Then, epithelial cells were detached from the colonic tissue with help of a syringe plunger. Free crypts were collected and incubated in 30 ml PBS containing 5 mM EDTA for 10 min at 4°C to dissociate the crypts into single epithelial cells. Dissociated cells were passed through a 40 µm cell strainer and centrifuged at 468 g for 15 min. The cell pellet was carefully suspended in 1 ml PBS containing 5 mM EDTA and immediately used for Ab labeling.

5.2.2.2 Lysis of erythrocytes

ACK lysis buffer is an iso-osmotic solution containing ammonium chloride, which causes rapid uptake of water into erythrocytes causing their burst. The process is far slower in leukocytes and therefore, erythrocytes can be removed from cells suspensions without harming leukocytes in a defined, short time frame.

Cell suspensions from spleen and, where indicated from BM and blood, were resuspended continuously for 15 s in 2 ml of ACK lysis buffer per sample. 90 s after addition of the lysis buffer, 7 ml of medium was added to stop the reaction. The cells were then filtered through a 40-70 µm cell-strainer to remove clumps and centrifuged at 468 g for 5 min. After removal of the supernatant, lymphocytes were suspended in 1x PBS containing 2 mM EDTA.

5.2.2.3 Characterization of cell subsets and phenotypes by flow cytometry

Flow cytometry allows the analysis of distinct cell populations based on their size, granularity and expression of different markers revealed by antibodies coupled to fluorophores. Cell suspensions enter a stream of fluid where each cell gets hydrodynamically focused before passing a laser beam. The laser beam excites the fluorophores and thus induces emission of

light. This light is detected and converted to an electronic signal. This signal can be amplified and is finally graphically presented.

Ab-labeling of cell surface antigens

Leucocytes were isolated from blood and lymphoid organs and approximately 1-5x10^6 cells were stained in a 1,5 ml tube or a well of a 96-well plate. Prior or simultaneously to staining with fluorophore-conjugated Abs, cells were incubated with anti-CD16/32 Abs to block unspecific binding of fluorophore-conjugated Abs by their constant region. Cells were labeled with a mix of fluorophore-conjugated Abs diluted in 1x PBS containing 2 mM EDTA and 0,5% BSA. As control, cells were incubated with isotype-matched fluorophore-conjugated control or single Abs and / or FMO (fluorescence minus one) controls. FMO controls contain all Abs in a panel, except of one. It is used to identify and gate cells in the context of data spread due to the multiple fluorophores in a panel. After the cells were incubated with the fluorophore-conjugated antibodies for at least 30 min at 4°C, they were washed once with 1x PBS containing 2 mM EDTA and centrifuged at 698 g for 2 min for 96-well plates. To increase the intensity of CD127 staining on colonic epithelial cells, the FASER Kit-APC was used in two sequential steps according to the manufacturer's recommendations. The cells were then resuspended in 50-200 µl 1x PBS + 2 mM EDTA solution and transferred into tubes suitable for analysis by a flow cytometer. Then, data were analyzed using Cell-Quest Pro software from BD Biosciences or FlowJo software from Tree Star.

Ab-labeling of intranuclear antigens

The cells were first incubated in an Ab mix to label cell surface molecules of interest as described in 5.2.2.1. Then, PBS containing 2 mM EDTA was added to each well and the plates were centrifuged at 698 g to remove unbound Ab mix. Next, the cell pellet was resuspended in 50 µl of FoxP3/Transcription Factor Fixation/Permeablization solution (eBioscience) and incubated for 30 min at 4°C in the dark. 200 µl of FoxP3/Transcription Factor Permeabilization buffer (eBioscience) was added and cells were again centrifuged at 698 g for 2 min to remove the fixative. The cell pellets were resuspended in Ab mix diluted in FoxP3/Transcription Factor Permeabilization buffer and incubated for at least 45 min at 4°C in the dark. The unbound Ab was removed by adding 200 µl of buffer and centrifugation before cells were resuspended in 80-150 µl 1x PBS containing 2 mM EDTA and measured by flow cytometry.

Ab-labeling of intracellular cytokines

Intracellular cytokine staining allows the determination of relative cytokine amounts produced by a cell of interest. In order to detect cytokines in cells, their secretion must be inhibited by protein transport inhibitors e.g. brefeldin A or monensin A. The cells are then fixed and permeabilized to allow the fluorophore-conjugated antibodies to penetrate the cells. In order

to detect cytokine production, 1-3x10^6 splenocytes were stimulated for 6 h at 37°C in 100-200 µl T cell stimulation medium/well in 96-well round bottom plates. Alternatively, PBMCs from blood were mixed with splenocytes from Rag^- mice as source of APCs (one spleen for 10 PBMC samples) and stimulated as indicated above. Cells were then centrifuged at 698 g for 2 min. The cell pellet was resuspended in an Ab mix to label cell surface molecules of interest as described above. PBS containing 2 mM EDTA was then added to each well and the plates were centrifuged at 698 g to remove unbound Ab mix. Next, the cell pellet was resuspended in 50 µl of Perm/Fix solution (BD Biosciences or Biolegend) and incubated for 30 min at 4°C in the dark. 200 µl of 1x Perm/Wash solution (BD Biosciences or Biolegend) was added and cells were again centrifuged at 698 g for 2 min to remove the fixative. The cell pellets were resuspended in anti-cytokine Ab mix diluted in 1x Perm/Wash solution and incubated for at least 45 min at 4°C in the dark. The unbound Ab was removed by adding 200 µl of 1x Perm/Wash solution and centrifugation before cells were resuspended in 80-150 µl 1x PBS containing 2 mM EDTA and measured by flow cytometry.

5.2.2.4 Isolation of OT-I T cells using AutoMACS

Cells of interest can be separated from other cells by labeling them with Abs conjugated to magnetic beads. The cells are then run through a column in which they are exposed to a magnetic field. The unlabeled cells pass through while the magnetically labeled cells are retained within the column. Upon removal of the magnetic field, labeled cells are liberated and eluted from the column.

OT-I TCR transgenic mice express the cDNA of the rearranged Vα2-Jα26 and Vβ5-Jβ2.6 TCR-chains, which recognize the peptide SIINFEKL bound to MHC-I H-2Kb (154). Thus, all $CD8^+$ T cells of these mice are reactive to the SIINFEKL peptide, a foreign peptide, which is derived from chicken ovalbumin. Therefore, these transgenic mice allow the study of cytotoxic T cell responses to a known antigen. Genotyping of OT-I and Rag^-OT-I mice was performed on isolated PBMCs as described in 4.2.2.1. These cells were labeled with Abs against CD8α, Vα2, CD19, B220, CD4 and the congenic markers CD90.1, CD90.2. OT-I-tg^+ mice were defined by expression of Vα2 on all $CD8α^+$ cells. Additionally, Rag^- OT-I-tg^+ mice were defined by low frequencies (<5%) of $CD4^+$ and/or $CD19^+$ or $B220^+$ cells.

In order to purify OT-I T cells, single cell suspensions pooled from spleen, brachial, inguinal and mesenteric lymph nodes from one mouse were suspended in 0,9-0,95 ml cold 1x PBS containing 2mM EDTA and 0,5% BSA solution and 50-100 µl α-CD8 microbeads per mouse were added and incubated for 20-30 min at 4°C with occasional shaking. Then, unbound microbeads were removed by addition of 30 ml 1x PBS containing 2 mM EDTA and centrifugation at 300 g for 15 min at 4°C. The cell pellet was suspended in 2 ml / mouse 1x PBS containing 2 mM EDTA and 0,5% BSA solution and filtered through a 40 µm cell-

strainer. The labeled cells were separated using the “positive selection” program of the AutoMACS or by manual cell separation on a LS column from Miltenyi according to the manufacturer’s recommendations. The purity and activation state of the $CD8^+$ OT-I T cells were analyzed by flow cytometry using Abs recognizing CD8, Vα2, CD44, CD62L, CD69, CD90.1 and CD90.2.

5.2.2.5 Labeling of $CD8^+$ T cells with CFSE

After the separation of $CD8^+$ OT-I T cells by AutoMACS, the cells were washed once with 1x PBS containing 2 mM EDTA and centrifuged at 300 g for 10 min at 4°C. $5x10^7$ $CD8^+$ T cells / ml were incubated with 5 µM Carboxyfluorescein diacetate succinimidylester (CFSE) in 1x PBS for 20 min at 37°C before the reaction was stopped by addition of 1x PBS containing 2 mM EDTA and 5% FCS. The cells were then washed twice with 1x PBS containing 2 mM EDTA and 5% FCS and centrifuged at 300 g for 10 min at 4°C.

5.2.2.6 Immunostaining

Tissues were embedded in Tissue Tek OCT compound and snap-frozen in liquid nitrogen or on dry ice. 6 µm thick tissue sections were cut with the help of a microtome, air dried for 20 min and then stored at -20°C until needed. Cells were grown on cover slips in cell culture dishes. After removal of the medium, coverslips were stored on glass slides at -20°C until needed.

For immunostaining, cells were fixed in cold acetone/methanol (1:1) for 3 min and then washed with PBS 3x for 5 min each. Cells were incubated for 30 min with PBS containing 1% BSA / 0,2% gelatin / 1% of serum from the species where the secondary Ab was generated in. Cells were then incubated with primary Abs for 1 h at RT. After washing with PBS / 1% BSA / 0,2% gelatin 3x for 5 min each, secondary Abs were added for 45 min at RT. As negative controls, samples were incubated with isotype-matched control Abs or secondary Abs only. Cells were washed once for 5 min in PBS / 1% BSA / 0,2% gelatin and incubated for 5 min with 1 µg/ml DAPI in PBS. Finally, cells were washed with PBS, then with distilled water and allowed to air dry. Samples were covered with Vectashield Mounting Medium and examined using a Zeiss Axioplan 200 microscope with AxioVision Release 4.5 software or a Leica DM-RE microscope with SPOT Advanced software.

5.2.3 Manipulations on laboratory mice

5.2.3.1 Transfer of cells by tail vein injection

Cells were prepared as described in 5.2.2.4, washed with 30 ml 1x PBS containing 2 mM EDTA and after centrifugation at 300 g for 12 min, they were finally suspended in 1x PBS. Cells were counted and the cell number was adjusted based on the purity of the preparation. 200 µl of the cell suspension were injected into the tail vein of recipient mice that had been shorty warmed by infrared light in order to widen the vein.

5.2.3.2 IL-7 therapy

Unless otherwise stated, 1,5 µg recombinant murine IL-7 was mixed with 10 µg anti-IL-7 Ab M25 and incubated for 20 min at RT. The mixture was then diluted with 1x PBS to a total volume of 200 µl per mouse and injected i.p every 3-4 days starting one day prior to T cell transfer.

5.2.3.3 Peptide vaccination

As mentioned previously, OT-I $CD8^+$ T cells express a transgenic TCR that recognizes the peptide SIINFEKL presented by the MHC-I molecule H-2Kb. SIINFEKL stock solutions were prepared by solving the powder in DMSO (10 mg/ml). This stock was stored at -20 °C until further use. In order to activate OT-I T cells *in vivo*, 50 µg SIINFEKL in 200 µl PBS was injected i.v. into recipient mice one day post T cell transfer.

5.2.3.4 Tumor cell challenge

E.G7-OVA (EG7) was derived in 1988 from the C57BL/6 (H-2b) mouse lymphoma cell line EL4 by electroporation with a plasmid that carries a complete copy of chicken ovalbumin (OVA) mRNA and the neomycin (G418) resistance gene (214). EG7 cells synthesize and secrete OVA constitutively, and thus activate OT-I T cells to kill the EG7 tumor cells. In this study, we have made use of the EG7 cell line to study the function of OT-I T cells in different hosts and treatments.

The tumor cells were cultivated in standard medium containing 0,4 mg/ml G418 in order to select ova-expressing cells before transfer into recipient mice. For *in vivo* cell inoculation, the cells were centrifuged at 468 g for 5 min and 2x washed with 1x PBS containing 2 mM EDTA to remove bovine proteins from the cell suspension. Then, cells were resuspended in 1x PBS and $1x10^6$ cells were subcutaneously injected in a volume of 100-200 µl at the flanks of mice.

5.2.3.5 *In vivo* imaging by bioluminescence detection

In order to visualize luciferase activity in live animals, BL signal detection was performed using the IVIS Imaging system and software (Xenogen). For all *in vivo* imaging experiments, the light absorbing black fur was removed by shaving the thorax and abdomen.

The IL-7GCDL reporter mice express click beetle green luciferase 99 under control of the *il-7* promoter (63). 3 mg of the luciferase substrate D-luciferin was injected i. v. into the tail vein of mice, which were immediately anesthetized by isofluoran inhalation and then transferred into the IVIS Imaging System for analysis of systemic BL intensities under anesthesia. For detection of BL in isolated organs, mice were injected i. v. with 3 mg D-luciferin 2 min prior to organ removal. Organs were collected in PBS containing 1,5 mg/ml D-luciferin, then transferred on Whatman paper and imaged subsequently. BL signals collected from organs were corrected for the background signals by subtracting the signal of an identically sized area of Whatman paper only.

The systemic abundance of OT-I T cells was determined with the help of ChRLuc-OT-I mice, which express the humanized sea pansy (Renilla reniformis) luciferase gene under control of the CAG promoter (215). In order to visualize luciferase expressing OT-I T cells in live animals, mice were first anesthetized by isofluoran inhalation and then retrobulbally injected with 100 µg of the luciferase substrate colenterazine. *In vivo* imaging was performed under anesthesia within 2 minutes post injection using the IVIS Imaging System.

5.2.3.6 Generation of bone marrow chimeric mice

BM was isolated from both femurs and tibia, which were shortly dipped in 70% ethanol, and then in PBS 2x subsequently. Bone caps were removed to access the BM. The marrow was flushed out of the bones with PBS containing 2 mM EDTA using a 27-gauge needle. Next, it was centrifuged at 468g and resuspended with a 1 ml pipette to generate a single cell suspension, filtered through a 40 µm cell strainer and counted. BM from one donor was used to reconstitute 3 recipients 6-18 hours post irradiation by tail vein injection. Recipients were irradiated with 7-11 Gy using a C^{137} source after anesthesia with 50 µl Ketamin/Rompun i.p. Irradiated mice received an antibiotics mix via the drinking water for 3-4 weeks *ad libitum*.

5.3 Statistical analysis

Statistical analysis and graphs were generated using Graph Pad Prism5 software. Data are shown as single dots or means of authentic values or as relative values with SD or SEM. To calculate relative values of an indicated molecule, the mean value of percentages or the MFI of the respective treatment group was set to one and the values of all groups were calculated in relation. Statistical significance was determined using the non-parametric two-tailed Mann-Whitney, paired Student's t test, 1- and 2-way Anova, log-rank test or Wilcoxon matched-pairs signed rank test. Significant differences were indicated as follows: * $p<0,05$; ** $p<0,01$; *** $p<0,001$.

6 References

1. Janeway, C. A. J., P. Travers, and M. Walport. 2001. Immunobiology: The Immune System in Health and Disease. 5th edition.

2. Blander, J. M., and L. E. Sander. 2012. Beyond pattern recognition: five immune checkpoints for scaling the microbial threat. *Nat. Rev. Immunol.* 12: 215–25.

3. Holers, V. M. 2014. Complement and its receptors: new insights into human disease. *Annu. Rev. Immunol.* 32: 433–59.

4. Mantovani, A., M. A. Cassatella, C. Costantini, and S. Jaillon. 2011. Neutrophils in the activation and regulation of innate and adaptive immunity. *Nat. Rev. Immunol.* 11: 519–31.

5. Soehnlein, O., and L. Lindbom. 2010. Phagocyte partnership during the onset and resolution of inflammation. *Nat. Rev. Immunol.* 10: 427–39.

6. Murray, P. J., and T. A. Wynn. 2011. Protective and pathogenic functions of macrophage subsets. *Nat. Rev. Immunol.* 11: 723–37.

7. Annette Plueddemann, Subhankar Mukhopadhyay, S. G. 2011. Innate immunity to intracellular pathogens : macrophage receptors and responses to microbial entry. *Immunol. Rev.* 240: 11–24.

8. Martinez, F. O., L. Helming, and S. Gordon. 2009. Alternative activation of macrophages: an immunologic functional perspective. *Annu. Rev. Immunol.* 27: 451–483.

9. Spits, H., and T. Cupedo. 2012. Innate lymphoid cells: emerging insights in development, lineage relationships, and function. *Annu. Rev. Immunol.* 30: 647–75.

10. Vivier, E., E. Tomasello, M. Baratin, T. Walzer, and S. Ugolini. 2008. Functions of natural killer cells. *Nat. Immunol.* 9: 503–510.

11. Steinman, R. M. 1991. The dendritic cell system and its role in immunogenicity. *Annu. Rev. Immunol.* 9: 271–296.

12. Mellman, I., R. M. Steinman, and N. Haven. 2001. Dendritic cells: specialized and regulated antigen processing machines. *Cell* 106: 255–258.

13. Joffre, O., M. A. Nolte, R. Spoerri, and C. Reis e Sousa. 2009. Inflammatory signals in dendritic cell activation and the induction of adaptive immunity. *Immunol. Rev.* 227: 234–247.

14. Janeway, C. A. 2001. How the immune system works to protect the host from infection: A personal view. *Proc. Natl Acad. Sci. USA* 98: 7461–7468.

15. Girard, J.-P., C. Moussion, and R. Förster. 2012. HEVs, lymphatics and homeostatic immune cell trafficking in lymph nodes. *Nat. Rev. Immunol.* 12: 762–73.

16. Kalia, V., S. Sarkar, T. S. Gourley, B. T. Rouse, and R. Ahmed. 2006. Differentiation of memory B and T cells. *Curr. Opin. Immunol.* 18: 255–64.

17. Hardy, R. R., and K. Hayakawa. 2001. B cell development pathways. *Annu. Rev. Immunol.* 595–621.

18. McHeyzer-Williams, M., S. Okitsu, N. Wang, and L. McHeyzer-Williams. 2012. Molecular programming of B cell memory. *Nat. Rev. Immunol.* 12: 24–34.

19. Klein, L., M. Hinterberger, G. Wirnsberger, and B. Kyewski. 2009. Antigen presentation in the thymus for positive selection and central tolerance induction. *Nat. Rev. Immunol.* 9: 833–44.

20. Koch, U., and F. Radtke. 2011. Mechanisms of T cell development and transformation. *Annu. Rev. Cell Dev. Biol.* 27: 539–62.

21. Janeway, C. A. J. 1994. Thymic Selection: Two Pathways to Life and Two to Death. *Immunity* 1: 3–6.

22. Zhu, J., and W. E. Paul. 2008. ASH 50th anniversary review CD4 T cells : fates, functions, and faults. *Blood* 112: 1557–1569.

23. Kaech, S. M., and W. Cui. 2012. Transcriptional control of effector and memory CD8+ T cell differentiation. *Nat. Rev. Immunol.* 12: 749–761.

24. Wolint, P., M. R. Betts, R. a Koup, and A. Oxenius. 2004. Immediate cytotoxicity but not degranulation distinguishes effector and memory subsets of CD8+ T cells. *J. Exp. Med.* 199: 925–36.

25. Jameson, S. C., and D. Masopust. 2009. Diversity in T cell memory: an embarrassment of riches. *Immunity* 31: 859–71.

26. Haring, J. S., V. P. Badovinac, and J. T. Harty. 2006. Inflaming the CD8+ T cell response. *Immunity* 25: 19–29.

27. Surh, C. D., and J. Sprent. 2005. Regulation of mature T cell homeostasis. *Semin. Immunol.* 17: 183–91.

28. Harty, J. T., and V. P. Badovinac. 2008. Shaping and reshaping CD8+ T-cell memory. *Nat. Rev. Immunol.* 8: 107–19.

29. Kolumam, G. A., S. Thomas, L. J. Thompson, J. Sprent, and K. Murali-Krishna. 2005. Type I interferons act directly on CD8 T cells to allow clonal expansion and memory formation in response to viral infection. *J. Exp. Med.* 202: 637–50.

30. Ridge, J. P., F. Di Rosa, and P. Matzinger. 1998. A conditioned dendritic cell can be a temporal bridge between a CD4+ T-helper and a T-killer cell. *Nature* 393: 474–8.

31. Schoenberger, S., and R. Toes. 1998. T-cell help for cytotoxic T lymphocytes is mediated by CD40–CD40L interactions. *Nature* 393: 4–7.

32. Bennett, S. R. M., F. R. Carbone, F. Karamalis, R. A. Flavell, J. F. A. P. Miller, and W. R. Heath. 1998. Help for cytotoxic-T-cell responses is mediated by CD40 signalling. *Nature* 393: 478–480.

33. Badovinac, V. P., B. B. Porter, and J. T. Harty. 2002. Programmed contraction of CD8+ T cells after infection. *Nat. Immunol.* 3: 619–26.

34. Teixeiro, E., M. A. Daniels, S. E. Hamilton, A. G. Schrum, R. Bragado, S. C. Jameson, and E. Palmer. 2009. Different T cell receptor signals determine CD8+ memory versus effector development. *Science* 323: 502–5.

35. Zehn, D., S. Lee, and M. Bevan. 2009. Complete but curtailed T cell response to very low affinity antigen. *Nature* 458: 211–214.

36. Sallusto, F., D. Lenig, R. Förster, M. Lipp, and A. Lanzavecchia. 1999. Two subsets of memory T lymphocytes with distinct homing potentials. *Nature* 401: 708–712.

37. Mueller, S. N., T. Gebhardt, F. R. Carbone, and W. R. Heath. 2013. Memory T cell subsets, migration patterns, and tissue residence. *Annu. Rev. Immunol.* 31: 137–61.

38. Jabbari, A., and J. T. Harty. 2005. Cutting edge: differential self-peptide/MHC requirement for maintaining CD8 T cell function versus homeostatic proliferation. *J. Immunol.* 175: 4829–33.

39. Wherry, E. J., V. Teichgräber, T. C. Becker, D. Masopust, S. M. Kaech, R. Antia, U. H. von Andrian, and R. Ahmed. 2003. Lineage relationship and protective immunity of memory CD8 T cell subsets. *Nat. Immunol.* 4: 225–34.

40. Masopust, D., V. Vezys, A. L. Marzo, and L. Lefrançois. 2001. Preferential localization of effector memory cells in nonlymphoid tissue. *Science* 291: 2413–7.

41. Ahmed, R., M. J. Bevan, S. L. Reiner, and D. T. Fearon. 2009. The precursors of memory: models and controversies. *Nat. Rev. Immunol.* 9: 662–8.

42. Chang, J. T., V. R. Palanivel, I. Kinjyo, F. Schambach, A. M. Intlekofer, A. Banerjee, S. A. Longworth, K. E. Vinup, P. Mrass, J. Oliaro, N. Killeen, J. S. Orange, S. M. Russell, W. Weninger, and S. L. Reiner. 2007. Asymmetric T Lymphocyte Adaptive Immune Responses. *Science* 315: 1687–1691.

43. Fearon, D. T., P. Manders, and S. D. Wagner. 2001. Arrested differentiation, the self-renewing memory lymphocyte, and vaccination. *Science* 293: 248–50.

44. Bannard, O., M. Kraman, and D. T. Fearon. 2009. Secondary replicative function of CD8+ T cells that had developed an effector phenotype. *Science* 323: 505–9.

45. Sallusto, F., J. Geginat, and A. Lanzavecchia. 2004. Central memory and effector memory T cell subsets: function, generation, and maintenance. *Annu. Rev. Immunol.* 22: 745–63.

46. Souza, W. N. D., and S. M. Hedrick. 2006. Cutting edge: latecomer CD8 T cells are imprinted with a unique differentiation program. *J. Immunol.* 177: 777–781.

47. Stemberger, C., K. M. Huster, M. Koffler, F. Anderl, M. Schiemann, H. Wagner, and D. H. Busch. 2007. A single naive CD8+ T cell precursor can develop into diverse effector and memory subsets. *Immunity* 27: 985–97.

48. Schepers, K., E. Swart, J. W. J. van Heijst, C. Gerlach, M. Castrucci, D. Sie, M. Heimerikx, A. Velds, R. M. Kerkhoven, R. Arens, and T. N. M. Schumacher. 2008. Dissecting T cell lineage relationships by cellular barcoding. *J. Exp. Med.* 205: 2309–18.

49. Stjernswärd, J., M. Jondal, F. Vanky, H. Wigzell, and R. Sealy. 1972. Lymphopenia and change in distribution of human B and T lymphocytes in peripheral blood induced by irradiation for mammary carcinoma. *Lancet* 299: 1352–1356.

50. Mackall, C. L., T. A. Fleisher, I. T. Magrath, A. T. Shad, M. E. Horowitz, and L. H. Wexler. 1994. Lymphocyte depletion during treatment with intensive chemotherapy for cancer. *Blood* 84: 2221–2228.

51. Goldrath, and Bevan. 1999. Low-affinity ligands for the TCR drive proliferation of mature CD8+ T cells in lymphopenic hosts. *Immunity* 11: 183–90.

52. Goldrath. 2002. Cytokine Requirements for Acute and Basal Homeostatic Proliferation of Naive and Memory CD8+ T Cells. *J. Exp. Med.* 195: 1515–1522.

53. Goldrath, Luckey, Park, Benoist, and Mathis. 2004. The molecular program induced in T cells undergoing homeostatic proliferation. *Proc. Natl. Acad. Sci. U. S. A.* 101: 16885–90.

54. Rogers, P. R., C. Dubey, and S. L. Swain. 2000. Qualitative Changes Accompany Memory T Cell Generation: Faster, More Effective Responses at Lower Doses of Antigen. *J. Immunol.* 164: 2338–2346.

55. Slifka, M. K., and J. L. Whitton. 2001. Functional avidity maturation of CD8+ T cells without selection of higher affinity TCR. *Nat Immunol* 2: 711–717.

56. Veiga-Fernandes, H., U. Walter, C. Bourgeois, A. McLean, and B. Rocha. 2000. Response of naïve and memory CD8+ T cells to antigen stimulation in vivo. *Nat Immunol* 1: 47–53.

57. Huster, K. M., M. Koffler, C. Stemberger, M. Schiemann, H. Wagner, and D. H. Busch. 2006. Unidirectional development of CD8+ central memory T cells into protective Listeria-specific effector memory T cells. *Eur. J. Immunol.* 36: 1453–1464.

58. Klebanoff, C. 2005. Central memory self/tumor-reactive CD8+ T cells confer superior antitumor immunity compared with effector memory T cells. *Proc. Natl. Acad. Sci.* 102: 9571–9576.

59. Chapuis, A. G., J. A. Thompson, K. A. Margolin, R. Rodmyre, I. P. Lai, K. Dowdy, E. A. Farrar, S. Bhatia, D. E. Sabath, J. Cao, Y. Li, and C. Yee. 2012. Transferred melanoma-specific CD8+ T cells persist, mediate tumor regression, and acquire central memory phenotype. *Proc. Natl. Acad. Sci. U. S. A.* 109: 4592–7.

60. Sprent, J., and C. D. Surh. 2012. Interleukin 7, maestro of the immune system. *Semin. Immunol.* 24: 149–50.

61. Namen, A. E., A. E. Schmierer, C. J. March, R. W. Overell, L. S. Park, D. L. Urdal, and D. Y. Mochizuki. 1988. B cell precursor growth-promoting activity. Purification and characterization of a growth factor active on lymphocyte precursors. *J. Exp. Med.* 167: 988–1002.

62. Namen, A. E., S. Lupton, K. Hjerrild, J. Wignall, D. Y. Mochizuki, A. Schmierer, B. Mosley, C. J. March, D. Urdal, and S. Gillis. 1988. Stimulation of B-cell progenitors by cloned murine interleukin-7. *Nature* 333: 571–3.

63. Shalapour, S., K. Deiser, O. Sercan, J. Tuckermann, K. Minnich, G. Willimsky, T. Blankenstein, G. J. Hämmerling, B. Arnold, and T. Schüler. 2010. Commensal microflora and interferon-gamma promote steady-state interleukin-7 production in vivo. *Eur. J. Immunol.* 40: 2391–400.

64. Mazzucchelli, R. I., S. Warming, S. M. Lawrence, M. Ishii, M. Abshari, A. V. Washington, L. Feigenbaum, A. C. Warner, D. J. Sims, W. Q. Li, J. A. Hixon, D. H. D. Gray, B. E. Rich, M. Morrow, M. R. Anver, J. Cherry, D. Naf, L. R. Sternberg, D. W. McVicar, A. G. Farr, R. N. Germain, K. Rogers, N. A. Jenkins, N. G. Copeland, and S. K. Durum. 2009. Visualization and identification of IL-7 producing cells in reporter mice. *PLoS One* 4: e7637.

65. Repass, J. F., M. N. Laurent, C. Carter, B. Reizis, M. T. Bedford, K. Cardenas, P. Narang, M. Coles, and E. R. Richie. 2009. IL7-hCD25 and IL7-Cre BAC transgenic mouse lines: new tools for analysis of IL-7 expressing cells. *Genesis* 47: 281–7.

66. Alves, N. L., O. Richard-Le Goff, N. D. Huntington, A. P. Sousa, V. S. G. Ribeiro, A. Bordack, F. L. Vives, L. Peduto, A. Chidgey, A. Cumano, R. Boyd, G. Eberl, and J. P. Di Santo. 2009. Characterization of the thymic IL-7 niche in vivo. *Proc. Natl. Acad. Sci. U. S. A.* 106: 1512–7.

67. Von Freeden-Jeffry, U., P. Vieira, L. A. Lucian, T. McNeil, S. E. Burdach, and R. Murray. 1995. Lymphopenia in interleukin (IL)-7 gene-deleted mice identifies IL-7 as a nonredundant cytokine. *J. Exp. Med.* 181: 1519–26.

68. Tsapogas, P., S. Zandi, J. Åhsberg, J. Zetterblad, E. Welinder, J. I. Jönsson, R. Månsson, H. Qian, and M. Sigvardsson. 2011. IL-7 mediates Ebf-1-dependent lineage restriction in early lymphoid progenitors. *Blood* 118: 1283–90.

69. Tan, J. T., B. Ernst, W. C. Kieper, E. LeRoy, J. Sprent, and C. D. Surh. 2002. Interleukin (IL)-15 and IL-7 Jointly Regulate Homeostatic Proliferation of Memory Phenotype CD8+ Cells but Are Not Required for Memory Phenotype CD4+ Cells. *J. Exp. Med.* 195: 1523–1532.

70. Schluns, K. S., W. C. Kieper, S. C. Jameson, and L. Lefrançois. 2000. Interleukin-7 mediates the homeostasis of naïve and memory CD8 T cells in vivo. *Nat. Immunol.* 1: 426–32.

71. Kim, G. Y., D. L. Ligons, C. Hong, M. A. Luckey, H. R. Keller, X. Tai, P. J. Lucas, R. E. Gress, and J.-H. Park. 2012. An In Vivo IL-7 Requirement for Peripheral Foxp3+ Regulatory T Cell Homeostasis. *J. Immunol.* 188: 5859–66.

72. Mertsching, E., C. Burdet, and R. Ceredig. 1995. IL-7 transgenic mice: analysis of the role of IL-7 in the differentiation of thymocytes in vivo and in vitro. *Int. Immunol.* 7: 401–14.

73. Kieper, W. C., J. T. Tan, B. Bondi-Boyd, L. Gapin, J. Sprent, R. Ceredig, and C. D. Surh. 2002. Overexpression of interleukin (IL)-7 leads to IL-15-independent generation of memory phenotype CD8+ T cells. *J. Exp. Med.* 195: 1533–9.

74. Geiselhart, L. A., C. A. Humphries, T. A. Gregorio, S. Mou, J. Subleski, and K. L. Komschlies. 2001. IL-7 administration alters the CD4:CD8 ratio, increases T cell numbers, and increases T cell function in the absence of activation. *J. Immunol.* 166: 3019–27.

75. Mackall, C. L., T. J. Fry, and R. E. Gress. 2011. Harnessing the biology of IL-7 for therapeutic application. *Nat. Rev. Immunol.* 11: 330–42.

76. Sereti, I., R. M. Dunham, J. Spritzler, E. Aga, M. A. Proschan, K. Medvik, C. A. Battaglia, A. L. Landay, S. Pahwa, M. A. Fischl, D. M. Asmuth, A. R. Tenorio, J. D. Altman, L. Fox, S. Moir, A. Malaspina, M. Morre, R. Buffet, G. Silvestri, and M. M. Lederman. 2009. IL-7 administration drives T cell-cycle entry and expansion in HIV-1 infection. *Blood* 113: 6304–14.

77. Watanabe, M., Y. Ueno, M. Yamazaki, and T. Hibi. 1999. Mucosal IL-7-mediated immune responses in chronic colitis-IL-7 transgenic mouse model. *Immunol. Res.* 20: 251–9.

78. Yamaji, O., T. Nagaishi, T. Totsuka, M. Onizawa, M. Suzuki, N. Tsuge, A. Hasegawa, R. Okamoto, K. Tsuchiya, T. Nakamura, H. Arase, T. Kanai, and M. Watanabe. 2012. The development of colitogenic CD4(+) T cells is regulated by IL-7 in collaboration with NK cell function in a murine model of colitis. *J. Immunol.* 188: 2524–36.

79. Noguchi, M., Y. Nakamura, S. M. Russell, S. F. Ziegler, M. Tsang, X. Cao, and W. J. Leonardt. 1993. Interleukin-2 Receptor gamma Chain: A Functional Component of the Interleukin-7 Receptor. *Science* 262: 1877–80.

80. Rochman, Y., R. Spolski, and W. J. Leonard. 2009. New insights into the regulation of T cells by gamma(c) family cytokines. *Nat. Rev. Immunol.* 9: 480–90.

81. Park, J.-H., Q. Yu, B. Erman, J. S. Appelbaum, D. Montoya-Durango, H. L. Grimes, and A. Singer. 2004. Suppression of IL7Ralpha transcription by IL-7 and other prosurvival cytokines: a novel mechanism for maximizing IL-7-dependent T cell survival. *Immunity* 21: 289–302.

82. Mazzucchelli, R., and S. K. Durum. 2007. Interleukin-7 receptor expression: intelligent design. *Nat. Rev. Immunol.* 7: 144–54.

83. Takada, K., and S. C. Jameson. 2009. Naive T cell homeostasis: from awareness of space to a sense of place. *Nat. Rev. Immunol.* 9: 823–32.

84. Murali-Krishna, K. 1999. Persistence of Memory CD8 T Cells in MHC Class I-Deficient Mice. *Science* 286: 1377–1381.

85. Rooke, R., C. Waltzinger, C. Benoist, and D. Mathis. 1997. Targeted complementation of MHC class II deficiency by intrathymic delivery of recombinant adenoviruses. *Immunity* 7: 123–34.

86. Lacombe, M., and M. Hardy. 2005. IL-7 receptor expression levels do not identify CD8+ memory T lymphocyte precursors following peptide immunization. *J. Immunol.* 175: 4400–4407.

87. Kaech, S. M., J. T. Tan, E. J. Wherry, B. T. Konieczny, C. D. Surh, and R. Ahmed. 2003. Selective expression of the interleukin 7 receptor identifies effector CD8 T cells that give rise to long-lived memory cells. *Nat. Immunol.* 4: 1191–8.

88. Tanchot, C., F. A. Lemonnier, B. Perarnau, A. A. Freitas, and B. Rocha. 1997. Differential Requirements for Survival and Proliferation of CD8 Naïve or Memory T Cells. *Science* 276: 2057–2062.

89. Carrette, F., and C. D. Surh. 2012. IL-7 signaling and CD127 receptor regulation in the control of T cell homeostasis. *Semin. Immunol.* 24: 209–17.

90. Ma, A., R. Koka, and P. Burkett. 2006. Diverse functions of IL-2, IL-15, and IL-7 in lymphoid homeostasis. *Annu. Rev. Immunol.* 24: 657–79.

91. Guimond, M., R. G. Veenstra, D. J. Grindler, H. Zhang, Y. Cui, R. D. Murphy, S. Y. Kim, R. Na, L. Hennighausen, S. Kurtulus, B. Erman, P. Matzinger, M. S. Merchant, and C. L. Mackall. 2009. Interleukin 7 signaling in dendritic cells regulates the homeostatic proliferation and niche size of CD4+ T cells. *Nat. Immunol.* 10: 149–57.

92. Jiang, Q., W. Li, and R. Hofmeister. 2004. Distinct regions of the interleukin-7 receptor regulate different Bcl2 family members. *Mol. Cell. Biol.* 24: 6501–6513.

93. Li, W. Q., Q. Jiang, E. Aleem, P. Kaldis, A. R. Khaled, and S. K. Durum. 2006. IL-7 promotes T cell proliferation through destabilization of p27Kip1. *J. Exp. Med.* 203: 573–82.

94. Barata, J. T., A. Silva, J. G. Brandao, L. M. Nadler, A. a Cardoso, and V. a Boussiotis. 2004. Activation of PI3K is indispensable for interleukin 7-mediated viability, proliferation, glucose use, and growth of T cell acute lymphoblastic leukemia cells. *J. Exp. Med.* 200: 659–69.

95. Sinclair, L. V, D. Finlay, C. Feijoo, G. H. Cornish, A. Gray, A. Ager, K. Okkenhaug, T. J. Hagenbeek, H. Spits, and D. A. Cantrell. 2008. Phosphatidylinositol-3-OH kinase and nutrient-sensing mTOR pathways control T lymphocyte trafficking. *Nat. Immunol.* 9: 513–21.

96. Wofford, J. A., H. L. Wieman, S. R. Jacobs, Y. Zhao, and J. C. Rathmell. 2008. IL-7 promotes Glut1 trafficking and glucose uptake via STAT5-mediated activation of Akt to support T-cell survival. *Blood* 111: 2101–11.

97. Li, Q., R. R. Rao, K. Araki, K. Pollizzi, K. Odunsi, J. D. Powell, and P. a Shrikant. 2011. A central role for mTOR kinase in homeostatic proliferation induced CD8+ T cell memory and tumor immunity. *Immunity* 34: 541–53.

98. Pellegrini, M., T. Calzascia, A. R. Elford, A. Shahinian, A. E. Lin, D. Dissanayake, S. Dhanji, L. T. Nguyen, M. A. Gronski, M. Morre, B. Assouline, K. Lahl, T. Sparwasser, P. S. Ohashi, and T. W. Mak. 2009. Adjuvant IL-7 antagonizes multiple cellular and molecular inhibitory networks to enhance immunotherapies. *Nat. Med.* 15: 528–36.

99. Park, J.-H., S. Adoro, P. J. Lucas, S. D. Sarafova, A. S. Alag, L. L. Doan, B. Erman, X. Liu, W. Ellmeier, R. Bosselut, L. Feigenbaum, and A. Singer. 2007. “Coreceptor tuning”: cytokine signals transcriptionally tailor CD8 coreceptor expression to the self-specificity of the TCR. *Nat. Immunol.* 8: 1049–59.

100. Henriques, C. M., J. Rino, R. J. Nibbs, G. J. Graham, and J. T. Barata. 2010. IL-7 induces rapid clathrin-mediated internalization and JAK3-dependent degradation of IL-7Ralpha in T cells. *Blood* 115: 3269–77.

101. Kerdiles, Y. M., D. R. Beisner, R. Tinoco, A. S. Dejean, D. H. Castrillon, R. A. DePinho, and S. M. Hedrick. 2009. Foxo1 links homing and survival of naive T cells by regulating L-selectin, CCR7 and interleukin 7 receptor. *Nat. Immunol.* 10: 176–84.

102. Kimura, M. Y., L. a Pobezinsky, T. I. Guinter, J. Thomas, A. Adams, J.-H. Park, X. Tai, and A. Singer. 2013. IL-7 signaling must be intermittent, not continuous, during $CD8^+$ T cell homeostasis to promote cell survival instead of cell death. *Nat. Immunol.* 14: 143–51.

103. Hammerbeck, C. D., and M. F. Mescher. 2008. Antigen Controls IL-7R Expression Levels on CD8 T Cells during Full Activation or Tolerance Induction. *J. Immunol.* 180: 2107–2116.

104. Vogt, T. K., A. Link, J. Perrin, D. Finke, and S. A. Luther. 2009. Novel function for interleukin-7 in dendritic cell development. *Blood* 113: 3961–8.

105. Hochweller, K., G. H. Wabnitz, Y. Samstag, J. Suffner, G. J. Hämmerling, and N. Garbi. 2010. Dendritic cells control T cell tonic signaling required for responsiveness to foreign antigen. *Proc. Natl. Acad. Sci. U. S. A.* 107: 5931–6.

106. Chen, Z., S. Kim, N. D. Chamberlain, S. R. Pickens, M. V Volin, S. Volkov, S. Arami, J. W. Christman, B. S. Prabhakar, W. Swedler, A. Mehta, N. Sweiss, and S. Shahrara. 2013. The novel role of IL-7 ligation to IL-7 receptor in myeloid cells of rheumatoid arthritis and collagen-induced arthritis. *J. Immunol.* 190: 5256–66.

107. Schlenner, S. M., V. Madan, K. Busch, A. Tietz, C. Läufle, C. Costa, C. Blum, H. J. Fehling, and H.-R. Rodewald. 2010. Fate mapping reveals separate origins of T cells and myeloid lineages in the thymus. *Immunity* 32: 426–36.

108. Mebius, R. E. 2003. Organogenesis of lymphoid tissues. *Nat. Rev. Immunol.* 3: 292–303.

109. Mebius, R. E., P. Rennert, and I. L. Weissman. 1997. Developing lymph nodes collect CD4+CD3-LT[beta]+ cells that can differentiate to APC, NK cells and follicular cells but not T or B cells. *Immunity* 7: 493–504.

110. Adachi, S., H. Yoshida, K. Maki, K. Saijo, K. Ikuta, T. Saito, and S. Nishikawa. 1998. Essential role of IL-7 receptor α in the formation of Peyer's patch anlage. *Int. Immunol.* 10: 1–6.

111. Yoshida, H., R. Shinkura, S. Adachi, S. Nishikawa, K. Maki, K. Ikuta, and S. Nishikawa. 1999. IL-7 receptor α+ CD3– cells in the embryonic intestine induces the organizing center of Peyer's patches. *Int. Immunol.* 11: 643–655.

112. Luther, S. A., K. M. Ansel, and J. G. Cyster. 2003. Overlapping roles of CXCL13, interleukin 7 receptor alpha, and CCR7 ligands in lymph node development. *J. Exp. Med.* 197: 1191–8.

113. Meier, D., C. Bornmann, S. Chappaz, S. Schmutz, L. a Otten, R. Ceredig, H. Acha-Orbea, and D. Finke. 2007. Ectopic lymphoid-organ development occurs through interleukin 7-mediated enhanced survival of lymphoid-tissue-inducer cells. *Immunity* 26: 643–54.

114. Scandella, E. 2008. Restoration of lymphoid organ integrity through the interaction of lymphoid tissue-inducer cells with stroma of the T cell zone. *Nat. Immunol.* 9: 667–675.

115. Sawa, S., M. Lochner, N. Satoh-Takayama, S. Dulauroy, M. Bérard, M. Kleinschek, D. Cua, J. P. Di Santo, and G. Eberl. 2011. RORγt+ innate lymphoid cells regulate intestinal homeostasis by integrating negative signals from the symbiotic microbiota. *Nat. Immunol.* 12: 320–6.

116. Hanash, A. M., J. A. Dudakov, G. Hua, M. H. O'Connor, L. F. Young, N. V Singer, M. L. West, R. R. Jenq, A. M. Holland, L. W. Kappel, A. Ghosh, J. J. Tsai, U. K. Rao, N. L. Yim, O. M. Smith, E. Velardi, E. B. Hawryluk, G. F. Murphy, C. Liu, L. A. Fouser, R. Kolesnick, B. R. Blazar, and M. R. M. van den Brink. 2012. Interleukin-22 protects intestinal stem cells from

immune-mediated tissue damage and regulates sensitivity to graft versus host disease. *Immunity* 37: 339–50.

117. Vonarbourg, C., and A. Diefenbach. 2012. Multifaceted roles of interleukin-7 signaling for the development and function of innate lymphoid cells. *Semin. Immunol.* 24: 165–174.

118. Iolyeva, M., D. Aebischer, S. T. Proulx, A.-H. Willrodt, T. Ecoiffier, S. Häner, G. Bouchaud, C. Krieg, L. Onder, B. Ludewig, L. Santambrogio, O. Boyman, L. Chen, D. Finke, and C. Halin. 2013. Interleukin-7 is produced by afferent lymphatic vessels and supports lymphatic drainage. *Blood* 122: 2271–2281.

119. Al-Rawi, M. A. A., K. Rmali, G. Watkins, R. E. Mansel, and W. G. Jiang. 2004. Aberrant expression of interleukin-7 (IL-7) and its signalling complex in human breast cancer. *Eur. J. Cancer* 40: 494–502.

120. Mazzucchelli, R. I., A. Riva, and S. K. Durum. 2012. The human IL-7 receptor gene: deletions, polymorphisms and mutations. *Semin. Immunol.* 24: 225–30.

121. Toraldo, G., C. Roggia, W.-P. Qian, R. Pacifici, and M. N. Weitzmann. 2003. IL-7 induces bone loss in vivo by induction of receptor activator of nuclear factor kappa B ligand and tumor necrosis factor alpha from T cells. *Proc. Natl. Acad. Sci. U. S. A.* 100: 125–30.

122. Hartgring, S. A. Y., C. R. Willis, J. W. J. Bijlsma, F. P. J. G. Lafeber, and J. A. G. van Roon. 2012. Interleukin-7-aggravated joint inflammation and tissue destruction in collagen-induced arthritis is associated with T-cell and B-cell activation. *Arthritis Res. Ther.* 14: R137.

123. Watanabe, M., Y. Ueno, T. Yajima, S. Okamoto, T. Hayashi, M. Yamazaki, Y. Iwao, H. Ishii, S. Habu, M. Uehira, H. Nishimoto, H. Ishikawa, J. Hata, and T. Hibi. 1998. Interleukin 7 transgenic mice develop chronic colitis with decreased interleukin 7 protein accumulation in the colonic mucosa. *J. Exp. Med.* 187: 389–402.

124. Lee, L.-F., K. Logronio, G. H. Tu, W. Zhai, I. Ni, L. Mei, J. Dilley, J. Yu, A. Rajpal, C. Brown, C. Appah, S. M. Chin, B. Han, T. Affolter, and J. C. Lin. 2012. Anti-IL-7 receptor-α reverses established type 1 diabetes in nonobese diabetic mice by modulating effector T-cell function. *Proc. Natl. Acad. Sci. U. S. A.* 109: 12674–9.

125. Penaranda, C., W. Kuswanto, J. Hofmann, R. Kenefeck, P. Narendran, L. S. K. Walker, J. A. Bluestone, A. K. Abbas, and H. Dooms. 2012. IL-7 receptor blockade reverses autoimmune diabetes by promoting inhibition of effector/memory T cells. *Proc. Natl. Acad. Sci. U. S. A.* 109: 12668–73.

126. Sawa, Y., Y. Arima, H. Ogura, C. Kitabayashi, J.-J. Jiang, T. Fukushima, D. Kamimura, T. Hirano, and M. Murakami. 2009. Hepatic interleukin-7 expression regulates T cell responses. *Immunity* 30: 447–57.

127. Bolotin, E., M. Smogorzewska, S. Smith, M. Widmer, and K. Weinberg. 1996. Enhancement of thymopoiesis after bone marrow transplant by in vivo interleukin-7. *Blood* 88: 1887–94.

128. Perales, M.-A., J. D. Goldberg, J. Yuan, G. Koehne, L. Lechner, E. B. Papadopoulos, J. W. Young, A. A. Jakubowski, B. Zaidi, H. Gallardo, C. Liu, T. Rasalan, J. D. Wolchok, T. Croughs, M. Morre, S. M. Devlin, and M. R. M. van den Brink. 2012. Recombinant human interleukin-7 (CYT107) promotes T-cell recovery after allogeneic stem cell transplantation. *Blood* 120: 4882–91.

129. Unsinger, J., M. McGlynn, K. R. Kasten, A. S. Hoekzema, E. Watanabe, J. T. Muenzer, J. S. McDonough, J. Tschoep, T. A. Ferguson, J. E. McDunn, M. Morre, D. A. Hildeman, C. C. Caldwell, and R. S. Hotchkiss. 2010. IL-7 promotes T cell viability, trafficking, and functionality and improves survival in sepsis. *J. Immunol.* 184: 3768–79.

130. Pellegrini, M., T. Calzascia, J. G. Toe, S. P. Preston, A. E. Lin, A. R. Elford, A. Shahinian, P. A. Lang, K. S. Lang, M. Morre, B. Assouline, K. Lahl, T. Sparwasser, T. F. Tedder, J.-H. Paik, R. A. DePinho, S. Basta, P. S. Ohashi, and T. W. Mak. 2011. IL-7 engages multiple mechanisms to overcome chronic viral infection and limit organ pathology. *Cell* 144: 601–13.

131. Andersson, A., S.-C. Yang, M. Huang, L. Zhu, U. K. Kar, R. K. Batra, D. Elashoff, R. M. Strieter, S. M. Dubinett, and S. Sharma. 2009. IL-7 promotes CXCR3 ligand-dependent T cell antitumor reactivity in lung cancer. *J. Immunol.* 182: 6951–8.

132. Nanjappa, S. G. S., J. H. J. Walent, M. Morre, and M. Suresh. 2008. Effects of IL-7 on memory CD8+ T cell homeostasis are influenced by the timing of therapy in mice. *J. Clin. Invest.* 118: 1027–1039.

133. Nanjappa, S. G., E. H. Kim, and M. Suresh. 2011. Immunotherapeutic effects of IL-7 during a chronic viral infection in mice. *Blood* 117: 5123–32.

134. Sportès, C., R. R. Babb, M. C. Krumlauf, F. T. Hakim, S. M. Steinberg, C. K. Chow, M. R. Brown, T. A. Fleisher, P. Noel, I. Maric, M. Stetler-Stevenson, J. Engel, R. Buffet, M. Morre, R. J. Amato, A. Pecora, C. L. Mackall, and R. E. Gress. 2010. Phase I study of recombinant human interleukin-7 administration in subjects with refractory malignancy. *Clin. Cancer Res.* 16: 727–35.

135. Restifo, N. P., M. E. Dudley, and S. A. Rosenberg. 2012. Adoptive immunotherapy for cancer: harnessing the T cell response. *Nat. Rev. Immunol.* 12: 269–81.

136. Lee, E. C., D. Yu, J. Martinez de Velasco, L. Tessarollo, D. A. Swing, D. L. Court, N. A. Jenkins, and N. G. Copeland. 2001. A highly efficient Escherichia coli-based chromosome engineering system adapted for recombinogenic targeting and subcloning of BAC DNA. *Genomics* 73: 56–65.

137. Szymczak, A. L., C. J. Workman, Y. Wang, K. M. Vignali, S. Dilioglou, E. F. Vanin, and D. a a Vignali. 2004. Correction of multi-gene deficiency in vivo using a single “self-cleaving” 2A peptide-based retroviral vector. *Nat. Biotechnol.* 22: 589–94.

138. Willimsky, G., and T. Blankenstein. 2005. Sporadic immunogenic tumours avoid destruction by inducing T-cell tolerance. *Nature* 437: 141–6.

139. Onder, L., E. Scandella, Q. Chai, S. Firner, C. T. Mayer, T. Sparwasser, V. Thiel, T. Rülicke, and B. Ludewig. 2011. A novel bacterial artificial chromosome-transgenic podoplanin-cre mouse targets lymphoid organ stromal cells in vivo. *Front. Immunol.* 2: 50.

140. Farr, A., A. Nelson, and S. Hosier. 1992. Characterization of an antigenic determinant preferentially expressed by type I epithelial cells in the murine thymus. *J. Histochem. Cytochem.* 40: 651–664.

141. Colby, W. W., and T. Shenk. 1982. Fragments of the simian virus 40 transforming gene facilitate transformation of rat embryo cells. *Proc. Natl Acad. Sci. USA* 79: 5189–5193.

142. Zamisch, M., B. Moore-Scott, D. Su, P. J. Lucas, N. Manley, and E. R. Richie. 2005. Ontogeny and Regulation of IL-7-Expressing Thymic epithelial cells. *J. Immunol.* 174: 60–67.

143. Katakai, T., T. Hara, M. Sugai, H. Gonda, and A. Shimizu. 2004. Lymph node fibroblastic reticular cells construct the stromal reticulum via contact with lymphocytes. *J. Exp. Med.* 200: 783–95.

144. Klug, D. B., C. Carter, E. Crouch, D. Roop, C. J. Conti, and E. R. Richie. 1998. Interdependence of cortical thymic epithelial cell differentiation and T-lineage commitment. *Proc. Natl Acad. Sci. USA* 95: 11822–11827.

145. Ariizumi, K., Y. Meng, P. R. Bergstresser, and A. Takashima. 1995. IFN-gamma-dependent IL-7 gene regulation in keratinocytes. *J. Immunol.* 154: 6031–9.

146. Huang, H.-Y., and S. A. Luther. 2012. Expression and function of interleukin-7 in secondary and tertiary lymphoid organs. *Semin. Immunol.* 24: 175–89.

147. Capitini, C. M., a. a. Chisti, and C. L. Mackall. 2009. Modulating T-cell homeostasis with IL-7: preclinical and clinical studies. *J. Intern. Med.* 266: 141–153.

148. Reinecker, H., and D. K. Podolsky. 1995. Human intestinal epithelial cells express functional cytokine receptors sharing the common yc chain of the interleukin 2 receptor. *Proc. Natl Acad. Sci. USA* 92: 8353–8357.

149. Boyman, O., C. Ramsey, D. M. Kim, J. Sprent, and C. D. Surh. 2008. IL-7/anti-IL-7 mAb complexes restore T cell development and induce homeostatic T Cell expansion without lymphopenia. *J. Immunol.* 180: 7265–75.

150. Fry, T. J. 2002. Interleukin-7: from bench to clinic. *Blood* 99: 3892–3904.

151. Peschon, J., and P. Morrissey. 1994. Early Lymphocyte Expansion Is Severely Impaired in Interleukin 7 Receptor-deficient Mice. *J. Exp. Med.* 180: 6–11.

152. Rose, S., A. Misharin, and H. Perlman. 2012. A novel Ly6C/Ly6G-based strategy to analyze the mouse splenic myeloid compartment. *Cytometry. A* 81: 343–50.

153. Schnorrer, P., G. M. N. Behrens, N. S. Wilson, J. L. Pooley, C. M. Smith, D. El-Sukkari, G. Davey, F. Kupresanin, M. Li, E. Maraskovsky, G. T. Belz, F. R. Carbone, K. Shortman, W. R. Heath, and J. A. Villadangos. 2006. The dominant role of CD8+ dendritic cells in cross-presentation is not dictated by antigen capture. *Proc. Natl. Acad. Sci. U. S. A.* 103: 10729–34.

154. Hogquist, K. A., S. C. Jameson, W. R. Heath, J. L. Howard, M. J. Bevan, and F. R. Carbone. 1994. T Cell Receptor Antagonist Peptides Induce Positive Selection. *Cell* 76: 17–27.

155. Cheung, K. P., E. Yang, and A. W. Goldrath. 2009. Memory-like CD8+ T cells generated during homeostatic proliferation defer to antigen-experienced memory cells. *J. Immunol.* 183: 3364–72.

156. Schuster, K., J. Gadiot, R. Andreesen, A. Mackensen, T. F. Gajewski, and C. Blank. 2009. Homeostatic proliferation of naïve CD8+ T cells depends on CD62L/L-selectin-mediated homing to peripheral LN. *Eur. J. Immunol.* 39: 2981–90.

157. Sportès, C., F. T. Hakim, S. A. Memon, H. Zhang, K. S. Chua, M. R. Brown, T. A. Fleisher, M. C. Krumlauf, R. R. Babb, C. K. Chow, T. J. Fry, J. Engels, R. Buffet, M. Morre, R. J. Amato, D. J. Venzon, R. Korngold, A. Pecora, R. E. Gress, and C. L. Mackall. 2008. Administration of rhIL-7 in humans increases in vivo TCR repertoire diversity by preferential expansion of naive T cell subsets. *J. Exp. Med.* 205: 1701–14.

158. Overwijk, W. W., M. R. Theoret, S. E. Finkelstein, D. R. Surman, L. A. de Jong, F. A. Vyth-Dreese, T. A. Dellemijn, P. A. Antony, P. J. Spiess, D. C. Palmer, D. M. Heimann, C. A. Klebanoff, Z. Yu, L. N. Hwang, L. Feigenbaum, A. M. Kruisbeek, S. A. Rosenberg, and N. P. Restifo. 2003. Tumor regression and autoimmunity after reversal of a functionally tolerant state of self-reactive CD8+ T cells. *J. Exp. Med.* 198: 569–80.

159. Joshi, N. S., W. Cui, A. Chandele, H. K. Lee, D. R. Urso, J. Hagman, L. Gapin, and S. M. Kaech. 2007. Inflammation directs memory precursor and short-lived effector CD8+ T cell fates via the graded expression of T-bet transcription factor. *Immunity* 27: 281–95.

160. Banerjee, A., S. M. Gordon, A. M. Intlekofer, M. a Paley, E. C. Mooney, T. Lindsten, E. J. Wherry, and S. L. Reiner. 2010. Cutting edge: The transcription factor eomesodermin enables CD8+ T cells to compete for the memory cell niche. *J. Immunol.* 185: 4988–92.

161. Li, G., Q. Yang, Y. Zhu, H.-R. Wang, X. Chen, X. Zhang, and B. Lu. 2013. T-Bet and Eomes Regulate the Balance between the Effector/Central Memory T Cells versus Memory Stem Like T Cells. *PLoS One* 8: e67401.

162. Takemoto, N., A. M. Intlekofer, J. T. Northrup, E. J. Wherry, and S. L. Reiner. 2006. Cutting Edge: IL-12 Inversely Regulates T-bet and Eomesodermin Expression during Pathogen-Induced CD8+ T Cell Differentiation. *J. Immunol.* 177: 7515–7519.

163. Dunkle, A., I. Dzhagalov, C. Gordy, and Y.-W. He. 2013. Transfer of CD8+ T cell memory using Bcl-2 as a marker. *J. Immunol.* 190: 940–7.

164. Holler, P. D., and D. M. Kranz. 2014. Quantitative Analysis of the Contribution of TCR/pepMHC Affinity and CD8 to T Cell Activation. *Immunity* 18: 255–264.

165. Maile, R., C. a. Siler, S. E. Kerry, K. E. Midkiff, E. J. Collins, and J. a. Frelinger. 2005. Peripheral “CD8 Tuning” Dynamically Modulates the Size and Responsiveness of an Antigen-Specific T Cell Pool In Vivo. *J. Immunol.* 174: 619–627.

166. Kuhns, M. S., M. M. Davis, and K. C. Garcia. 2006. Deconstructing the form and function of the TCR/CD3 complex. *Immunity* 24: 133–9.

167. Azzam, H. S., A. Grinberg, K. Lui, H. Shen, E. W. Shores, and P. E. Love. 1998. CD5 Expression Is Developmentally Regulated By T Cell Receptor (TCR) Signals and TCR Avidity. *J. Exp. Med.* 188: 2301–2311.

168. Zinselmeyer, B. H., S. Heydari, C. Sacristán, D. Nayak, M. Cammer, J. Herz, X. Cheng, S. J. Davis, M. L. Dustin, and D. B. McGavern. 2013. PD-1 promotes immune exhaustion by inducing antiviral T cell motility paralysis. *J. Exp. Med.* 210: 757–74.

169. Wherry, E. J. 2011. T cell exhaustion. *Nat. Immunol.* 131: 492–499.

170. Von Freeden-Jeffry, U., N. Solvason, M. Howard, and R. Murray. 1997. The Earliest T Lineage – Committed Cells Depend on IL-7 for Bcl-2 Expression and Normal Cell Cycle Progression. *Immunity* 7: 147–154.

171. Lenz, D. C., S. K. Kurz, E. Lemmens, S. P. Schoenberger, J. Sprent, M. B. A. Oldstone, and D. Homann. 2004. IL-7 regulates basal homeostatic proliferation of antiviral CD4+ T cell memory. *Proc. Natl. Acad. Sci.* 101: 9357–9362.

172. Welsh, D. K., and S. A. Kay. 2005. Bioluminescence imaging in living organisms. *Curr. Opin. Biotechnol.* 16: 73–8.

173. Colin, M., S. Moritz, H. Schneider, J. Capeau, C. Coutelle, and M. C. Brahimi-Horn. 2000. Haemoglobin interferes with the ex vivo luciferase luminescence assay: consequence for detection of luciferase reporter gene expression in vivo. *Gene Ther.* 7: 1333–6.

174. Hara, T., S. Shitara, K. Imai, H. Miyachi, S. Kitano, H. Yao, S. Tani-Ichi, and K. Ikuta. 2012. Identification of IL-7-Producing Cells in Primary and Secondary Lymphoid Organs Using IL-7-GFP Knock-In Mice. *J. Immunol.* 189: 1577–84.

175. Miller, C. N., D. J. Hartigan-O'Connor, M. S. Lee, G. Laidlaw, I. P. Cornelissen, M. Matloubian, S. R. Coughlin, D. M. McDonald, and J. M. McCune. 2013. IL-7 production in murine lymphatic endothelial cells and induction in the setting of peripheral lymphopenia. *Int. Immunol.* 25: 471–83.

176. Link, A., T. K. Vogt, S. Favre, M. R. Britschgi, H. Acha-Orbea, B. Hinz, J. G. Cyster, and S. A. Luther. 2007. Fibroblastic reticular cells in lymph nodes regulate the homeostasis of naive T cells. *Nat. Immunol.* 8: 1255–65.

177. Malhotra, D., A. L. Fletcher, J. Astarita, V. Lukacs-Kornek, P. Tayalia, S. F. Gonzalez, K. G. Elpek, S. K. Chang, K. Knoblich, M. E. Hemler, M. B. Brenner, M. C. Carroll, D. J. Mooney, and S. J. Turley. 2012. Transcriptional profiling of stroma from inflamed and resting lymph nodes defines immunological hallmarks. *Nat. Immunol.* 13: 499–510.

178. Zhang, F., X. Liang, D. Pu, K. I. George, P. J. Holland, S. T. R. Walsh, and R. J. Linhardt. 2012. Biophysical characterization of glycosaminoglycan-IL-7 interactions using SPR. *Biochimie* 94: 242–9.

179. Onder, L., P. Narang, E. Scandella, Q. Chai, M. Iolyeva, K. Hoorweg, C. Halin, E. Richie, P. Kaye, J. Westermann, T. Cupedo, M. Coles, and B. Ludewig. 2012. IL-7-producing stromal cells are critical for lymph node remodeling. *Blood* 120: 4675–83.

180. Nemoto, Y., T. Kanai, M. Takahara, S. Oshima, T. Nakamura, R. Okamoto, K. Tsuchiya, and M. Watanabe. 2013. Bone marrow-mesenchymal stem cells are a major source of interleukin-7 and sustain colitis by forming the niche for colitogenic CD4 memory T cells. *Gut* 62: 1142–52.

181. Huang, M., S. Sharma, L. X. Zhu, M. P. Keane, J. Luo, L. Zhang, M. D. Burdick, Y. Q. Lin, M. Dohadwala, B. Gardner, R. K. Batra, R. M. Strieter, and S. M. Dubinett. 2002. IL-7 inhibits fibroblast TGF-β production and signaling in pulmonary fibrosis. *J. Clin. Invest.* 109: 931–937.

182. Zhang, L., M. P. Keane, L. X. Zhu, S. Sharma, E. Rozengurt, R. M. Strieter, S. M. Dubinett, and M. Huang. 2004. Interleukin-7 and transforming growth factor-beta play counter-regulatory roles in protein kinase C-delta-dependent control of fibroblast collagen synthesis in pulmonary fibrosis. *J. Biol. Chem.* 279: 28315–9.

183. Yang, B.-G., T. Tanaka, M. H. Jang, Z. Bai, H. Hayasaka, and M. Miyasaka. 2007. Binding of Lymphoid Chemokines to Collagen IV That Accumulates in the Basal Lamina of

High Endothelial Venules: Its Implications in Lymphocyte Trafficking. *J. Immunol.* 179: 4376–4382.

184. Duś, D., A. Krawczenko, P. Załęcki, M. Paprocka, A. Więdłocha, C. Goupille, and C. Kieda. 2003. IL-7 receptor is present on human microvascular endothelial cells. *Immunol. Lett.* 86: 163–168.

185. Li, R., A. Paul, K. W. S. Ko, M. Sheldon, B. E. Rich, T. Terashima, C. Dieker, S. Cormier, L. Li, E. a Nour, L. Chan, and K. Oka. 2012. Interleukin-7 induces recruitment of monocytes/macrophages to endothelium. *Eur. Heart J.* 33: 3114–23.

186. Roye, O., N. Delhem, F. Trottein, F. Remoué, S. Nutten, J. P. Decavel, M. Delacre, V. Martinot, J. Y. Cesbron, C. Auriault, and I. Wolowczuk. 1998. Dermal endothelial cells and keratinocytes produce IL-7 in vivo after human Schistosoma mansoni percutaneous infection. *J. Immunol.* 161: 4161–8.

187. Hirosue, S., E. Vokali, V. R. Raghavan, M. Rincon-Restrepo, A. W. Lund, P. Corthésy-Henrioud, F. Capotosti, C. Halin Winter, S. Hugues, and M. A. Swartz. 2014. Steady-state antigen scavenging, cross-presentation, and CD8+ T cell priming: a new role for lymphatic endothelial cells. *J. Immunol.* 192: 5002–11.

188. Lund, A. W., F. V Duraes, S. Hirosue, V. R. Raghavan, C. Nembrini, S. N. Thomas, A. Issa, S. Hugues, and M. A. Swartz. 2012. VEGF-C promotes immune tolerance in B16 melanomas and cross-presentation of tumor antigen by lymph node lymphatics. *Cell Rep.* 1: 191–9.

189. Förster, R., A. Braun, and T. Worbs. 2012. Lymph node homing of T cells and dendritic cells via afferent lymphatics. *Trends Immunol.* 33: 271–80.

190. Mueller, S. N., and R. N. Germain. 2009. Stromal cell contributions to the homeostasis and functionality of the immune system. *Nat. Rev. Immunol.* 9: 618–29.

191. Zaft, T., A. Sapoznikov, R. Krauthgamer, D. R. Littman, and S. Jung. 2005. Lymphopenia-Driven Proliferation of Naive and Memory CD8+ T cells. *J. Immunol.* 175: 6428–6435.

192. Park, B. L. S., U. Martin, K. Garka, B. Gliniak, J. P. Di Santo, W. Muller, D. A. Largaespada, N. G. Copeland, N. A. Jenkins, A. G. Farr, S. F. Ziegler, P. J. Morrissey, R. Paxton, and J. E. Sims. 2000. Cloning of the Murine Thymic Stromal Lymphopoietin (TSLP) Receptor : Formation of a Functional Heteromeric Complex Requires Interleukin 7 Receptor. *J. Exp. Med.* 192: 659–669.

193. Al-Shami, A., R. Spolski, J. Kelly, A. Keane-Myers, and W. J. Leonard. 2005. A role for TSLP in the development of inflammation in an asthma model. *J. Exp. Med.* 202: 829–39.

194. Kitajima, M., and S. F. Ziegler. 2013. Cutting edge: identification of the thymic stromal lymphopoietin-responsive dendritic cell subset critical for initiation of type 2 contact hypersensitivity. *J. Immunol.* 191: 4903–7.

195. Wendland, M., S. Willenzon, J. Kocks, A. C. Davalos-Misslitz, S. I. Hammerschmidt, K. Schumann, E. Kremmer, M. Sixt, A. Hoffmeyer, O. Pabst, and R. Förster. 2011. Lymph node T cell homeostasis relies on steady state homing of dendritic cells. *Immunity* 35: 945–57.

196. Rubinstein, M. P., N. a Lind, J. F. Purton, P. Filippou, J. A. Best, P. A. McGhee, C. D. Surh, and A. W. Goldrath. 2008. IL-7 and IL-15 differentially regulate CD8+ T-cell subsets during contraction of the immune response. *Blood* 112: 3704–12.

197. Kittipatarin, C., W. Li, S. K. Durum, and A. R. Khaled. 2010. Cdc25A-driven proliferation regulates CD62L levels and lymphocyte movement in response to interleukin-7. *Exp. Hematol.* 38: 1143–56.

198. Martin, C. E., E. M. M. van Leeuwen, S. J. Im, D. C. Roopenian, Y.-C. Sung, and C. D. Surh. 2013. IL-7/anti-IL-7 mAb complexes augment cytokine potency in mice through association with IgG-Fc and by competition with IL-7R. *Blood* 121: 4484–92.

199. Gagnon, J., X. L. Chen, M. Forand-Boulerice, C. Leblanc, C. Raman, S. Ramanathan, and S. Ilangumaran. 2010. Increased antigen responsiveness of naive CD8 T cells exposed to IL-7 and IL-21 is associated with decreased CD5 expression. *Immunol Cell Biol* 88: 451–460.

200. Aiello, F. B., J. R. Keller, K. D. Klarmann, G. Dranoff, R. Mazzucchelli, and S. K. Durum. 2007. IL-7 induces myelopoiesis and erythropoiesis. *J. Immunol.* 178: 1553–63.

201. Gunnarsson, S., D. Bexell, A. Svensson, P. Siesjö, A. Darabi, and J. Bengzon. 2010. Intratumoral IL-7 delivery by mesenchymal stromal cells potentiates IFN-gamma-transduced tumor cell immunotherapy of experimental glioma. *J. Neuroimmunol.* 218: 140–4.

202. Pickens, S. R., N. D. Chamberlain, M. V Volin, R. M. Pope, N. E. Talarico, A. M. Mandelin, and S. Shahrara. 2011. Characterization of interleukin-7 and interleukin-7 receptor in the pathogenesis of rheumatoid arthritis. *Arthritis Rheum.* 63: 2884–93.

203. Al-Rawi, M. A. A., G. Watkins, R. E. Mansel, and W. G. Jiang. 2005. Interleukin 7 upregulates vascular endothelial growth factor D in breast cancer cells and induces lymphangiogenesis in vivo. *Br. J. Surg.* 92: 305–10.

204. Hou, L., Z. Jie, Y. Liang, M. Desai, L. Soong, and J. Sun. 2014. Type 1 interferon-induced IL-7 maintains CD8+ T-cell responses and homeostasis by suppressing PD-1 expression in viral hepatitis. *Cell Mol Immunol* .

205. Rao, R. R., Q. Li, M. R. Gubbels Bupp, and P. A. Shrikant. 2012. Transcription factor Foxo1 represses T-bet mediated effector functions and promotes memory CD8+ T cell differentiation. *Immunity* 36: 374–387.

206. Nakarai, T., M. J. Robertson, M. Streuli, Z. Wu, T. L. Ciardeui, K. A. Smith, and J. Ritz. 1994. Interleukin 2 Receptor gamma Chain Expression on Resting and Activated Lymphoid Cells. *J. Exp. Med.* 180: 241–251.

207. Quinci, A. C., S. Vitale, E. Parretta, A. Soriani, M. L. Iannitto, M. Cippitelli, C. Fionda, S. Bulfone-Paus, A. Santoni, and F. Di Rosa. 2012. IL-15 inhibits IL-7Rα expression by memory-phenotype $CD8^+$ T cells in the bone marrow. *Eur. J. Immunol.* 42: 1129–39.

208. Intlekofer, A. M., N. Takemoto, E. J. Wherry, S. a Longworth, J. T. Northrup, V. R. Palanivel, A. C. Mullen, C. R. Gasink, S. M. Kaech, J. D. Miller, L. Gapin, K. Ryan, A. P. Russ, T. Lindsten, J. S. Orange, A. W. Goldrath, R. Ahmed, and S. L. Reiner. 2005. Effector and memory CD8+ T cell fate coupled by T-bet and eomesodermin. *Nat. Immunol.* 6: 1236–44.

209. Wakita, D., K. Sumida, Y. Iwakura, H. Nishikawa, T. Ohkuri, K. Chamoto, H. Kitamura, and T. Nishimura. 2010. Tumor-infiltrating IL-17-producing gammadelta T cells support the progression of tumor by promoting angiogenesis. *Eur. J. Immunol.* 40: 1927–37.

210. Kryczek, I., Y. Lin, N. Nagarsheth, D. Peng, L. Zhao, E. Zhao, L. Vatan, W. Szeliga, Y. Dou, S. Owens, W. Zgodzinski, M. Majewski, G. Wallner, J. Fang, E. Huang, and W. Zou. 2014. IL-22(+)CD4(+) T cells promote colorectal cancer stemness via STAT3 transcription factor activation and induction of the methyltransferase DOT1L. *Immunity* 40: 772–84.

211. Lukacs-Kornek, V., D. Malhotra, A. L. Fletcher, S. E. Acton, K. G. Elpek, P. Tayalia, A. Collier, and S. J. Turley. 2011. Regulated release of nitric oxide by nonhematopoietic stroma controls expansion of the activated T cell pool in lymph nodes. *Nat. Immunol.* 12: 1096–104.

212. Yang, C.-Y., T. K. Vogt, S. Favre, L. Scarpellino, H.-Y. Huang, F. Tacchini-Cottier, and S. A. Luther. 2014. Trapping of naive lymphocytes triggers rapid growth and remodeling of the fibroblast network in reactive murine lymph nodes. *Proc. Natl. Acad. Sci. U. S. A.* 111: E109–18.

213. Mombaerts, P., J. Iacomini, R. S. Johnson, K. Herrup, S. Tonegawa, and V. E. Papaioannou. 1992. RAG-1-deficient mice have no mature B and T lymphocytes. *Cell* 68: 869–77.

214. Moore, M. W., F. R. Carbone, and M. J. Bevan. 1988. Introduction of Soluble Protein into the Class I Pathway of Antigen Processing and Presentation. *Cell* 54: 777–785.

215. Charo, J., C. Perez, C. Buschow, A. Jukica, M. Czeh, and T. Blankenstein. 2011. Visualizing the dynamic of adoptively transferred T cells during the rejection of large established tumors. *Eur. J. Immunol.* 41: 3187–97.

7 Abbreviations

7-AAD	7-amino-actinomycin D
α	anti or alpha
Ab	antibody
Ag	antigen
ACK	ammonium-chloride-potassium
Actb	beta-actin
ATT	adoptive T cell therapy
AKT	protein kinase B (PKB)
APC	antigen-presenting cell
Bcl-2	B cell lymphoma 2
BCR	B cell receptor
BAC	bacterial artificial chromosome
bp	base pair
BIM	Bcl-2-interacting mediator of cell death
BL	bioluminescence
BLI	bioluminescence intensity
BM	bone marrow
BSA	bovine serum albumin
CCR	C-C chemokine receptor
CFSE	carboxyfluorescein succinimidyl ester
CEC	colonic epithelial cell
CLP	common lymphoid progenitor
CMP	common myeloid progenitor
cDNA	complementary DNA
ctrl	control
cTEC	cortical thymic epithelial cell
CTL	cytotoxic T lymphocyte
DAPI	4',6-diamidino-2-phenylindole
DC	dendritic cell
DNA	deoxyribonucleic acid
DMSO	Dimethylsulfoxid
DN	double-negative
DP	double-positive
dNTP	deoxynucleotide triphosphate
EDTA	ethylenediamine-N, N, N’, N’-tetraacetic acid
Eomes	Eomesodermin

FCS	fetal calf serum
FMO	fluorescence minus one
FOXO1	forkhead box protein O1
FRC	fibroblastic reticular cell
FSC	forward scatter
ɣc-chain	common gamma chain
GLUT1	glucose transporter 1
GFP	green fluorescent protein
hprt	hypoxanthine phosphoribosyltransferase 1
IgG	Immunoglobulin G
IL-7R^{-}	Interleukin-7-receptor-deficient
IL-7R^{+}	Interleukin-7-receptor-competent
i.p.	intraperitoneally
i.v.	intravenously
ICAM-1	intracellular adhesion molecule-1, CD54
IFN	interferon
IL	interleukin
ILC	innate lymphoid cell
IRES	internal ribosome entry site
JAK	Janus kinase
JAX	The Jackson Laboratory
Klf2	Kruppel-like factor 2
KLRG-1	killer cell lectin-like receptor subfamily G member 1
LN	lymph node
LEC	lymphatic endothelial cell
LTi	lymphoid tissue inducer cell
LIP	lymphopenia-induced proliferation
m	murine
MACS	magnetic-activated cell sorting
mTOR	mammalian target of rapamycin
MHC	major histocompatibility complex
MHC-I	major histocompatibility complex class 1
MHC-II	major histocompatibility complex class 2
MFI	mean fluorescence intensity
mTEC	medullary thymic epithelial cell
MLN	mesenteric lymph node
mRNA	messenger RNA

MCL1	myeloid cell leukemia 1
NK cell	Natural killer cell
Neo	neomycin
PAMP	pathogen-associated molecular pattern
PRR	pattern-recognition receptor
PBMC	peripheral blood mononuclear cell
PBS	phosphate-buffered saline
PCR	polymerase chain reaction
PI3K	phosphoinositol 3-phosphate
PD-1	programmed death-1
P27KIP1	cyclin-dependent kinase inhibitor 1B
r	recombinant
Rag	recombination activating gene
RNA	ribonucleic acid
SP	single-positive
SSC	side scatter
STAT	signal transducer and acitvator of transcription
SD	standard deviation
SEM	standard error of the mean
SLEC	short-lived effector cells
SLO	secondary lymphoid organs
SI	small intestine
s.c.	subcutaneously
TAE	Tris-Acetate-EDTA
T_{CM}	central memory T cells
T_{EM}	effector memory T cells
T_{EFF}	effector T cells
T_{EM}	effector memory T cells
T_{M}	memory T cells
T_{N}	naive T cells
T_{SLEC}	short-lived effector T cells
TCR	T cell receptor
tg	transgenic
TE	Tris-EDTA
TGF-β	transforming growth factor-beta
TLR	Toll-like receptor
TNF	tumor necrosis factor

TSLP	thymic stromal lymphopoietin
VCAM-1	vascular cell adhesion molecule-1; CD106
WT	wild-type